

THE UNIVERSITY OF CALGARY

**Stability and
the Descending Limb of the Force-Length Relation
in Mouse Skeletal Muscle --
a Theoretical and Experimental Examination**

by

Todd Lawrence Allinger

A DISSERTATION

SUBMITTED TO THE FACULTY OF GRADUATE STUDIES
IN PARTIAL FULFILLMENT OF THE REQUIREMENTS FOR THE
DEGREE OF DOCTOR OF PHILOSOPHY

DEPARTMENT OF MECHANICAL ENGINEERING

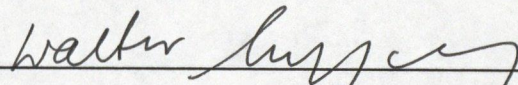
CALGARY, ALBERTA

AUGUST, 1995

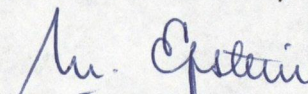
© Todd Lawrence Allinger 1995

THE UNIVERSITY CALGARY
FACULTY OF GRADUATE STUDIES

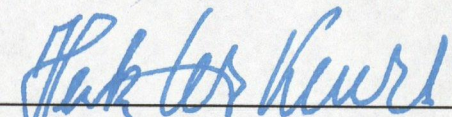
The undersigned certify that they have read, and recommend to the Faculty of Graduate Studies for acceptance, a dissertation entitled "Stability and the Descending Limb of the Force-Length Relation in Mouse Skeletal Muscle -- a Theoretical and Experimental Examination" submitted by Todd Lawrence Allinger in partial fulfillment of the requirements for the degree of Doctor of Philosophy.



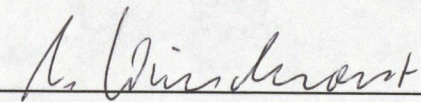
Supervisor, Dr. W. Herzog
Faculty of Kinesiology



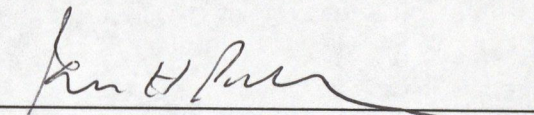
Dr. M. Epstein
Department of Mechanical Engineering



Dr. H.E.D.J. ter Keurs
Department of Medical Physiology



Dr. U. Windhorst
Department of Clinical Neuroscience



External Examiner, Dr. G.H. Pollack
Department of Bioengineering
University of Washington, USA

August 2, 1995

Abstract

The isometric force-length (F-L) relation for skeletal muscle has a negative slope on the descending limb, and it has been suggested that sarcomeres are unstable at lengths corresponding to the descending limb (Hill, 1953). Instability results in sarcomeres diverging in length on the descending limb of the F-L relation: the short (strong) sarcomeres shorten at the expense of the long (weak) sarcomeres. Two of the purposes of this dissertation were to identify the mechanical conditions for which sarcomeres in a muscle fiber are stable -- analytically, and determine if sarcomeres in muscle exhibit stable length behavior at lengths on the descending limb of the F-L relation. Stability was defined to exist if the potential energy function (derived from the F-L properties) of a fiber has a minimum. Theoretically it was shown that all sarcomeres in a fiber except one must possess a positively sloped force-displacement relation for stability to occur. It was also demonstrated that a stable sarcomere can produce a negatively sloped, isometric F-L relation, that could be misinterpreted as unstable. Sarcomere length-time behavior was measured using laser diffraction in the serratus anterior muscle of mouse during fixed-end tetani (i.e., the ends of the muscle were held at constant length). All sarcomere length-time traces measured experimentally; as well as, almost all of those in the literature exhibited a decrease in speed with time (stable behavior).

Other purposes of the dissertation were to determine theoretically the properties necessary to explain the differences between the theoretical and fixed-end F-L relations, and to determine if these properties exist in the mouse serratus anterior muscle. The fixed-end F-L relation exhibited larger forces than the theoretical F-L relation at corresponding sarcomere lengths on the descending limb of the F-L relation for the serratus anterior muscle. Analytically it was shown that sarcomeres must possess an effective stiffness (slope of the force-displacement curve for sarcomeres) that increases with increasing initial sarcomere length to explain the differences between the theoretical and fixed-end F-L relations. Experimentally, this occurred and could provide an explanation for the differences between the theoretical and fixed-end F-L relations.

Preface

Chapters 4 and 5 of this dissertation are based, respectively, on the following manuscripts:

Allinger, T.L., Epstein, M., and Herzog, W. (1995) Stability of muscle fibers on the descending limb of the force-length relation -- a theoretical consideration (*accepted, J. Biomech.*).

Allinger, T.L., Herzog, W. and Epstein, M. (1995) Force-length properties in stable skeletal muscle fibers -- theoretical considerations (*submitted, J. Biomech.*).

Acknowledgements

I would like to express my sincere thanks to:

Walter Herzog for his dedication to research excellence, keenness in the search for knowledge, excellent guidance, and for making me revise each article 10 times;

Henk ter Keurs for his vast store of knowledge about muscles;

Marcelo Epstein for his superb analytical mind which verges on the abstractness of math;

Uwe Windhorst and Gerald Pollack for serving on my dissertation defense committee;

Brian Macintosh for the use of the experimental equipment;

Tim Leonard for making the strain gauges;

F.G. Biddle for providing animal specimens;

Warren Veale and Benno Nigg for consultations and guidance;

fellow graduate students who have helped me, especially: Lynda, Janet, Andy, Tony, Michael, Gerald;

the Alberta Heritage Foundation for Medical Research for three years of financial support.

Dedication

. . . . to my Calgary family (Cathy, Leah, Alicia, and Colten) for supporting my pursuits both at work and in our daily life, and for putting up with my late nights (early mornings). Maybe now I can get a real job, Cathy .

. . . . to my parents who taught me the value of family, the perseverance to accomplish anything, and the conviction of strong principles.

Table of Contents

Approval Page	ii
Abstract	iii
Preface	v
Acknowledgements	vi
Dedication	vii
Table of Contents	viii
List of Tables	xi
List of Figures	xii
 Chapter 1: Introduction	 1
New and notable	8
Overview of thesis	9
 Chapter 2: Review of Relevant Literature	 10
Sarcomere stability, nonuniformity, and the F-L relation	10
History dependent sarcomere properties	19
Summary of relevant literature	21
 Chapter 3: The Muscle Preparation and Experimental Setup	 23
Choice of muscle preparation	23
Dissection of muscle preparation	25
Experimental Setup	32
Bathing solution	32
Experimental apparatus	32
Stimulation	36
Data Collection	36
Pilot tests	38
Sarcomere clamping	38
Segment length measurements	39

Chapter 4: Stability of muscle fibers on the descending limb of the force-length relation -- a theoretical consideration	41
Introduction	41
Methods	43
Results	47
Stability of a Two Sarcomere Fiber	47
Stability of an $n + 1$ Sarcomere Fiber	49
Discussion	51
Conditions of stability	51
Is stability consistent with the descending limb of the F-L relation?	53
Conclusion	57
 Chapter 5: Force-length properties in stable skeletal muscle fibers -- theoretical considerations	 58
Introduction	58
Methods	61
Sarcomere properties	61
Rules of stability	65
Results	69
Model 1: Classic force-length model	69
Model 2: Cross-bridge stiffness model	70
Model 3: Effective stiffness model	71
Discussion	72
Evaluation of F-L Properties of the Three Models	72
 Chapter 6: Sarcomere stability on the Descending Limb of the Force-Length Relation of Mouse Skeletal Muscle	 77
Introduction	77
Methods	80
Stable and unstable fiber models	81
Experimental sarcomere length measurements	85
Sarcomere length measurement errors	93
Experimental results	95
Sarcomere length nonuniformities at rest	95
Sarcomere length nonuniformities during contraction	97
Stability considerations	100
Discussion	103
Sarcomere length nonuniformity in muscle vs. single fibers..	103
Support for stability	105
Support for instability	107
Conclusions	108
Appendix	109

Chapter 7: Reason for the Difference Between the Theoretical and Fixed-end Force-length Relation in Mouse Skeletal Muscle	112
Introduction	112
Methods	116
Experimental procedure	116
Data analysis	119
Results	123
Discussion	133
Comparison with other investigations	133
Stability considerations	134
Reason for a shift in the fixed-end F-L relation	136
Chapter 8: Summary	138
Chapter 9: References	141

List of Tables

Table 3.1. Muscles examined and ranked for testing (best to worst)	25
Table 6.1. Rate of change in sarcomere length for the last 40 ms of a fixed-end contraction	102
Table 6.2. Comparison of types of sarcomere length behaviors between muscle (this study) and single fibers (Edman and Reggiani, 1984, Figure 5 and 6)	104
Table 6.3. List of the number of sarcomere length-time traces demonstrating stable and unstable behavior	105

List of Figures

Figure 1.1. The structural components of muscle	2
Figure 1.2. F-L relation for frog single fibers (Gordon et al., 1966b). Active force producing regions (ascending limb, plateau, and descending limb) plus the resting force (dashed line) equals the total force. A representation of the myofilament overlap at various sarcomere lengths is shown above	3
Figure 1.3. Total F-L relation for frog single fibers (Gordon et al., 1966b). Sarcomeres that begin on the descending limb (hollow circles) are unstable until they are on positively sloped regions (solid circles)	4
Figure 1.4. Force-displacement relation (A) that is unstable over a portion of the curve (negative slope, dashed line) for a structure (B) with two elastic beams of stiffness k	5
Figure 1.5. Fixed-end (thin line) and theoretical (thick line) F-L relations for frog single fibers (Gordon et al., 1966b)	7
Figure 2.1. Fixed-end (thin line) and theoretical (thick line) F-L relations for frog single fibers (Gordon et al., 1966b) (A). Schematic of force-time traces during a fixed-end contraction at two different muscle lengths (B)	11
Figure 2.2. Illustration of the amount a monochromatic beam of light will diffract after transmission through a grating or muscle. SL - sarcomere length, λ - wavelength of light, n number of diffraction order, θ - angle of diffracted beam	15
Figure 3.1. Superficial muscles of the thorax. Lateral view with skin and cutaneous maximus muscle removed	27

Figure 3.2. Deeper muscles of the thorax. Lateral view with acromiotrapezius, spinotrapezius, latissimusdorsi, spinodeltoideus, and upper arm muscles removed	28
Figure 3.3. Muscle preparation after extraction from thorax and with muscles on scapula removed (infraspinatus, supraspinatus, subscapularis)	29
Figure 3.4. Top view of muscle preparation (distal head of serratus anterior) with all extra muscles removed. Scapula is reflected so anterior side (subscapularis origin) is visible	30
Figure 3.5. Top view of muscle preparation in experimental apparatus	31
Figure 3.6. Schematic of experimental apparatus. Bathing solution flowed past muscle from the force transducer end to the motor end of the bath. A - muscle specimen, B - bath, C - cover slip, F - micro-manipulator, H - half cylindrical lens, L - laser beam, M - motor, O - microscope objective, P - photodiode array, S - strain gauge transducer, T - converging lens	33
Figure 3.7. Cable connections (thick lines) are shown between the electrical equipment used in the experimental setup	37
Figure 4.1. Demonstration of the expected unstable sarcomere behavior on the descending limb of the F-L curve (after Hill, 1953). Two sarcomeres at different initial lengths (open circles) diverge in length until stability occurs (solid circles). Note, the F-L relation shown contains the characteristics of actual F-L relations (e.g., Gordon et al., 1966), but does not represent the properties of any specific muscle. The passive force was represented as a straight line starting at sarcomere lengths where the force of the descending limb becomes zero	42
Figure 4.2. Fiber model (A) consisting of $n + 1$ sarcomeres in series and n nodes. Displacement (x_i) of node i is from the equilibrium condition. Force-displacement properties (B) for an individual sarcomeres. A sarcomere is considered to either have a positive stiffness (k_A , solid line) or a negative stiffness ($-k_D$, solid line)	44

Figure 4.3. Stability -- response of the two sarcomere model at different initial lengths. All sarcomeres follow the F-L curves (solid line) given by slopes k_A and $-k_D$. <i>Case 1</i> : a stable fiber begins with both sarcomeres on the ascending limb. The sarcomeres initial lengths are a_{0s} and a_{1s} (open circles) and reach equilibrium at a_{0e} and a_{1e} (solid circle). <i>Case 2</i> : a different fiber begins with both sarcomeres on the descending limb (d_{0s} and d_{1s}). The system is unstable and the sarcomeres diverge	47
Figure 4.4. Stability -- response of a stable ($k_A > k_D$), two sarcomere model with different initial lengths for <i>case 3</i> . One sarcomere is always on the ascending limb and one sarcomere always on the descending limb. Sarcomeres f_0 and f_1 represent one fiber and sarcomeres g_0 and g_1 represent a different fiber. Initial sarcomere lengths are given by open circles and the stable, steady-state conditions are shown by solid circles	48
Figure 4.5. Illustration of a comb experiment that demonstrates how a sarcomere can be stable yet possess a F-L relation with a negative slope. A) Combs in resting condition before engaging bristles. B) Force-deflection relation for a single bristle. C) Comb configuration after engaging all bristles and pulling the ends of the comb apart by Δ . D) Comb configuration after engaging two bristles and pulling the ends of the comb apart by Δ	54
Figure 4.6. F-L plot of the comb experiment. Thick shaded line shows the F-L relation after "activation" when combs are pulled apart a distance Δ . Solid lines represent the force-displacement curves for individual trials with all bristles engaged (C) and with two bristles engaged (D)	56
Figure 5.1. Schematic representation of the force-length (F-L) relation for a small group of sarcomeres under isometric contraction conditions using segment-clamping methods (thick line). Also shown is the F-L relation (using average sarcomere length) for a muscle fiber under fixed-end contraction conditions (thin line)	59
Figure 5.2. F-L properties of individual sarcomeres for model 1 (A), model 2 (B), and model 3 (C). Sarcomeres that shorten are illustrated with squares; sarcomeres that lengthen are illustrated with circles	62

Figure 5.3. Model 1-- stable lengths of sarcomeres (open circles) for average sarcomere lengths of a fiber ("x"). The thick line represents the classic F-L relation for a sarcomere. See text for details	66
Figure 5.4. Model 2-- behavior of a two-sarcomere model with sarcomeres that follow the cross-bridge stiffness curves (solid lines). "x" indicates the force and average sarcomere length at equilibrium. The classic F-L curve for a sarcomere is represented (shaded line) along with the cross-bridge stiffness curves (solid lines, k_1 and k_2)	67
Figure 5.5. Model 3 -- response of a two-sarcomere model with sarcomeres that have individual shortening and stretching behaviors. Shortening sarcomeres follow the segment-clamped F-L curve (shaded line) and stretching sarcomeres follow their effective stiffness curves (k_2 and k_4). Equilibrium (solid circles) is reached at an average sarcomere length and force indicated by "x". Sarcomere behavior for a fiber length near the plateau is illustrated by sarcomeres 1 and 2 with the postscript "s" designating the initial sarcomere length, and "e" the equilibrium sarcomere length. Sarcomere behavior for a fiber at a long length is illustrated by sarcomeres 3 and 4	68
Figure 5.6. Model 1 -- force vs. average sarcomere length for the two-sarcomere model under fixed-end conditions and at stable equilibrium (thin line). The classic F-L curve for a sarcomere is represented by the thick line	69
Figure 5.7. Model 2 -- force vs. average sarcomere length for the two-sarcomere model under fixed-end conditions and stable equilibrium (thin line). The classic F-L curve for a sarcomere is represented by the thick line	71
Figure 5.8. Model 3 -- force vs. average sarcomere length for the two-sarcomere model under fixed-end conditions and stable equilibrium (thin line). The classic F-L curve for a sarcomere is represented by the thick line	72

Figure 6.1. Sarcomere force-length relation for mouse skeletal muscle under isometric conditions based on an thin myofilament length of 1.14 μm (Phillips and Woledge, 1992) and a thick myofilament length of 1.63 μm (Sosa et al., 1994). Open circles represent two sarcomeres in the same fiber that begin a contraction at different initial lengths and then become more nonuniform in length during the contraction (an unstable behavior)	78
Figure 6.2. (A) Muscle fiber model composed of two sarcomeres. (B) Force-length relation for sarcomeres. The circles represent the initial length of the two sarcomeres and the boxes represent the behavior during contraction. Filled symbols illustrate the behavior of the stable fiber, and the hollow symbols represent the behavior of the unstable fiber. (C) Additional force that depends on the speed of shortening (-) or lengthening (+) and is added to the F-L relation to get the total sarcomere force	82
Figure 6.3. Sarcomere length-time behaviors from the unstable (thin line) and the stable (thick line) fiber composed of two sarcomeres ..	83
Figure 6.4. Diagram of the serratus anterior muscle as seen from a left lateral view of the mouse (4A). Schematic of the experimental set-up (4B). Bathing solution flowed past the muscle from the force transducer end to the motor end of the bath. A - muscle specimen, B - bath, C - cover slip, F - micro-manipulator, H - half cylindrical lens, L - laser beam, M - motor, O - microscope objective, P - photodiode array, S - strain gauge transducer, T - converging lens	86
Figure 6.5. Characteristic sarcomere length-time traces which were classified as types 1 (shortening), 2 (lengthening), 12 (shortening-lengthening), and 21 (lengthening-shortening) according to the mean sarcomere length during the time periods shown	91
Figure 6.6. Resting sarcomere length measured across the width of a muscle at two distances from the rib end at a constant muscle length. The mean sarcomere lengths of the traces (\pm S.D.) were $2.670 \pm 0.023 \mu\text{m}$ and $2.585 \pm 0.012 \mu\text{m}$ at a distance of 1/8 [file: f2393.c3] and 1/4 [file: f2393.c4] of the muscle length from the rib end, respectively. Distances across the muscle width are not to scale	95

Figure 6.7. Resting sarcomere length along the length of the muscle measured near one edge for four muscle lengths. The mean sarcomere lengths (\pm S.D.) at each muscle length were $2.551 \pm 0.026 \mu\text{m}$ (A; file: f2493.a7), $2.638 \pm 0.027 \mu\text{m}$ (B; file: f2493.a9), $2.754 \pm 0.038 \mu\text{m}$ (C; file: f2493.a13), and $2.890 \pm 0.026 \mu\text{m}$ (D; file: f2493.a19). Distances along the muscle, parallel to the fiber axes, are not to scale	96
Figure 6.8. (A) Sarcomere length-time traces during a contraction at three positions across the width of a muscle (proximal edge, a1; center, a2; distal edge, a3) near the rib end. Mean and standard deviations of the three traces during rest (0 - 25 ms) and during the tetanic plateau (230 - 270 ms) were $2.19 \pm 0.040 \mu\text{m}$ and $2.380 \pm 0.041 \mu\text{m}$, respectively. (B) Corresponding force-time curves for the above contraction (stimulation 250 ms) [muscle: j293; plateau force 290 mN/mm ² ; cross sectional area 0.10 mm ²]	97
Figure 6.9. Typical sarcomere length-time traces at different locations along the length of four muscles. Traces for a given muscle were at one muscle length. Raw data were represented by dots and the smoothed data by the solid lines. The time of contraction was determined from the force-time traces (Figure 6.10). Stimulation occurred from 0 - 250 ms (A [m994], B [a1994]) and 0 - 300 ms (C [j2293], D [a2894])	99
Figure 6.10. Force-time histories for the corresponding traces in Figure 6.9. The forces were normalized to the peak force during the plateau (last 40 ms of contraction). Stimulation occurred from 0 - 250 ms (A, B) and 0 - 300 ms (C, D). Muscles A [m994], B [a1994], C [j2293], and D [a2894] had plateau forces of 86, 75, 490, and 100 mN/mm ² ; and cross sectional areas of 0.18, 0.08, 0.32, and 0.35 mm ² , respectively	100
Figure 6.11. Illustration of the exponential ($SL(t) = a + b e^{-c t}$) approximation during the contraction (thick line) of a type 1 (A; file: m994.a23) and a type 2 (C; file: j2293.a7) sarcomere length-time trace from Figure 6.9	101
Figure 7.1. Schematic of the force-length relations for sarcomeres (thick line) and for fixed-end methods (thin line) from frog single fibers	113

Figure 7.2. Diagram of serratus anterior muscle during dissection (2A). Schematic of experimental apparatus (2B). Bathing solution flowed past muscle from the force transducer end to the motor end of the bath. A - muscle specimen, B - bath, C - cover slip, F - micro-manipulator, H - half cylindrical lens, L - laser beam, M - motor, O - microscope objective, P - photodiode array, S - strain gauge transducer, T - converging lens	117
Figure 7.3. Illustration of the four types of sarcomere length-time traces. Two regions in muscle A and C were measured at the same muscle length. Muscle A had type 2 (a20) and type 12 (a19), while muscle C had type 1 (a3) and type 21 (a27) sarcomere length behaviors. Force curves in B and D correspond to the curves in A and C, respectively. Vertical lines indicate time periods where mean sarcomere length was calculated. Stimulation in the two muscles was 250 ms. [A and B from muscle: m994; C and D from muscle: m1894]	120
Figure 7.4. Sarcomere length-time (A) and force-time (B) traces at four different muscle lengths. Sarcomere length was measured from the same group of sarcomeres in all four traces. Note, stimulation of a23 was for 400 ms while it was 250 ms for the other three contractions [muscle: m1894]	124
Figure 7.5. Sarcomere length-time (A) and force-time (B) traces for one muscle at two different muscle lengths (subscripts 1 and 2). Sarcomere length was measured at three different location along the length of the muscle (labelled a, b, and c). [muscle: j2293; line-file: a ₁ -a ₂ , b ₁ -a ₄ , c ₁ -a ₅ , a ₂ -a ₁₀ , b ₂ -a ₁₁ , c ₂ -a ₁₂]	125
Figure 7.6. Change in force producing potential for one group of sarcomeres at various muscle lengths (same muscle as Figure 7.4). Arrows connect the theoretical force at the resting sarcomere length (open boxes) with the force and sarcomere length during the plateau of the tetanus (filled boxes)	126

Figure 7.7. Change in force producing potential for three different groups of sarcomeres along the length of the muscle (same muscle as in Figure 7.5). Arrows connect the theoretical force at the resting sarcomere length (open symbols) with the force and sarcomere length during the tetanic plateau (filled symbols) for type 1 sarcomeres. Type 12 sarcomeres have an intermediate point (diamond) after shortening and before lengthening. Letters (a, b, and c) identify the location where sarcomere length was measured. Three different muscle lengths are designated by the different symbols (boxes, circles, triangles)	127
Figure 7.8. Plots of effective stiffness (Ks) for shortening sarcomeres of type 1 (A) and the shortening phase of type 12 (B) sarcomeres. Each symbol represents a different muscle. Combined results of plots A and B are included in C. Insets show the sarcomere length-time trace for each type of behavior between which the effective stiffness was measured.	129
Figure 7.9. Plots of effective stiffness (Kl) for lengthening sarcomeres of type 2 (A) and the lengthening phase of type 12 (B) sarcomeres. Each symbol represents a different muscle. Combined results of plots A and B are included in C. Insets show the sarcomere length-time trace for each type of behavior between which the effective stiffness was measured	130
Figure 7.10. Fixed-end F-L relation for all data points (n = 143) along with a best fit line (thin line). Also shown are the theoretical F-L relations (thick line) and resting F-L relation for two muscles (cross and plus symbols; fit line, $y = -29.2 + 57.7x - 45.2x^2 + 17.5x^3 - 3.37x^4 + 0.257x^5$, $r = 0.93$, $n = 29$)	131
Figure 7.11. Sarcomere F-L relation using the extrapolation method for all data points (12 muscles, n = 143) along with a linear fit line for data points above 2.65 μm (thin line). Theoretical F-L relations also shown (thick line)	132
Figure 7.12. F-L relations from lines fit to data of this study. The difference curve computed as the fixed-end minus the extrapolated F-L relations	133

Chapter 1

Introduction

Muscles are fascinating engines. Take these facts into consideration:

- 1) Heart muscle contracts over 2,500,000,000 times in a human's life.
- 2) Muscles propel frogs to jump 5 times their body length.
- 3) Muscles accelerate a cheetah to over 100 Km/hr.

Muscles are the pistons that drive living structures (skeletons), by converting chemical energy into mechanical energy. These biological engines are more efficient and can produce more power per mass (1 kW/kg) than any man-made motor ever produced.

Although we use muscles every day and muscles are outstanding engines, our understanding of how they work is limited. Muscle is structurally partitioned into fiber bundles, fibers (single cells), sarcomeres (literally translated, muscle unit), myofibrils, and myofilaments (Figure 1.1). Muscle fibers contain all the necessary components to store chemical energy, and to convert chemical energy into mechanical energy when stimulated by a nerve action potential. Fibers are composed of a large number of sarcomeres in series which are the basic units of contraction. Within a sarcomere, contraction occurs by an interaction between the thick (myosin) and thin (actin) myofilaments. Although the exact mode of interaction is unknown, the accepted theory is that cross-bridges from the thick myofilament attach to a neighboring thin myofilament; the

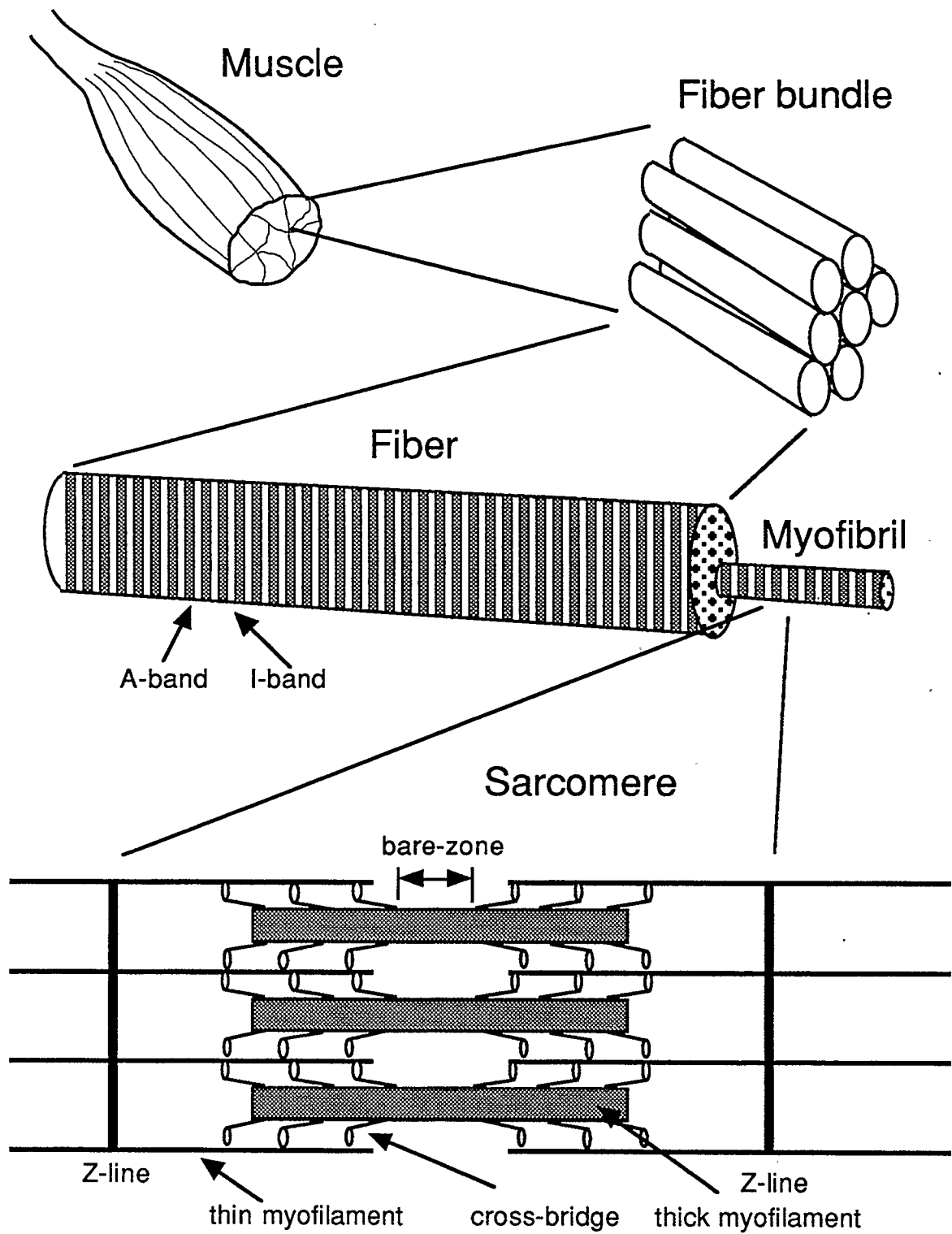


Figure 1.1. The structural components of muscle.

cross-bridges rotate, sliding the thin myofilament past the thick myofilament; and then the cross-bridges detach. This method of muscle contraction is termed the “cross-bridge theory” and has existed for less than 40 years (Huxley, 1957) .

Strong experimental evidence in support of the cross-bridge theory is found in the force-length (F-L) relation. The force-length relation refers to the dependence of maximal isometric force on sarcomere length. A maximally stimulated muscle (tetanus) contains an active force-length relation with an ascending limb, a plateau, and a descending limb (Figure 1.2). An unstimulated muscle possesses a resting (or passive) F-L relation: force increases with increasing sarcomere length. The sum of the active and passive F-L relations gives the total F-L property of a sarcomere or muscle (Figure 1.2).

Because the F-L relation has a negative slope on the descending limb, it has been suggested that sarcomeres are unstable on the descending limb (Hill,

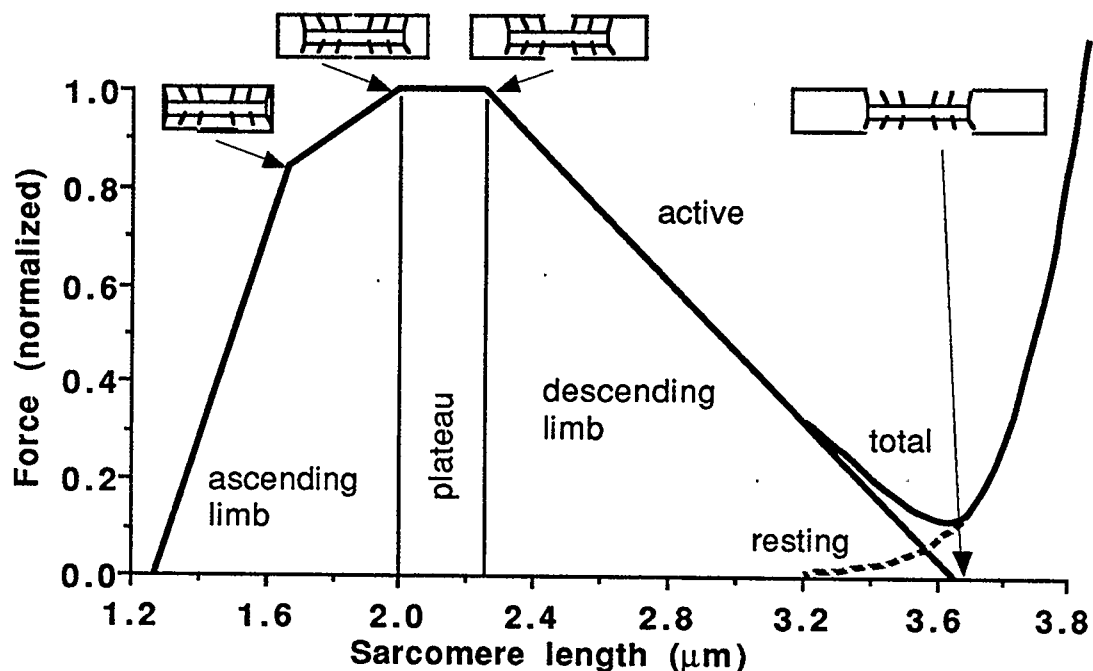


Figure 1.2. F-L relation for frog single fibers (Gordon et al., 1966b). Active force producing regions (ascending limb, plateau, and descending limb) plus the resting force (dashed line) equals the total force. A representation of the myofilament overlap at various sarcomere lengths is shown above.

1953). Instability refers to the idea that two sarcomeres in a fiber which are at different initial lengths on the descending limb of the F-L relation diverge in length: the short (strong) sarcomere shortens at the expense of the long (weak) sarcomere (Figure 1.3). According to this hypothesis, muscle fibers would “pull themselves apart” during a contraction.

Structures that possess a negatively sloped force-displacement relation are unstable (Figure 1.4). For example, an unloaded structure may begin in an equilibrium state (filled circle, Figure 1.4A). If an increasing load (P) is applied to the structure, the displacement (x) will increase along the solid force-displacement curve. At a critical displacement (x_c) the structure will suddenly flip into a reversed orientation. In the unstable region of the force-displacement curve (dotted line) the structure can not remain at these displacements or any slight perturbation in the displacement will cause a radical shift in displacement.

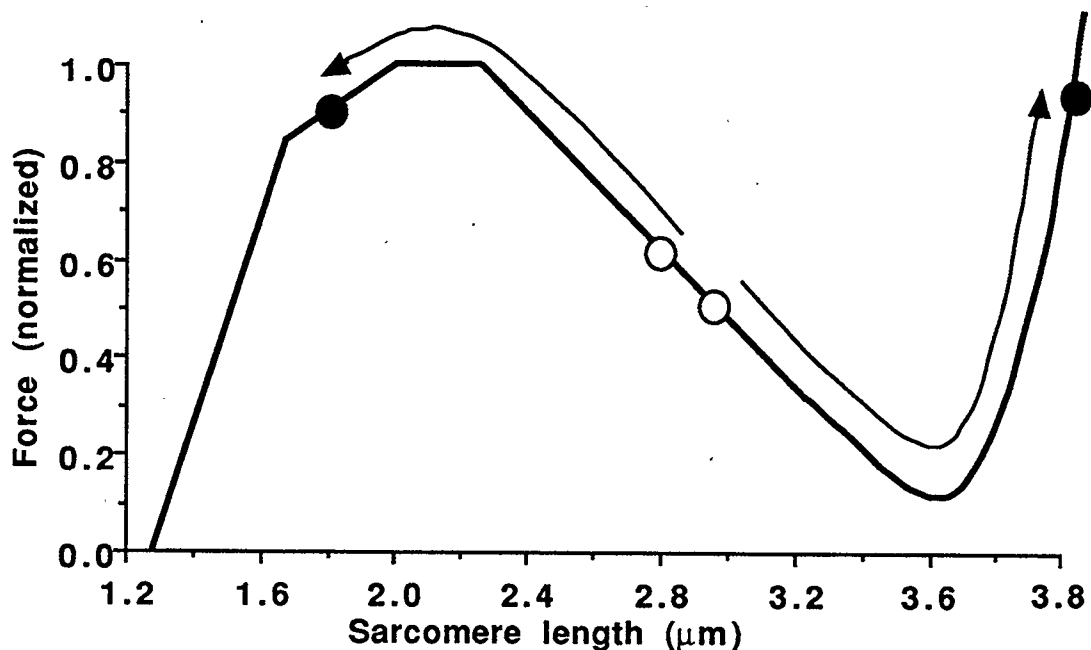


Figure 1.3. Total F-L relation for frog single fibers (Gordon et al., 1966b). Sarcomeres that begin on the descending limb (hollow circles) are unstable until they are on positively sloped regions (solid circles).

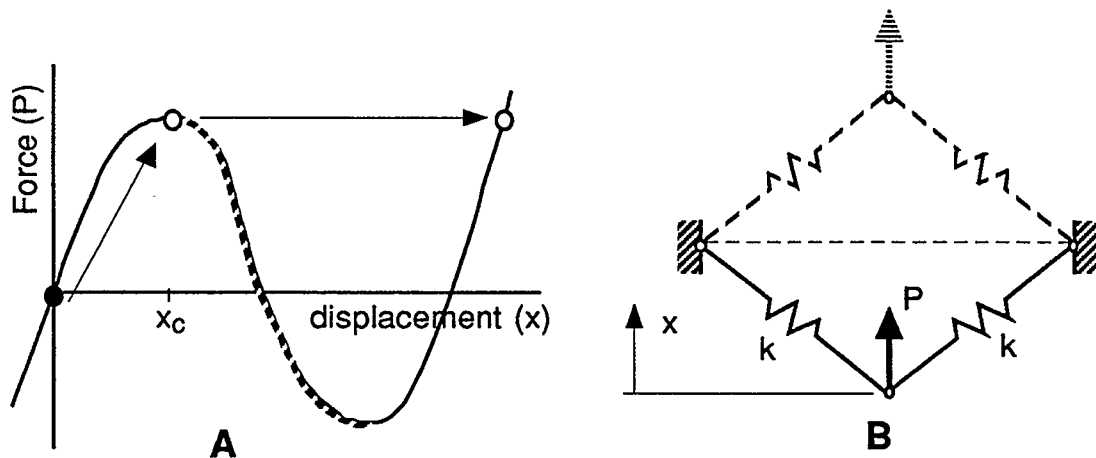


Figure 1.4. Force-displacement relation (A) that is unstable over a portion of the curve (negative slope, dashed line) for a structure (B) with two elastic beams of stiffness k .

If muscle fibers were unstable over a portion of their working range, many difficulties could arise during contraction. As mentioned, muscle fibers would pull themselves apart so that the force of sarcomeres located on the passive limb could no longer be actively controlled (Morgan, 1990). Muscle fibers have no apparent capabilities to control such highly stretched sarcomeres.

Unstable muscle fibers would also imply unstable joint moment-angle relationships. The moment-angle relationship describes the maximal, isometric moment a muscle produces as a function of the joint angle. Although the human neuromotor system has feed-back circuits to control muscle forces, nerve signals have not been identified that are responsible for controlling such an instability in a joint. As a result, erratic and uncontrollable joint motion would occur as a result of the unstable muscle properties.

It is possible that muscle fibers are stable over their entire working length. If the force-displacement curve of a sarcomere was identical to the descending limb of the F-L relation, sarcomeres would be unstable at these lengths. However, the F-L relation of a muscle can not be directly compared to the force-displacement relation of a structure. The force-displacement relation of a

structure is determined by small incremental displacements. In a stable structure, this relation has a positive slope (solid line portions of Figure 1.4A). The F-L relation in muscle is obtained by measuring the maximal, isometric force at different lengths and then connecting these points. So, the muscle does not undergo incremental length changes while stimulated during the F-L experiments. If sarcomere length is changed (or perturbed) during a contraction, the force output changes in a stable manner. For example, if a muscle fiber on the descending limb of the F-L relation is stretched and then held isometrically while stimulated, the final force is larger than the force before the stretch (Edman et al., 1982). The muscle fiber exhibits a force-displacement behavior with a positive slope, which is stable. It is my belief that the instability hypothesis is a misinterpretation of the properties of skeletal muscle on the descending limb of the F-L relation, and that muscle is inherently stable at these lengths.

Stability is defined to exist if a minimum of the potential energy function exists, which is derived from the force-displacement properties. A sarcomere with a positively sloped force-displacement curve is stable, and a sarcomere with a negatively sloped force-displacement curve is unstable. A stable sarcomere will eventually reach a steady-state (constant) length. Since no velocity terms are included in the potential energy functions, dampening (e.g., force-velocity) properties do not affect the evaluation of stability, but only affect the rate at which a steady-state will be reached.

The issues of stability presented in this dissertation are analyzed in terms of unforced, passive structures. F-L properties of sarcomeres are assumed to be represented by springs. The dynamic behavior of a sarcomere is analyzed as an unforced system. A sarcomere can be represented by a spring and damper in parallel, and a fiber represented as a number of these spring-damper elements in series (i.e., sarcomeres in series). When the sarcomere elements

begin a contraction at lengths that are not at equilibrium, the sarcomeres will change length until a steady-state length is reached in a stable system. Oscillations in spring-damper length will occur if the system is under-damped; one oscillation in spring-damper length will occur if the system is critically-damped; and an exponential change in the spring-damper length will occur if the system is over-damped. The behavior of sarcomeres under forced oscillations was not considered. Thus, the stability results are limited in terms of the dynamic behavior. Statements related to the stable behavior in muscle as determined experimentally, may be limited to the period of tetanus.

The supposed instabilities of the F-L relation have been thought to affect the F-L relation. Two different F-L relations have been determined from muscle fibers (Figure 1.5; Granzier and Pollack, 1990, their Figure 5; Pollack, 1990, his Figure 2.8). The “theoretical” F-L relation is based on the cross-bridge theory where a small number of consecutive sarcomeres is held isometric during the entire contraction. The “fixed-end” F-L relation is derived from an experiment

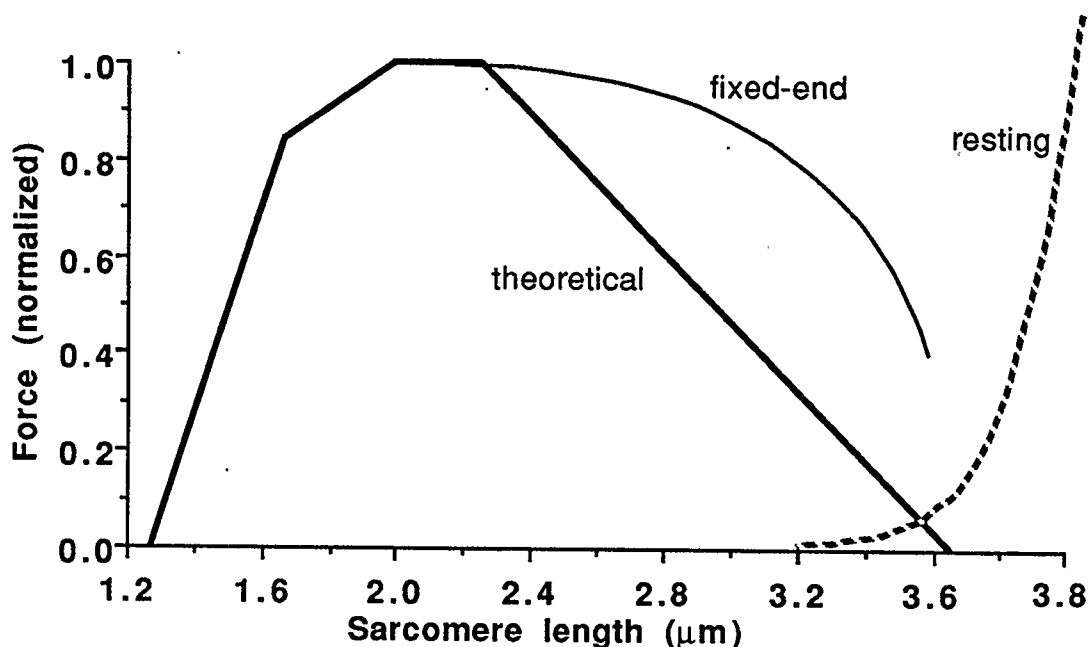


Figure 1.5. Fixed-end (thin line) and theoretical (thick line) F-L relations for frog single fibers (Gordon et al., 1966b).

where only the ends of a fiber are held fixed (constant muscle-tendon length) during contraction, and sarcomeres within the fiber may shorten or lengthen. It has been found in previous studies that the difference between the two F-L relations is caused by sarcomere stretching and the force-velocity properties (i.e, additional force changes caused by the speed of lengthening) of the stretching sarcomeres. However, if sarcomeres are in fact stable and a steady-state sarcomere length is reached, force-velocity properties can not explain the differences between the two curves.

The purposes of this dissertation are to:

- 1) identify the mechanical conditions for which sarcomeres in a muscle fiber are stable -- analytically;*
- 2) determine theoretically the fixed-end F-L relation of a muscle fiber when sarcomeres are at a stable, steady-state length;*
- 3) measure the nonuniformities in sarcomere length in mouse skeletal muscle and determine whether or not sarcomeres exhibit stable length behavior at lengths on the descending limb of the F-L relation during a fixed-end contraction;*
- 4) determine the theoretical and the fixed-end F-L relations in mouse skeletal muscle, and determine if the mechanical properties exist which can explain the differences between the two F-L relations exist.*

New and Notable

Several results that are new and notable should be emphasized. This study is the first to:

- 1) describe the sarcomere F-L properties necessary for a fiber to be stable (Chapter 4);

- 2) demonstrate how a sarcomere with stable mechanical properties can produce an apparently unstable F-L relation (Chapter 4);
- 3) show that the isometric properties of sarcomeres following lengthening or shortening (history dependence) can explain the differences in the theoretical and fixed-end F-L relations -- analytically (Chapter 5);
- 4) use the mouse serratus anterior muscle experimentally, which has no apparent series elasticity (i.e., no visible tendon), has bony attachments, and requires minimal dissection (Chapters 2, 6, and 7);
- 5) show that the sarcomeres exhibit a stable length-time behavior, using data from mouse serratus anterior muscle and data from other investigations found in the literature; (Chapter 6);
- 6) determine the force-sarcomere length relation (using laser diffraction) for mouse skeletal muscle during fixed-end tetani (Chapter 7);
- 7) demonstrate that sarcomeres in the mouse serratus anterior muscle possess the history dependent properties that can explain the differences between the theoretical and the fixed-end F-L relations.

Overview of thesis

The dissertation continues with a review of relevant literature (Chapter 2), aimed at providing a historical background of the research related to stability and the F-L relation in skeletal muscle. The section on the muscle preparation and experimental setup (Chapter 3) details the choice of the muscle used in the experimental work, the dissection of the muscle preparation, and the experimental apparatus developed for the studies. Chapters 4 to 7 address each of the four purposes of this dissertation in the order stated previously, and were written so each chapter could stand alone as a journal manuscript. A summary (Chapter 8) concludes the dissertation.

Chapter 2

Review of Relevant Literature

Sarcomere stability, nonuniformity, and the F-L relation

A chronological review of the relevant literature is presented here to understand the history behind the issues of sarcomere stability, nonuniform changes in sarcomere length, and the F-L relation of skeletal muscle. In a nutshell, past researchers thought that unstable sarcomeres caused nonuniform length changes in a fixed-end fiber, and these nonuniformities resulted in differences between the theoretical and the fixed-end F-L relations.

A.V. Hill (1953) coined the idea that muscle is unstable on the descending limb of the F-L relation. He noticed that the force-time curves exhibit a “creep” phase during a fixed-end contraction on the descending limb in toad and frog sartorius muscle (at lengths greater than optimum, L_0). Creep refers to the slow rise component of the force-time curve. Fixed-end contractions near optimal muscle length (curve at L_0 , Figure 2.1A) had little creep, while contractions at longer lengths exhibited creep (curve above L_0 , Figure 2.1A). Hill (1953) presumed that this creep was associated with nonuniform changes in length in different regions of the muscle (i.e., some segments of the muscle shorten while others lengthen), even though no measurements of length changes in small regions of the muscle were made. It was shown earlier by Fischer (1926) that some regions of this muscle shorten while others are

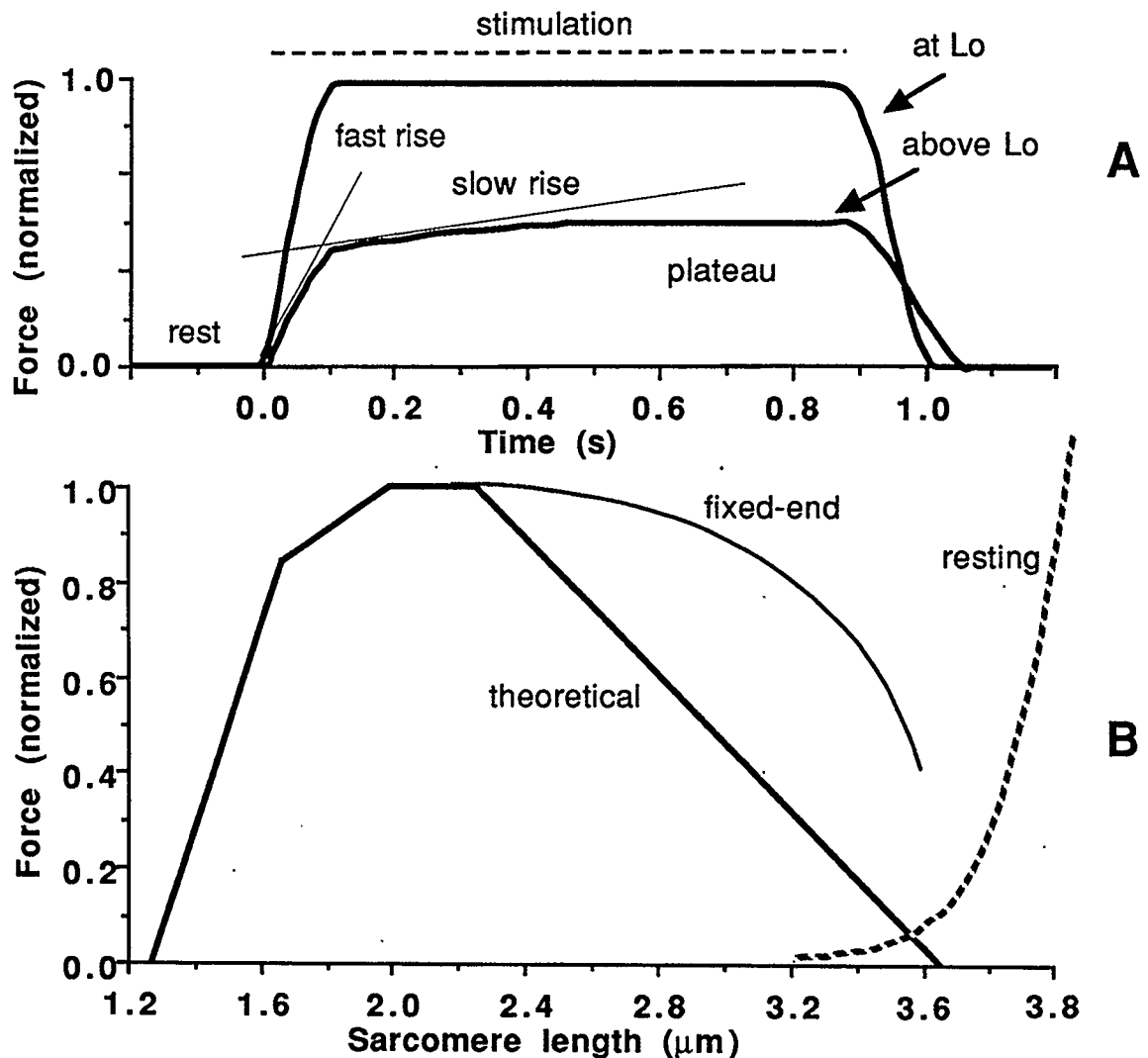


Figure 2.1. Fixed-end (thin line) and theoretical (thick line) F-L relations for frog single fibers (Gordon et al., 1966b) (A). Schematic of force-time traces during a fixed-end contraction at two different muscle lengths (B).

stretched during a fixed-end tetanus.

Instability was presumed to occur because of the negative slope of the descending limb of the F-L relation (Hill, 1953). According to Hill, at muscle lengths greater than optimum, a short (strong) region would shorten and stretch a weak (long) region of the muscle (Figure 1.3). Thus, tension creep only occurs at lengths greater than optimum where the muscle is unstable. During contraction, this force creep continues until a stable equilibrium occurs (i.e., until

one region of the muscle is on the ascending limb and another region on the resting limb of the F-L relation (solid circles, Figure 1.3). Tension creep did not occur at lengths less than or equal to optimum, because the muscle is stable and nonuniform length changes within the muscle did not occur. On the ascending limb of the F-L relation, the muscle is said to be stable since a steady tension is reached without creep.

Relevant studies from 1953 on, concentrated on determining muscle properties using single fibers. The following studies all used single fibers of frog muscle at temperatures close to zero °C. These low temperatures slow the chemical processes of contraction to allow for a detailed analysis of the results.

The “sliding filament theory” was developed to explain how length changes occurred in striated muscle (Huxley, 1953; Huxley and Hanson, 1954; Huxley and Niedergerke, 1954), around the time the instability concept was introduced. The sliding filament theory assumes that thick and thin myofilaments are constant in length and that these myofilaments slide past one another during changes in muscle length. Although this theory could explain how changes in muscle length occur, the mechanism causing force development was unknown.

A.F. Huxley (1957) proposed a hypothesis for the mechanism of force production which was quickly adopted as the “cross-bridge theory” of muscle contraction. This theory added an explanation for how the thick and thin myofilaments interacted to produce the forces of contraction. The cross-bridge theory assumes that force is produced by cyclic interactions of extensions from the thick to the thin myofilament. Since these extensions or cross-bridges are assumed to be independent of each other, have no time-dependent properties, and produce equal average forces, force production in a sarcomere is

proportional to the number of attached cross-bridges. Since cross-bridges are assumed to be arranged uniformly along the thick myofilaments, the number of cross-bridges that can interact with the thin filaments is proportional to the amount of thick-thin myofilament overlap. The cross-bridge theory closely predicted the experimental findings of heat production, and force during concentric contractions reported by A.V. Hill (1938).

Although the sliding filament and cross-bridge theories were developed based on myofilament lengths measured using electron microscopy and x-ray diffraction, no F-L data from isometric contractions clearly verified these theories. Huxley and Peachey (1961) reported that the maximum sarcomere length where active force could be developed corresponded to a length where no thick-thin myofilament overlap occurred. They did find that force was developed at lengths longer than thick-thin myofilament overlap; however, they attributed this force to the slow component of the force rise (creep phase). Their measurements of different segments along the length of a fiber (using markers attached to the fiber surface) demonstrated that the ends of the fiber were shortening while the central segments were lengthening during the creep phase of a fixed-end contraction. Huxley and Peachey (1961) concluded that no force was developed by sarcomeres which remain isometric, but that sarcomeres which were stretching produced the passive forces that were measured. The slow rise in force (creep) was attributed to instability of sarcomeres on the descending limb of the F-L relation (Hill, 1953).

Because sarcomeres within a fiber change length during a fixed-end contraction, the "true" isometric force of a sarcomere had not been measured. Gordon et al. (1966a) developed a servo device to hold a group of consecutive sarcomeres at constant length during a tetanus. Surface markers were attached to a central region of a fiber to denote a segment (6 -11 mm long). During a

tetanus, the distance between the markers was kept constant by changing the fiber length. This method (known as “segment clamping”) keeps a small number of consecutive sarcomeres at a constant length, and it reduced or eliminated the force creep. F-L measurements using this system (Gordon et al., 1966b) corresponded closely to the sliding filament and cross-bridge theories.

Even with the segment clamping method, tension creep was exhibited at sarcomere lengths on the descending limb of the F-L relation (Gordon et al., 1966b). The reason suggested for this creep was that sarcomeres located between the markers did not remain at uniform lengths during the contraction. Thus, an “extrapolation” technique was used to determine the force developed by sarcomeres before any nonuniformities would develop between the markers. In the extrapolation technique, a straight line is fit to the fast rise and another straight line to the slow rise phases of the force-time trace (Figure 2.1A). The intersection of these two lines determines the time when force and sarcomere length are used for the F-L plots. Gordon et al. (1966b) thought that force creep still existed in their experiments because of nonuniform changes in sarcomere length between the segment markers as a result of instability, although no direct evidence was reported.

Using surface markers is one technique for determining the average sarcomere length in a small region of a fiber and laser diffraction is another. In laser diffraction, a laser beam is directed perpendicular to the long axis of a fiber. The differing refractive indices caused by the thick (anisotropic band) and thin filaments (isotropic band) form an interference pattern from the transmitted light. This interference pattern formed by the dark and light bands in a fiber is similar to what occurs when a laser is transmitted through a grating. This so called “diffraction pattern” exhibits a zero-order (nondiffracted beam), first-order, and higher order intensity peaks. The angle formed between the zero and first-

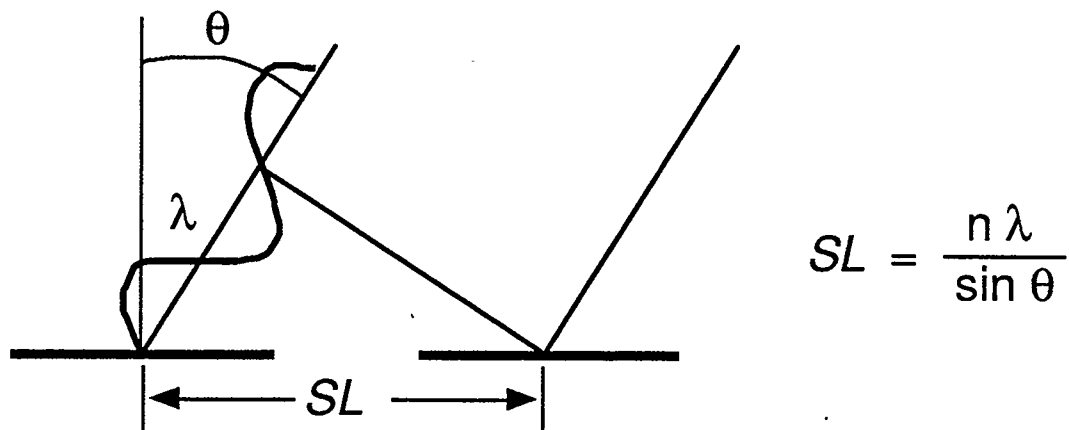


Figure 2.2. Illustration of the amount a monochromatic beam of light will diffract after transmission through a grating or muscle. SL - sarcomere length, λ - wavelength of light, n number of diffraction order, θ - angle of diffracted beam.

order diffraction patterns is proportional to the sarcomere length (Figure 2.2). A uniform sarcomere spacing within the illuminated beam will produce a narrow, high intensity first-order diffraction pattern while a nonuniform sarcomere spacing will produce a wide, low intensity first-order diffraction pattern. Thus, the width of the diffraction pattern is a measure of sarcomere length uniformity within the illuminating beam.

Cleworth and Edman (1972) used the laser diffraction technique to determine if nonuniform changes in sarcomere length occur in a group of consecutive sarcomeres. They observed that the width of the first-order laser diffraction line remained constant during the plateau of a fixed-end tetanus. Thus, Cleworth and Edman (1972) did not verify that the tension creep observed by Gordon et al. (1966b) was a result of nonuniform changes in sarcomere length in the test region of the fiber. These data indicate that sarcomeres during a fixed-end contraction are isometric and reach a steady-state length (stable behavior).

Other researchers argued that the true isometric force of a sarcomere is the force reached during the plateau of the tetanus and not the force reached at

the extrapolation point (Figure 2.1A). ter Keurs et al. (1978b) selectively chose fibers that were uniform in sarcomere length ($< 0.2 \mu\text{m}$ peak-to-peak variation along the length of the fiber). During fixed-end tetani, force creep was still evident even though sarcomere length appeared to remain constant. They argued that the sarcomeres in their fibers were isometric throughout the contraction; and thus, represented the true F-L relation of sarcomeres. Their fixed-end F-L relation exhibited an extended plateau and forces on the descending limb that were larger than those of the extrapolated F-L relation at corresponding sarcomere lengths (Figure 2.1B). Although sarcomeres were uniform along the length of the fibers, sarcomere length did not remain constant from rest to the plateau (sarcomere length increased by less than 4% or about $0.1 \mu\text{m}$). These small changes in sarcomere length during a fixed-end contraction could be related to the observed force creep and other investigations demonstrated this possibility.

Julian and Morgan (1979a) measured the length of central segments of a fiber using surface markers and the end regions using light microscopy during fixed-end contractions. They determined that the central region of a fiber lengthens and the end regions of a fiber shortens during tetani. The lengthening segments were stretched most rapidly during the slow rise phase of the force-time curve, but the lengthening continued throughout the tetanus at a slower rate. They concluded that this behavior represented a damped instability. Similar findings and conclusions were later reported by Lieber and Baskin (1983) using laser diffraction. Again, data were presented that supported the idea that sarcomere length changes during fixed-end tetani were the cause of creep and the cause for the differences between the fixed-end and the theoretical force-length relations.

Theoretical research indicated that even small changes in sarcomere length (like those of ter Keurs et al., 1978a) could result in force creep. Morgan et al. (1982) used a quantitative model of intersarcomere dynamics during fixed-end contractions that used the theoretical F-L relation (Gordon et al., 1966b), which is unstable on the descending limb of the F-L relation. Morgan et al. (1982) found that even a fiber with very uniform sarcomere length will produce a slow rise in force without compromising the peak tension reached. A limitation of their model is that adjacent sarcomeres can not act independently. Morgan's model forced a short sarcomere to shorten its neighbors, and a long sarcomere to lengthen its neighbors. This constraint was necessary to prevent gross nonuniformities in adjacent sarcomeres which are known to not occur (Cleworth and Edman, 1972; Tameyasu et al., 1982). However, this constraint on adjacent sarcomeres contradicts the experimental findings that adjacent sarcomeres act independently in isolated fibers (Huxley, 1957, their Figure 4).

Tameyasu et al. (1982) found that sarcomere length nonuniformities were not large in a group of consecutive sarcomeres, using a more detailed analysis than Cleworth and Edman (1972). They analyzed the microstructure of the first-order laser diffraction line from resting and tetanically stimulated fibers. They found no rapid fluctuations, nor slow shortening or lengthening of sarcomere length during the plateau of a fixed-end tetanus. Differences in sarcomere length within the laser beam were between $0.010\ \mu\text{m}$ and $0.130\ \mu\text{m}$ during the plateau of the tetanus. During the tension of a 2-3 s tetanus for a fixed-end contraction, sarcomeres reached a steady-state length. More data supported the idea that sarcomeres in a small region of a fiber exhibit stable properties. If sarcomeres were unstable and independent, adjacent sarcomeres should develop length differences larger than $1.6\ \mu\text{m}$ (Figure 1.3).

Edman and Reggiani (1984) further investigated the changes in sarcomere length along the length of a fiber during a fixed-end contraction. They used surface markers to record length changes in successive segments (0.5 - 0.8 mm long) on a fiber which underwent fixed-end tetani. These segments changed length rapidly during the steep rise of force; and subsequently, the segments changed length slowly for the remainder of the contraction. Generally, the central segments (central 90% of fiber) elongated while the end segments (5% on each end of fiber) shortened during the slow rise of force, which confirmed the results of earlier studies (Huxley and Peachey, 1961; Julian and Morgan, 1979a; Lieber and Baskin, 1983). Edman and Reggiani (1984) also found that adjacent segments in the central region of the fiber do not all follow the same behavior. Some central segments shortened ($< 0.10 \mu\text{m}$) while others lengthened ($< 0.07 \mu\text{m}$) during the fast rise of force. Some segments subsequently shortened ($< 0.06 \mu\text{m}$) while others lengthened ($< 0.06 \mu\text{m}$) during the slow rise and plateau of force. There was no apparent correlation between the sarcomere length changes that occurred between the fast rise phase and the slow rise-plateau phase of force production.

After the work of ter Keurs et al. (1978), several studies verified that the forces produced by isometrically contracting sarcomeres are close to the theoretical F-L relation proposed by Gordon et al. (1966b). Better servo (feedback) controlled systems, and smaller segments (fewer sarcomeres in the test region) were used to measure the F-L relation with segment clamping techniques (Julian et al., 1978; Edman and Reggiani, 1987; Bagni et al., 1988; Granzier and Pollack, 1990) and laser diffraction systems (Granzier and Pollack, 1990).

Granzier and Pollack (1990) reinvestigated the reasons for the differences between the theoretical and fixed-end F-L relations. They used laser

diffraction and segment length measurement methods simultaneously to measure sarcomere length in the central region of the preparations during tetanus. They performed fixed-end and sarcomere length-clamped contractions on the same fibers. Results from their study demonstrated that at the end of the tetanus, sarcomeres were lengthening (60 nm/s on average). They found that active and passive force increases associated with sarcomere lengthening during the plateau could account for the difference between the theoretical and fixed-end F-L relations.

Sarcomere length-time traces from many investigators exhibited a decreasing stretch velocity during the fixed-end contractions (Huxley and Peachey, 1961; Julian and Morgan, 1979a; Edman and Reggiani, 1984; Granzier and Pollack, 1990). If the velocity of these lengthening sarcomeres continued to decrease, sarcomere length would become constant, as other studies have shown (Cleworth and Edman, 1972; Haskell and Carlson, 1981; Tameyasu et al., 1982). At this point in time, force-velocity properties could not explain the differences in the F-L relations, because sarcomeres would be isometric. Thus, a change in the isometric F-L properties of sarcomeres from the theoretical F-L relation (Gordon et al., 1966b) would be necessary to explain the difference between the theoretical and the fixed-end F-L relations. Such a change in F-L properties as a function of the contractile history has been found in sarcomeres.

History dependent sarcomere properties

It is known that the history of contraction affects the current force response (e.g. Abbot and Aubert, 1952). Although the cross-bridge theory does not contain history-dependent conditions (Huxley, 1957), many studies have

shown that the isometric force produced by sarcomeres depends on the changes in sarcomere length preceding the isometric state. These history-dependent properties may be critical in explaining the differences between the theoretical and the fixed-end F-L relations since sarcomeres change their lengths during a fixed-end contraction.

The isometric force of a muscle preparation after a stretch is typically larger than the isometric force predicted theoretically on the descending limb of the F-L relation. This result has been found using whole muscle (Abbott and Aubert, 1952; D  l  ze, 1961) and isolated fibers (Hill, 1977; Edman et al., 1978; Edman et al., 1982; Sugi and Tsuchiya, 1988).

Contradictory evidence exists on what the isometric force is after sarcomere shortening. Horowitz et al. (1992) reported that the isometric force was greater than what would be predicted by the theoretical F-L relation after small sarcomere shortenings ($0.02 - 0.16 \mu\text{m}$ / sarcomere) on the descending limb of the F-L relation. Edman et al. (1993) found that after sarcomeres shorten (0.25 and $0.33 \mu\text{m}$ / sarcomere) onto the plateau of the theoretical F-L relation, the isometric force is maximal. Other researchers have demonstrated a decrease in isometric force below the theoretical F-L relation after sarcomere shortening (Abbott and Aubert, 1952; D  l  ze, 1961; Julian and Morgan, 1979b; Mar  chal and Plaghki, 1979; Edman, 1980; Sugi and Tsuchiya, 1988; Granzier and Pollack, 1989).

The altered force output of a sarcomere *while* it shortens or lengthens during stimulation is referred to as the force-velocity property (Hill, 1938). The force-velocity property is often represented as a nonlinear damper which is in parallel to the isometric F-L properties of the fiber (Hill, 1938). During a stretch, the force produced by a sarcomere increases rapidly to about 1.6x the isometric force at the corresponding length (Katz, 1939). During sarcomere shortening,

the force produced is less than the corresponding isometric force (Hill, 1938).

Summary of relevant literature

Nonuniform changes in sarcomere length (i.e., some sarcomeres shorten while others lengthen) appear to be responsible for the fast rise and slow rise phases of the force-time traces for fixed-end tetani ¹. Generally, it is believed that changes in sarcomere length are caused by the apparent instability of sarcomere length on the descending limb of the F-L relation ². However, others have stated that the descending limb of the F-L relation may be stable ³. A number of studies have demonstrated that sarcomeres achieve a steady-state length during fixed-end tetani ⁴, which indicates a stable behavior.

The "true" F-L relation for an isometric sarcomere produces a different curve than the F-L relation measured with the ends of a fiber fixed ⁵. These differences in the theoretical and the fixed-end F-L relations are a result of the nonuniform changes in sarcomere length during fixed-end tetani. However, when the sarcomeres reach a steady-state length during the fixed-end tetani ⁴, the theoretical and the fixed-end F-L curves should coincide, but they do not. Thus, the isometric properties of sarcomeres must change as a function of the previous length changes to explain the differences between the theoretical and the fixed-end F-L curves; such history dependent properties exist ⁶.

Footnotes to summary of relevant literature

- 1 Hill, 1953; Huxley and Peachey, 1961; Gordon et al., 1966; Julian et al., 1978; Julian and Morgan, 1979a; Morgan et al., 1982; Lieber and Baskin, 1983; Edman and Reggiani, 1984; Sugi and Tsuchiya, 1988; Granzier and Pollack, 1990.
- 2 Hill, 1953; Huxley and Peachey, 1961; Gordon et al., 1966; Julian et al., 1978; Julian and Morgan, 1979a; Morgan et al., 1982; Lieber and Baskin, 1983; Edman and Reggiani, 1984; Morgan, 1990.
- 3 D  l  ze, 1961; Hill, L., 1977; ter Keurs et al., 1978; Pollack, 1983; Pollack, 1990.
- 4 Cleworth and Edman, 1972; Paolini and Roos, 1975; Hill, 1977; Fabiato and Fabiato, 1978; Iwazumi, 1978; ter Keurs et al., 1978a,b; Haskell and Carlson, 1981; Tameyasu et al., 1982.
- 5 Granzier and Pollack, 1990, their Figure 5; Pollack, 1990, his Figure 2.8.
- 6 Hill, 1950; Hill 1951; Abbott and Aubert, 1952; D  l  ze, 1961; Hill, 1977; Julian and Morgan, 1979b; Mar  chal and Plaghki, 1979; Edman et al., 1978; Edman, 1980; Edman et al., 1982; Sugi and Tsuchiya, 1988; Granzier and Pollack, 1989; Horowitz et al., 1992; Edman et al., 1993.

Chapter 3

The Muscle Preparation and Experimental Setup

This chapter details the selection of the muscle preparation, the dissection procedure, and the setup used for the experimental work. Also included in this chapter are the results of attempts at using sarcomere clamping and making segment length measurements.

Choice of muscle preparation

It was decided that mammalian muscle would be used in the experimental work, since little data regarding sarcomere length behavior was available from mammals. As seen in the review of relevant literature (Chapter 2), many investigations have used amphibian muscle preparations. Only a few studies have measured sarcomere length in mammalian muscle (fiber bundles from the rat extensor digitorum longus, ter Keurs et al., 1984; omohyoideus muscle from mouse, Phillips and Woledge, 1992). Amphibian muscle is often chosen rather than mammalian muscle because it is easier to remove a viable single fiber from amphibian muscle.

A whole muscle instead of a single fiber preparation was chosen for these experimental studies in order to determine sarcomere behavior in an undisturbed setting, or as unaltered as possible. Although it may be more appropriate to use single fibers to isolate sarcomere properties, sarcomeres may not behave the same properties in a single fiber as they have in a whole

muscle. Extensive and delicate dissection practices are required to extract a viable single fiber from a muscle. The mechanical properties of the fiber may be altered during these teasing and cutting procedures. Also, sarcomeres in a single fiber may not behave the same as in the intact muscle because of the interaction of adjacent fibers in a muscle. In a muscle, adjacent fibers (parallel to each other) are attached by connective tissues (Totter, 1990; Totter and Purslow, 1992) and the mechanics of a selected fiber may be altered by those fibers connected to it.

The criteria for selecting a muscle preparation were as follows:

- 1) mammalian;
- 2) whole muscle;
- 3) thin enough for sarcomere length measurements with laser diffraction;
- 4) fusiform -- fibers aligned parallel to the direction of pull;
- 5) rigid attachments to experimental apparatus;
- 6) little tendon, to reduce effects of series elasticity;
- 7) minimal dissection, so preparation is not altered from *in vivo*.

The mouse was chosen as the species because it was a mammal, readily available, and was most likely to have muscles small enough to use for laser diffraction. Many potential mouse muscles were examined in the experimental apparatus based on the above criteria (Table 3.1).

The distal head of the serratus anterior muscle was chosen as the preparation for experimentation. This head of the muscle has fibers that originate from the vertebral border (distal end) of the scapula and insert into rib 7. Minimal dissection was required to separate this head of the muscle from other musculature. In the serratus anterior muscle, the head attached to rib 6 is connected to the edge of the distal head along only about half of the distal head's length. The other sides of the distal head are free from other muscle

Table 3.1. Muscles examined and ranked for testing (best to worst).

Muscle	Comments
distal head of serratus anterior	chosen muscle
clavotrapezius	
sternothyroideus	small bony attachments
sternohyoideus	small bony attachments
flex. hallucis longus	weak attachment (origin, interosseous membrane)
ext. hallucis longus	weak attachment (origin, interosseous membrane)
omohyoideus	weak diffraction signal
epitrochlearis	muscle attaches to tendon of latissimus dorsi
rectus (eye)	weak tissue attachments (eye ball)
superior oblique (eye)	weak tissue attachments (eye ball)
inferior oblique (eye)	weak tissue attachments (eye ball)
levator auris longus (ear)	weak diffraction signal
lumbrical (rear foot)	unipennate muscle
levator claviculae	difficult attachment sites (origin at spine)
tail muscles	difficult attachment sites (origin at spine)
one head of ext. digitorum longus	diffraction signal at edge of muscle only
gracilis anticus	too thick for good diffraction signal
brachioradialis	diffraction signal at edge of muscle only
palmaris longus	diffraction signal at edge of muscle only
soleus	too thick for good diffraction signal
biceps femoris (lateral head)	too thick for good diffraction signal

attachments. After dissection, the distal head of the serratus anterior muscle is a flat band of fibers about 10.9 ± 1.1 mm long (scapula to rib 7), 0.7 ± 0.2 mm wide, and 0.3 ± 0.1 mm thick at resting length. There is no visible tendon between the muscle fibers and the bony attachments. Fibers of approximately the same length enter the bone surfaces at a slightly oblique angle of about 120 degrees on both the scapula and rib. Because the preparation is left virtually intact, this preparation is considered to be a whole muscle.

Dissection of muscle preparation

It takes between 1 and 2 hours to dissect the muscle from the mouse and attach it into the experimental apparatus. Use mice of about 2 weeks old (14.9 ± 4.0 g, mean \pm S.D., $n = 15$). Weigh a mouse and anaesthetize it with an

interperitoneal injection of sodium pentobarbital ($2 \mu\text{l/g}$). After the animal is sedated, pin it through the feet and hands to a dissection board. Use scissors to cut a slit in the skin of the abdomen. Separate the skin from the underlying tissue by inserting the closed tips of the scissors and then expanding the tips in the desired locations. Separate and remove the skin from the entire thorax.

The blood in the muscle is then replaced by a physiological solution so the blood will not scatter light during the laser diffraction measurements. Cut and retract the abdominal muscles at their attachments to the ribs. After cutting the sternum along the long axis of the body retract the rib cage to expose the beating heart. Insert a needle into the left ventricle and allow the physiological solution to flow into the heart. Cut a small slit into the right ventricle and absorb the ejected blood with swabs. Once the heart is pumping the clear physiological solution out of the hole in the right ventricle, the thorax is isolated. Separate the thorax from the rest of the animal at the neck (spine), below the last rib (spine), and at both shoulder joints. Place the thorax immediately in a dissection bath.

The dissection bath consisted of a plastic cylinder with a glass and rubber bottom. The glass bottom allowed the preparation to be back lit and the rubber held dissection pins that were used to anchor the preparation during dissection. Physiological solution was continuously refreshed by drip through one port in the plastic cylinder and then extracted by a peristaltic pump through another port in the bath. Back light conditions were provided by a circular fluorescent tube under the bath with a black background in the middle of the light. These back light conditions were used during the final stages of dissection.

While the muscle and bony attachments were being removed from the thorax, the preparation was lit from the side. The distal head of the serratus anterior muscle was difficult to delineate from the other muscles on the thorax

unless a light beam was placed perpendicular to the line of sight and in the plane of the muscle. This placement of the light throws a shadow on the fibers and makes dissection procedures easier. Direct light, parallel to the line of sight, makes the muscle appear clear and invisible. The remainder of the dissection is done while viewing the specimen through a binocular dissection microscope (10X).

Position the thorax in the bath to expose the lateral-dorsal side. Several heads of the serratus anterior are visible as they enter the ribs, past the distal edge of the latissimus dorsi muscle (Figure 3.1). Remove excess back muscles (spinotrapezius and acromiotrapezius) by cutting their distal insertions at the spine of the scapula and their origins at the spines of the vertebrae. Similarly,

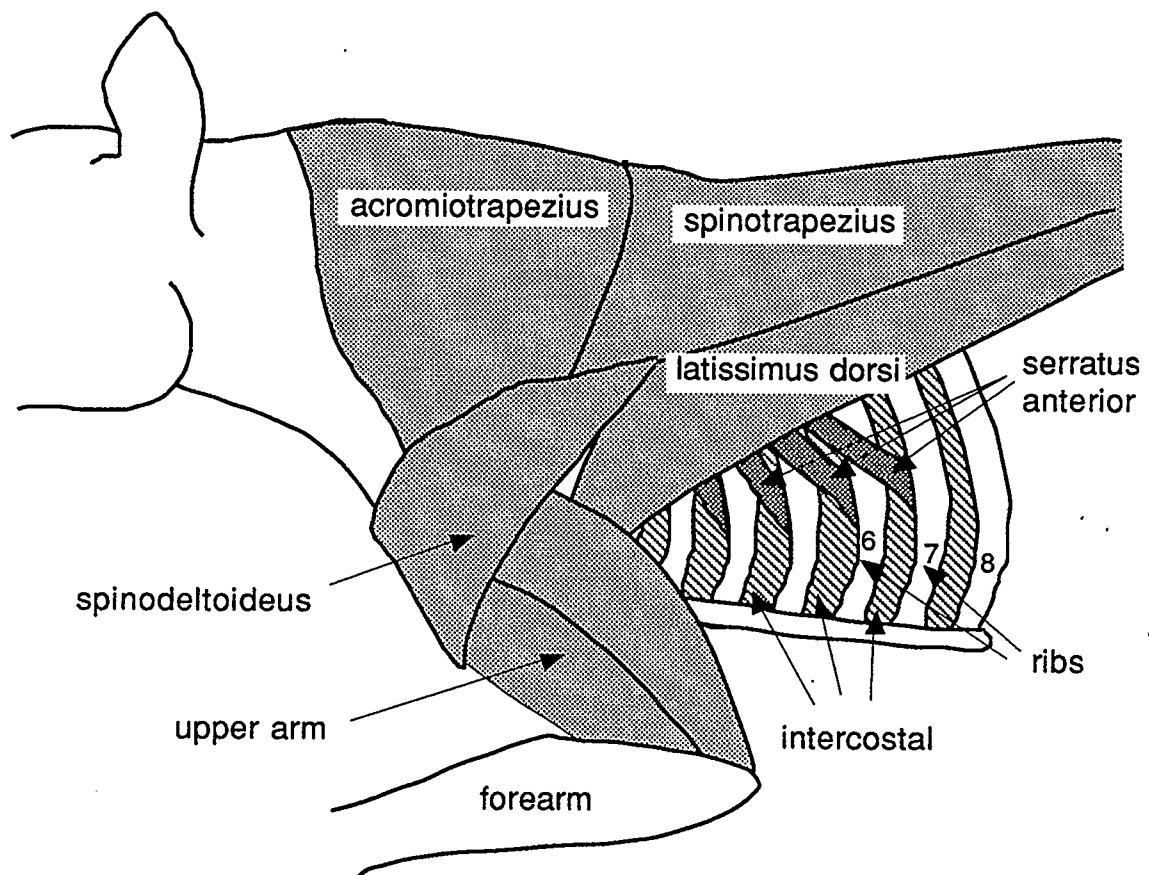


Figure 3.1. Superficial muscles of the thorax. Lateral view with skin and cutaneous maximus muscle removed.

remove latissimus dorsi by cutting its origin at the spines of the vertebrae and the distal tendon as it enters the axilla. Separate spinodeltoideus from the scapula and the humerus.

Many heads of the serratus anterior muscle are now visible when the thorax is positioned for a lateral view (Figure 3.2). Identify the insertion of the distal head of the serratus anterior into rib 7. Carefully, cut the intercostal muscles on either side of rib 7 for 5 mm on either side of the muscle insertion. Cut rib 7 so that 1 cm of bone remains with the muscle in the center of the bone piece. Carefully, retract the rib piece superiorly toward the scapula while cutting any connective tissue attaching the muscle to the thorax. Where the head of the serratus anterior from rib 7 attaches to the head from rib 6, stop. Cut all

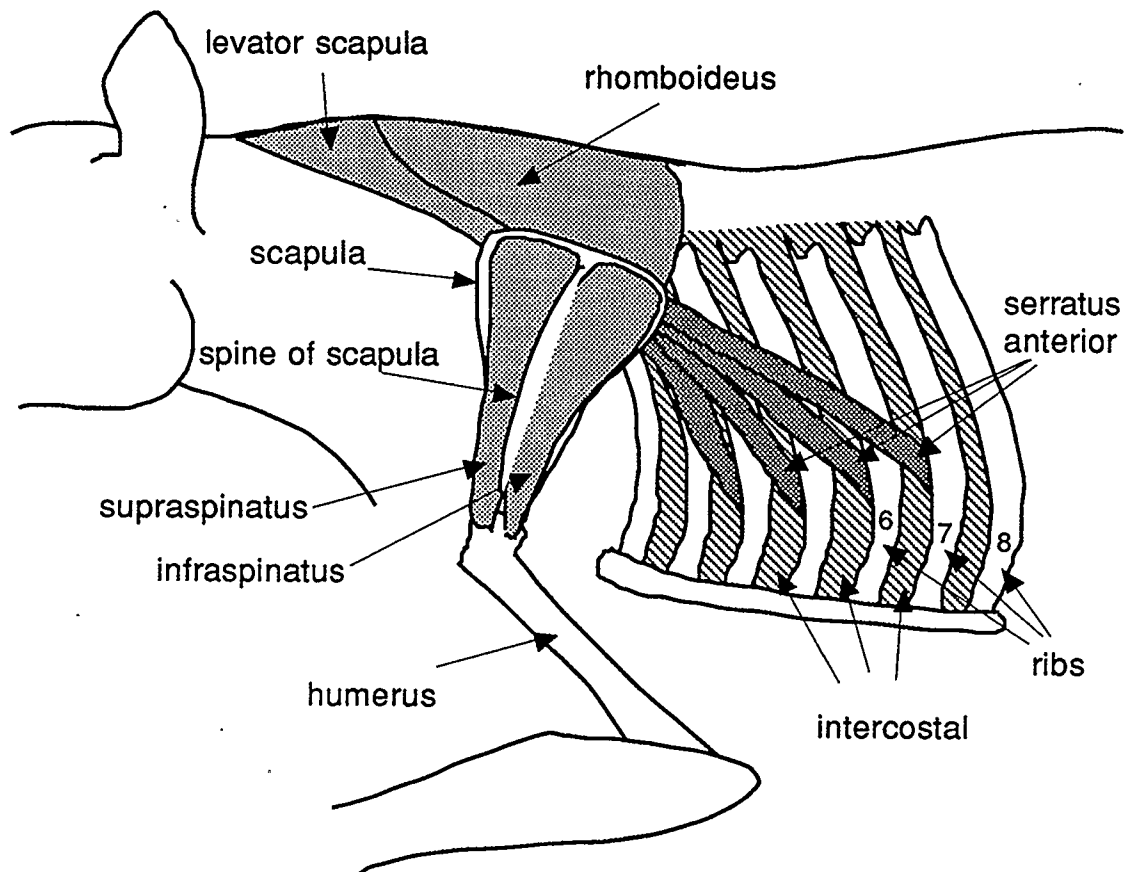


Figure 3.2. Deeper muscles of the thorax. Lateral view with acromiotrapezius, spinotrapezius, latissimusdorsi, spinodeltoideus, and upper arm muscles removed.

remaining heads of the serratus anterior between the origin and insertion. Cut all muscle connecting the scapula to the thorax (rhomboides and levator scapulae). Separate the humerus and scapula by cutting through the joint and through any musculature (infraspinatus, supraspinatus, subscapularis, teres major and teres minor). Now the scapula, distal head of serratus anterior, and the rib should be free from the thorax for further dissection over the back light area of the dissection bath.

Excess muscles need to be removed from the bones and the distal head of the serratus anterior muscle (Figure 3.3). Remove all extra muscles on the scapula (subscapularis, teres major, teres minor, supraspinatus, infraspinatus) by scraping the bone plate. Cut any muscle close to the origin of the serratus anterior muscle (vertebral border of the scapula), because the serratus anterior attachment to the scapula can inadvertently be scraped off.

Remove the 6th head from the 7th head of the serratus anterior muscle. Anchor the rib (through an end of the rib piece) and scapula (through the bone near the shoulder socket) using dissection pins stuck into rubber base of the dissection dish. With forceps, gently pull the 6th head away from the 7th head

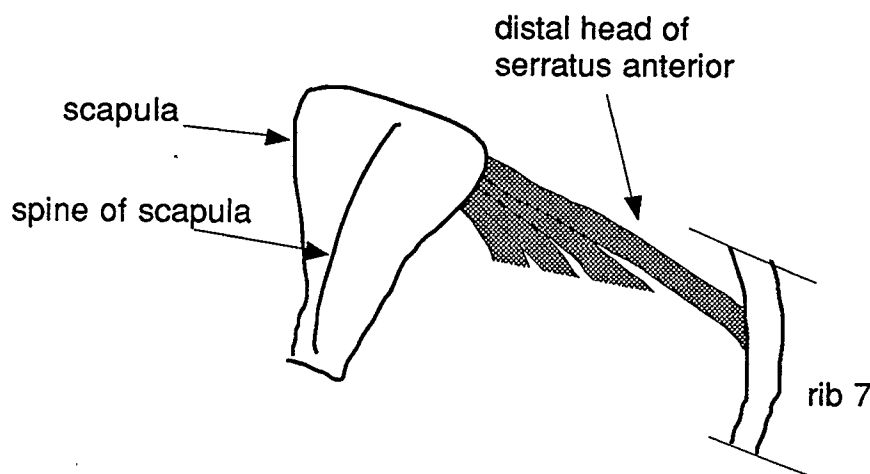


Figure 3.3. Muscle preparation after extraction from thorax and with muscles on scapula removed (infraspinatus, supraspinatus, subscapularis).

and cut the connective tissue attaching the two with scissors. The division between the two heads is very evident. Connective tissue attaches the dorsal and ventral sides of the zone separating the heads. The muscle will twitch when the nerve is cut, about 1/3 of the muscle length from the scapula (blood supply enters at the same location as the nerve). Continue separating the 6th and 7th heads up to the scapula. Then cut and remove the 6th and other heads of the serratus anterior muscle not required, as close to the scapula as possible. Remove any excess connective tissue around the muscle belly. Clear any fragments of the intercostal muscles left attached to the rib. Be careful not to cut too close to the serratus anterior muscle; its attachment to the rib can be damaged. If some of the serratus anterior muscle is accidentally cut, the muscle will twitch.

The muscle should now be isolated so the bones can be trimmed to fit in the experimental bath (Figure 3.4). Cut the rib so that 1 - 2 mm remain on either side of the muscle. Cut a square piece out of the scapula about 3 mm wide (across muscle attachment) and 5 mm long. Cut a hole in the scapula for mounting onto the motor arm. The hole in the scapula should not be larger than

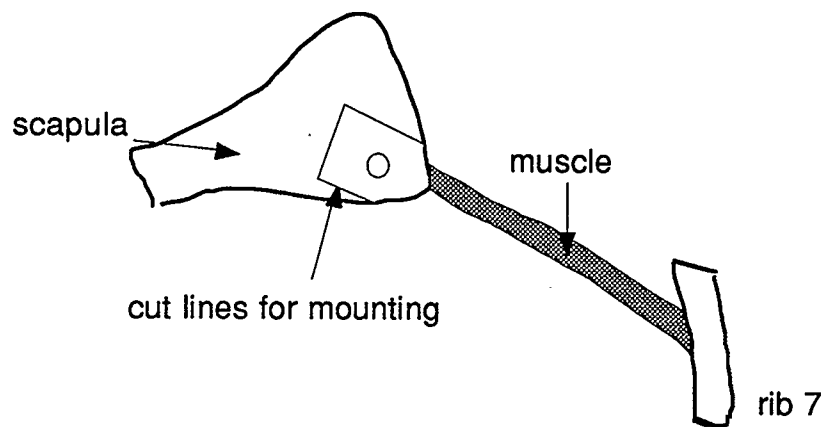


Figure 3.4. Top view of muscle preparation (distal head of serratus anterior) with all extra muscles removed. Scapula is reflected so anterior side (subscapularis origin) is visible.

the pin attached to the motor. Do not pierce the scapula with a pin because the scapula may split. The hole in the scapula should be 2 - 3 mm from the muscle insertion to avoid damaging the insertion site.

The preparation is now ready to be mounted in the experimental bath (Figure 3.5). Adjust the motor arm to its shortest position. Turn the bathing solution supply off so fluid remains in the experimental bath, but is not flowing. Transfer the preparation from the dissection bath to the experimental bath in a spoon. Surface tension from the fluid in the dissection bath may over-stretch the muscle when removing it. Slide the scapula over the pin attached to the motor arm. Place the rib in the cradle of the hooks attached to the strain gauge (Figure 3.5). The side of the rib that forms an acute angle with the muscle fibers must be placed in the cradle that has the extra wire that restrains the rib from sliding during contraction. Make sure the muscle is not twisted while connecting the rib.

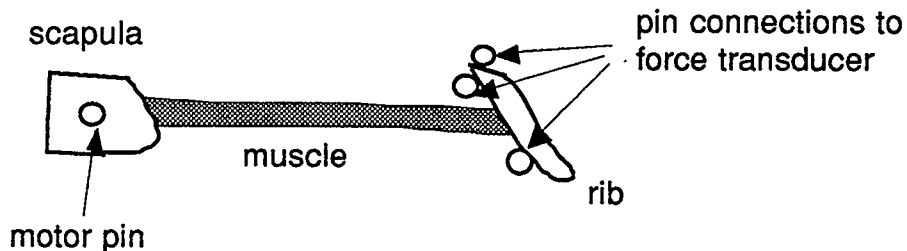


Figure 3.5. Top view of muscle preparation in experimental apparatus.

Place a cover slip over the surface of the bath and begin the flow of the bathing solution. Adjust the motor height and strain gauge height so they are as close to the bottom of the bath as possible without touching. The muscle should be adjusted so it is parallel to the bottom of the bath by focusing the microscope on the strain gauge end and then adjusting the motor height so that this end is in focus. Adjust the strain gauge end of the muscle (using micromanipulators) so the long axis of the muscle is parallel to the motor arm pull direction. The preparation is now ready for the conditioning contractions.

Experimental Setup

Bathing solution

The bathing solution used for perfusion, dissection, and during the experiment consisted of 118.1 mM NaCl, 3.4 mM KCl, 0.8 mM MgSO₄, 1.2 mM KH₂PO₄, 1.8 mM CaCl₂, 24 mM NaH₂CO₃, and 10 mM dextrose. The solution was vigorously bubbled with 95% O₂ and 5% CO₂ both during dissection and experimentation (pH 7.5). The bathing solution continuously flowed through both the dissection chamber and the experimental chamber (rate 6 ml/min) at room temperature (20°C).

Experimental apparatus

The experimental apparatus consisted of an experimental chamber, a motor, a force transducer, and a sarcomere length measurement system (Figure 3.6). The apparatus was mounted on a plate attached to the stage of an inverted microscope.

The experimental chamber was constructed with plexiglass walls and with a glass slide bottom. During the experiment a cover slip was placed over the top of the chamber to remove light aberrations caused by the surface vibrations and meniscus effects of the bathing solution. A motor (Model 6350, Cambridge Technology., Watertown, Massachusetts) controlled the length of the muscle at the scapula end.

Muscle force

Muscle force was measured with a semiconductor strain gauge transducer connected to an amplifier (PM1000, CWE Inc., Ardmore, Pennsylvania) in a half-bridge configuration. The force transducer had a sensitivity of 31 mN/V at an amplifier sensitivity of 10 mV (1000x amplification) and a resonant frequency of 2300 Hz (m26.95/d3.dat). The force transducer

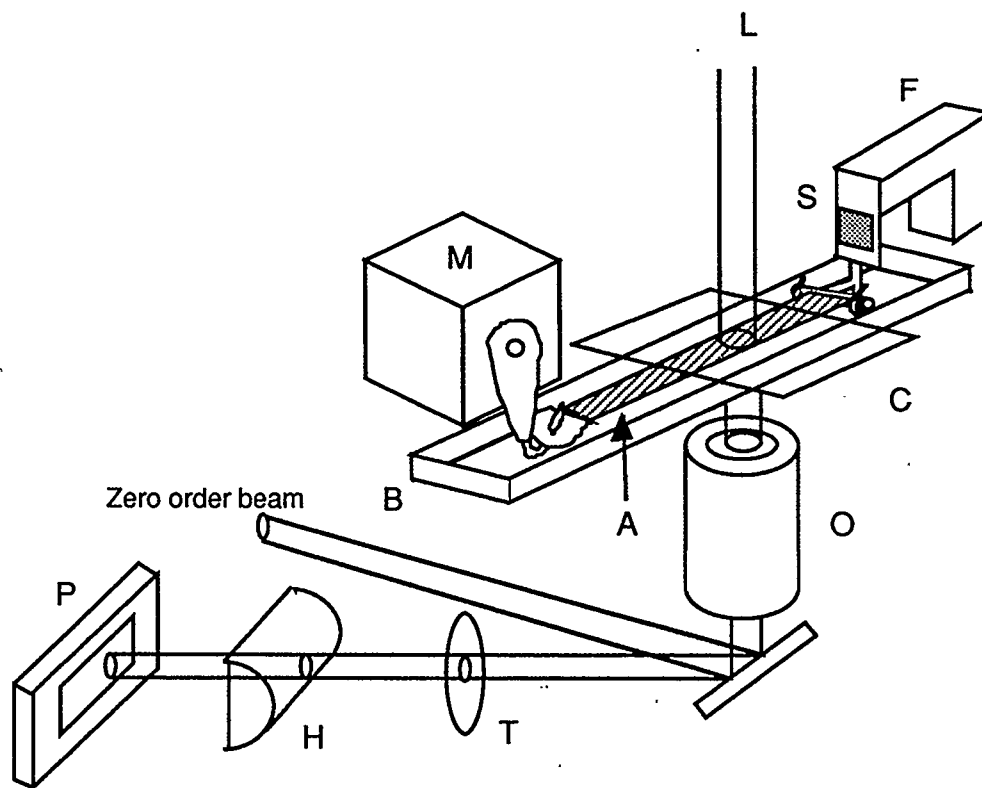


Figure 3.6. Schematic of experimental apparatus. Bathing solution flowed past muscle from the force transducer end to the motor end of the bath. A - muscle specimen, B - bath, C - cover slip, F - micro-manipulator, H - half cylindrical lens, L - laser beam, M - motor, O - microscope objective, P - photodiode array, S - strain gauge transducer, T - converging lens.

was attached to a micromanipulator capable of orienting the muscle perpendicular to a laser beam and parallel to the pull direction of the motor. The force transducer remained in a fixed position throughout the experiment.

This force transducer was built in-house. A stainless steel scalpel blade (No. 10) was shaped (cut and filed) into a 5 mm X 10 mm piece for use as the base metal. A thin layer of adhesive (M-Bond 610, Inter technology Inc., Calgary, Alberta) was applied to the base metal according to the manufacturers instructions. This precoat electrically isolates the strain gauge from the base metal. Another application of the adhesive was placed over the precoat and the strain gauge (Entran semiconductor strain gauge, ESU-60-350, bulk

unmatched, 350 Ω impedance, Intertechnology Inc., Calgary, Alberta) was attached. The same procedure was used to apply a second strain gauge to the opposite side of the base metal. The unit was then cured. Wire leads were soldered from the strain gauge to an electrically isolated pad on the base metal to act as a stress relief point for the wire leads. The strain gauge, base metal, and leads were then encased in a flexible silicon rubber (RTV) to make an insulated, water impermeable seal around the unit. Another epoxy (Barrier-D flexible epoxy, BLH Electronics, Canton, Massachusetts) may be placed under the silicon rubber to provide an additional barrier against water; however, this barrier is more rigid than the silicon rubber. Hooks, where the rib of the preparation was mounted, were glued to one end of the base metal. The other end of the base metal was screwed to a rigid aluminium block that was then screwed to the micromanipulators on the experimental apparatus.

Leads from the strain gauge were connected in a Wheatstone bridge (half bridge configuration) with 350 Ω balance resistors. With this configuration, the transducer was sensitive to bending and was temperature compensating.

Sarcomere length

Sarcomere length was measured with a laser diffraction system. When a laser beam is projected through a muscle, the different refractive indices of the A and I bands of the sarcomeres produce a diffraction pattern (Figure 1.1). Measurement of the deviation of the first-order diffraction peak from the zero-order peak gives a direct measure of sarcomere length. Thus, this system measured the average sarcomere length of the sarcomeres within the region illuminated by the beam (resolution about 5 nm). A 10 mW He-Ne laser (Model 1125, Uniphase, Manteca, California) with a beam diameter of 0.8 mm was directed through the top of the experimental chamber perpendicular to the long axes of the muscle fibers. The diffracted beam from the muscle was collected in

a 10X objective lens (N.A. 0.5, Nikon) and reflected through the access port in the microscope. The diffracted beam was then refracted by a telescopic lens and a cylindrical lens to compress the diffraction pattern onto a photodiode array (RL-128A, Reticon Corp., Sunnyvale, California). An amplifier (ter Keurs et al., 1978) produced an analog signal proportional to sarcomere length based on the median intensity of the first-order diffraction pattern measured by the photodiode array (2000 Hz). The quality of the diffracted beam was continuously monitored during testing. An oscilloscope displayed the intensity profile of the diffracted beam along with the median sarcomere length continuously throughout the experiments.

The sarcomere length measurement system was calibrated using a 12.5 μm grating which was placed in the experimental chamber with the bathing solution and cover slip. The 4th, 5th, and 6th order diffraction patterns (3.125, 2.500, 2.083 μm , respectively) were visible on the oscilloscope. Using the adjustments on the amplifier, the window was adjusted so only the 2.500 μm peak was visible on the oscilloscope and the zero pot was adjusted to read 2.500 μm on the computer screen (0 V at the "relative" connection; $\text{SL } (\mu\text{m}) = \text{relative (V)} + 2.500 (\mu\text{m})$). The window was then moved to show only the 2.083 μm peak and the gain pot was adjusted to read 2.083 μm on the computer screen (-0.417 V at the "relative" connection). The 3.125 μm peak was then checked, as it should read 3.125 μm . At longer sarcomere lengths the amplifier had to be adjusted using the 3rd, 4th, and 5th order diffraction patterns (4.167, 3.125, 2.500 μm , respectively).

Muscle length

Muscle length was determined using the position signal from the Cambridge motor. Motor position (2 V/mm) was converted into muscle length using a calibration from a video camera mounted on a dissecting microscope

above the muscle preparation. Muscle length was passively set. The microscope stage was translated under the microscope from one end of the fiber to another. A calibrated material was then placed in the plane of the muscle and recorded on video. The video tape was manually digitized using a frame capture system to determine the muscle length at several motor positions. Linear regression analysis revealed a linear relation between the measured motor position and the actual muscle length ($r = 0.99$).

Stimulation

The muscle preparations were stimulated tetanically through two platinum wires running the entire length of the chamber, parallel to the muscle fibers, and attached to the bottom of the test chamber. Tetanic stimulation was achieved using a square wave pulse of 0.5 ms duration at 200 Hz and with a train duration of 250 - 300 ms (Model S88F, Grass Instruments, Quincy, Massachusetts). The stimulation voltage was set supramaximally (typically 20 - 30 V) before the conditioning twitches and reset with tetanic contractions before the experimental protocol. A rest period of at least 100 seconds was provided between tetanic stimulations.

Data Collection

Data collection and initiation of the contractions were controlled (Figure 3.7) by a personal computer (IPC 386). The computer digitally recorded muscle length (from motor), sarcomere length (laser diffraction system), and force (force transducer) at a sampling frequency of 1000 Hz. The analog signals from the equipment were digitally collected (12 bit resolution) through an A/D/A board (DT 2821, Data Translation Inc., Marlborough, Massachusetts) and were displayed on the computer monitor after each contraction. The stimulator was triggered by a digital signal (DIO) from the computer. On the stimulator, the train

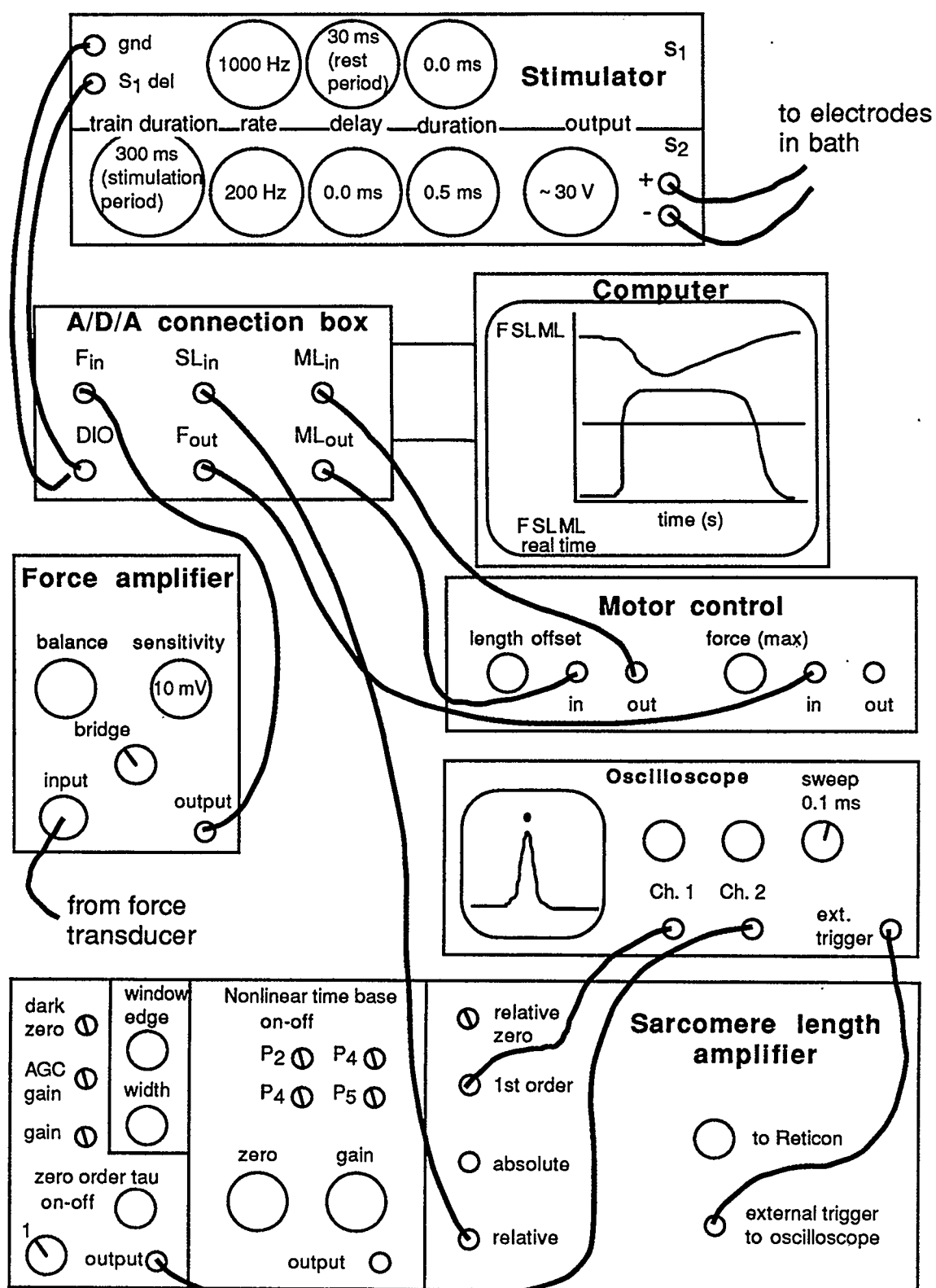


Figure 3.7. Cable connections (thick lines) are shown between the electrical equipment used in the experimental setup.

duration controlled the length of the stimulation and the delay in the S_1 circuit controlled the amount of data collected during the rest period, before stimulation began.

Pilot Tests

Several pilot experiments were attempted with the serratus anterior muscle preparation. Results from these pilot tests were not included in the main body of the dissertation as they were unsuccessful. The program I wrote to collect and display the data could also control muscle length through a second A/D/A board (in D/A mode). The type of muscle length changes (e.g., an isokinetic stretch) desired during contraction could be input into a buffer. When the contraction was executed, the ATLAB subroutines triggered the 2nd A/D/A board to send length control signals from the buffer to the motor (stream mode), the 1st A/D/A board collected 3 channels of data into another buffer (stream mode), and then the stimulator was triggered by a DIO signal. The length of time that data were collected before stimulation was set on the stimulator using the delay dial.

Sarcomere clamping

An attempt was made to keep sarcomere length constant throughout a contraction using a feed forward system with error correction. A fixed-end contraction was executed and force, sarcomere length, and muscle length were collected. The sarcomere length trace was then digitally smoothed using either a moving average or Butterworth filter. This filtered sarcomere length data was subtracted from the desired behavior (constant sarcomere length in this case). This error signal multiplied by a gain constant was subtracted from the previous muscle length signal. Then, a contraction was initiated with this new muscle

length control. This error correction method was repeated until the desired sarcomere length trace was obtained (Peterson et al., 1989; Smith and Barsotti, 1993).

Results from this technique were marginal, as the force-time traces did not show a steady force during contraction as was found by others using segment-control on single fibers of the frog (e.g., Granzier and Pollack, 1990). The force-time curve had a number of peaks and valleys corresponding to the changes in muscle length. These difficulties may be caused by sarcomere nonuniformities across the width of the muscle. Nonuniformities may produce a first-order diffraction pattern that contains excess noise. Such noise is then transferred into motor length control signal for the next contraction. Since this method was unsuccessful, the extrapolation method was used to determine the force produced by an isometric sarcomere.

Segment length measurements

An attempt was made to measure segment lengths in the serratus anterior muscle preparation. Small pieces (about 0.2 mm long) of 6-0 silk were attached to the surface of the muscle by natural adhesion. During a contraction the surface marker motion was recorded on video tape (200 Hz) through a camera attached to a dissection microscope positioned above the preparation. Simultaneously, sarcomere length for the segment of interest was recorded using laser diffraction. Surface markers were then digitized using a calibrated frame capture system.

Although segment length and sarcomere length showed similar behaviors during most of the tetani, the length changes from the two methods were of differing magnitudes. In some cases the segment and sarcomere length results showed very different behaviors. Based on personal observation, it was determined that the surface markers were adhering to a thin layer of loose

connective tissue above the fibers. During a contraction this connective tissue (e.i., the surface markers) did not move proportionally to the sarcolemma (and thus the sarcomeres) of the underlying fibers. Thus, surface markers were assumed to be an inadequate measure of the average sarcomere length in a particular region of the fiber.

Chapter 4

Stability of Muscle Fibers on the Descending Limb of the Force-Length Relation -- a Theoretical Consideration

Introduction

The force-length (F-L) relation for skeletal muscles has been studied extensively both on the sarcomere (e.g. Gordon et al., 1966) and whole fiber level (e.g. ter Keurs et al., 1978). In this study, the term "F-L relation" represents the tension producing potential of a fiber or a sarcomere under isometric conditions (i.e., constant length of a fiber or constant length of a group of sarcomeres). Qualitatively the F-L relation contains four regions: an ascending limb, a plateau, a descending limb, and a passive limb (Figure 4.1). Since a muscle fiber contains a large number of sarcomeres in series, a number of issues arise related to sarcomere behavior within a fiber -- one of these issues being stability.

Over the past 40 years, most researchers have believed that the descending limb of the F-L relation is unstable (Hill, 1953; Huxley and Peachey, 1961; Gordon et al., 1966; Julian and Morgan, 1979a; Morgan et al., 1982; Lieber and Baskin, 1983; Edman and Reggiani, 1984) because the descending limb has a negative slope. Instability in this context refers to a muscle fiber "pulling itself apart." On the descending limb of the F-L relation, any non-

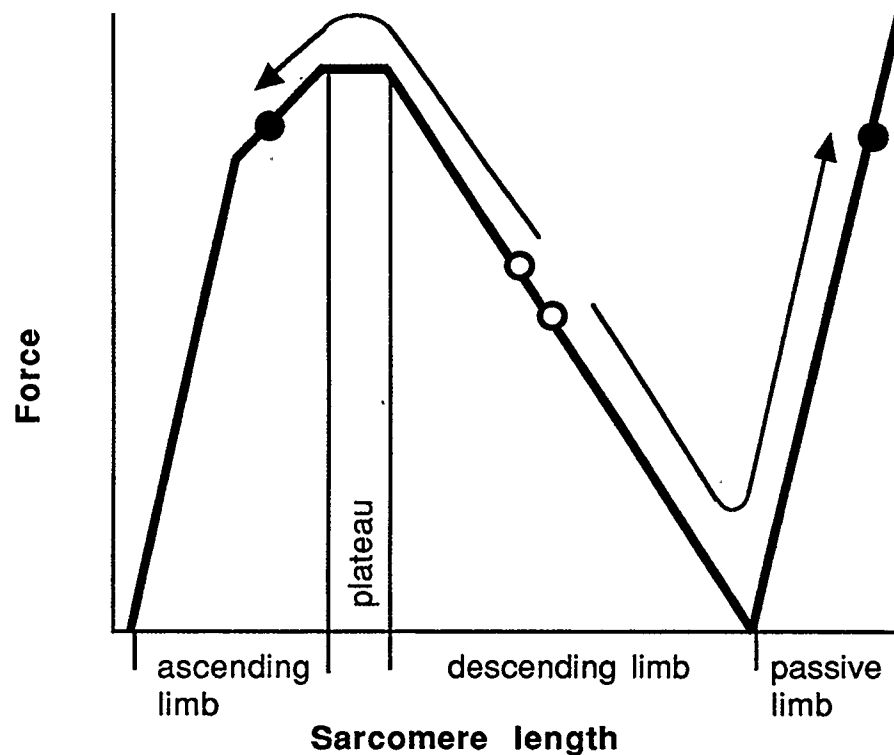


Figure 4.1. Demonstration of the expected unstable sarcomere behavior on the descending limb of the F-L curve (after Hill, 1953). Two sarcomeres at different initial lengths (open circles) diverge in length until stability occurs (solid circles). Note, the F-L relation shown contains the characteristics of actual F-L relations (e.g., Gordon et al., 1966), but does not represent the properties of any specific muscle. The passive force was represented as a straight line starting at sarcomere lengths where the force of the descending limb becomes zero.

uniformities in length of the sarcomeres along the fiber are associated with short (strong) sarcomeres shortening at the expense of the long (weak) sarcomeres (Figure 4.1). Thus, during a tetanic contraction the strong sarcomeres are thought to "pull apart" the weak sarcomeres (Morgan, 1990). This behavior is believed to continue until a stable, equilibrium force level is achieved in all sarcomeres; i.e., until the strong sarcomeres have shortened onto the active ascending limb of the F-L relation and the weak sarcomeres have stretched past thin-thick myofilament overlap onto the passive limb of the F-L relation (Figure 4.1).

Intuitively, the thought of a muscle fiber being unstable over a large portion of its operating range is unattractive. Instability would result in:

- 1) gross differences in sarcomere lengths along a fiber,
- 2) sarcomere extension being limited only by passive structures where force production can not be regulated,
- 3) fibers that are incapable of regulating their length over extended contractions,
- 4) large sarcomere length changes resulting in increased cross-bridge cycling (ATP splitting) and increased energy requirements, compared to a more stable behavior, and
- 5) unstable torque-angle relations at joints caused by the unstable muscle properties, leading to problems in movement control.

Stability may, in fact, be an inherent property of the active force producing process within a sarcomere, and the instability theory may be a misinterpretation based on viewing the descending limb of the F-L relation in isolation. A few researchers have suggested that sarcomeres and fibers are stable over the whole working range (Délèze, 1961; ter Keurs et al., 1978; Pollack, 1990), however the exact regulation of stability has not been identified.

The purpose of this research was (1) to demonstrate analytically the mechanical conditions for which sarcomeres in a muscle fiber are stable and (2) to demonstrate that a fiber composed of a large number of sarcomeres can be stable, while exhibiting an apparent unstable (negatively sloped) descending limb of the F-L curve.

Methods

In order to determine the conditions for sarcomere stability in a muscle fiber, a muscle fiber was modelled as a number of sarcomeres in series. The

muscle fiber containing $n+1$ independent sarcomeres in series with n nodes (Figure 4.2A). Sarcomeres were modelled to follow a force-displacement curve similar to that of a spring. Two types of sarcomeres existed: one type exhibiting a positive stiffness (K_A , Figure 4.2B), representing sarcomeres on the ascending or passive limb of the F-L relation, and a second type with a negative stiffness ($-K_D$, Figure 4.2B) representing sarcomeres on the descending limb of the F-L relation. Stiffness in this context refers to the slope of the force-displacement curve. The force of each sarcomere was related to the displacement of the nodes which was related to sarcomere length by a constant (resting sarcomere

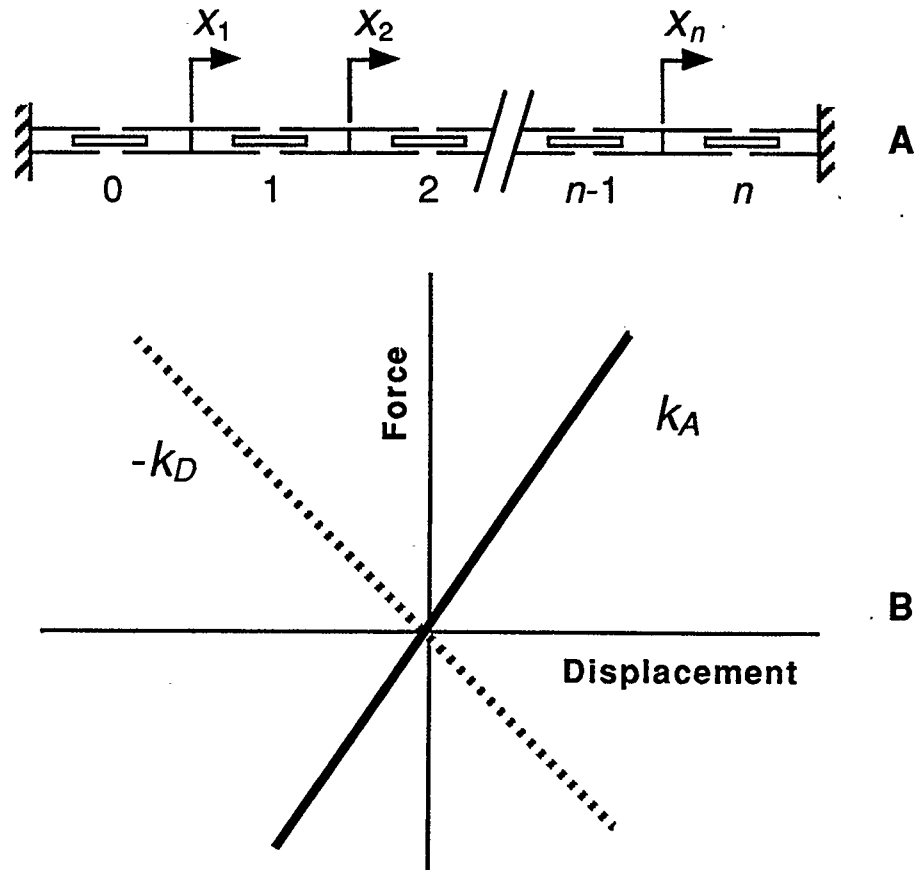


Figure 4.2. Fiber model (A) consisting of $n + 1$ sarcomeres in series and n nodes. Displacement (x_i) of node i is from the equilibrium condition. Force-displacement properties (B) for an individual sarcomeres. A sarcomere is considered to either have a positive stiffness (k_A , solid line) or a negative stiffness ($-k_D$, dotted line).

length). Fiber ends remained fixed (representing a fixed-end or isometric contraction), so the sum of the sarcomere lengths (i.e., the total fiber length) remained constant.

Force-velocity properties of sarcomeres were not included in this model, as they do not affect the evaluation of stability. Force-velocity properties can not cause an unstable sarcomere to achieve a steady-state sarcomere length, but only alter the rate at which the steady-state is reached. Neglecting the force-velocity properties thus implies, that we are not concerned with the time history of the sarcomere length changes during contraction, or the time in which stability may be reached, but with the attainment of stability exclusively.

Stability of the fiber was evaluated using the potential energy function (*PE*) and the positive definiteness of the stiffness matrix. The potential energy equation for the fiber (Figure 4.2A) can be written in matrix form as,

$$PE = 1/2 [\mathbf{x}]^T [\mathbf{K}] [\mathbf{x}] \quad (1)$$

where:

$$[\mathbf{x}] = \begin{bmatrix} x_1 \\ x_2 \\ x_3 \\ \vdots \\ x_n \end{bmatrix}$$

$[\mathbf{x}]$ is the displacement matrix and x_i is the displacement of node i .

$$[\mathbf{K}] = \begin{bmatrix} m_{11} & m_{12} & \cdots & m_{1n} \\ m_{21} & m_{ij} & & \vdots \\ \vdots & & & \vdots \\ m_{n1} & \cdots & \cdots & m_{nn} \end{bmatrix}$$

$[\mathbf{K}]$ is the stiffness matrix and m_{ij} is the stiffness of element ij .

$$[\mathbf{x}]^T$$

is the transpose of $[\mathbf{x}]$.

The stiffness matrix for the fiber composed of $n+1$ sarcomeres and n nodes is symmetric and banded,

$$[\mathbf{K}] = \begin{bmatrix} k_0+k_1 & -k_1 & 0 & 0 & \dots & \dots & 0 \\ -k_1 & k_1+k_2 & -k_2 & 0 & & & \vdots \\ 0 & -k_2 & k_2+k_3 & -k_3 & & & \vdots \\ \vdots & & & & & & \vdots \\ \vdots & & & -k_{n-3} & k_{n-3}+k_{n-2} & -k_{n-2} & 0 \\ \vdots & & & 0 & -k_{n-2} & k_{n-2}+k_{n-1} & -k_{n-1} \\ 0 & \dots & \dots & 0 & 0 & -k_{n-1} & k_{n-1}+k_n \end{bmatrix} \quad (2)$$

where k_i represents the stiffness of sarcomere i .

Stability of the system exists if the matrix $[\mathbf{K}]$ is positive definite. $[\mathbf{K}]$ is defined to be positive definite if, $[\mathbf{x}]^T [\mathbf{K}] [\mathbf{x}] > 0$ for all $[\mathbf{x}] \neq 0$ (Hildebrand, 1965). Thus, a positive definite matrix will always yield a positive potential energy (PE) when multiplied by an arbitrary matrix $[\mathbf{x}]$, except $[\mathbf{x}] = 0$. If a matrix $[\mathbf{x}]$ is found that yields a negative potential energy, the system is unstable. For the fiber model presented here, positive definiteness exists when (1) the determinant of the final stiffness matrix is positive ($|\mathbf{K}| > 0$), (2) the determinant of the principal minors is positive ($|m_{ij}| > 0$), and (3) the elements of the main diagonal are all positive ($m_{ij} > 0$) (Kardestuncer, 1974).

In order to gain an understanding of the behavior of the system which could be visualized easily, the stability of a two sarcomere system with one degree of freedom was evaluated for three cases. *Case 1* describes the situation where both sarcomeres are located on the ascending limb of the F-L relation (sarcomeres labelled a_0 and a_1 , Figure 4.3). *Case 2* describes the situation where both sarcomeres are located on the descending limb of the F-L relation (sarcomeres labelled d_0 and d_1 , Figure 4.3). *Case 3* describes the situation where one sarcomere is located on the ascending and the other sarcomere on the descending limb of the F-L relation (Figure 4.4).

The stability criteria for a general solution was evaluated for $n+1$ sarcomeres in series. The general solution was used to evaluate how many

sarcomeres in a fiber could possess a negative stiffness and still remain stable.

Results

Stability of a Two Sarcomere Fiber

Stability criteria for the muscle fiber containing two sarcomeres and one degree of freedom were evaluated for three cases. Based on equation (2) with $n = 1$, the stiffness matrix was $[K] = [k_0 + k_1]$.

Case 1: Assume that the fiber consists of two sarcomeres both located on the ascending limb of the F-L relation ($k_0 = k_1 = k_A$). This system of sarcomeres is

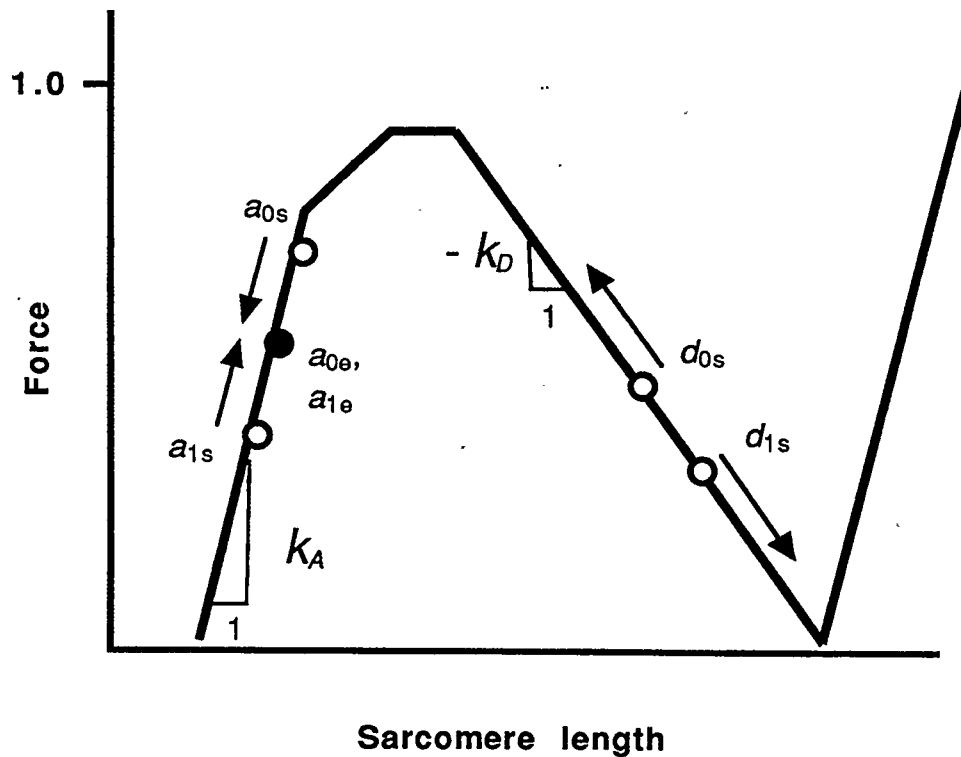


Figure 4.3. Stability -- response of the two sarcomere model at different initial lengths. All sarcomeres follow the F-L curves (solid line) given by slopes k_A and $-k_D$. *Case 1:* a stable fiber begins with both sarcomeres on the ascending limb. The sarcomeres initial lengths are a_{0s} and a_{1s} (open circles) and reach equilibrium at a_{0e} and a_{1e} (solid circle). *Case 2:* a different fiber begins with both sarcomeres on the descending limb (d_{0s} and d_{1s}). The system is unstable and the sarcomeres diverge.

stable since $[K]$ is positive definite ($[K] = 2k_A > 0$), and will reach equilibrium at the average sarcomere length of the fiber (Figure 4.3). The labels a_{0s} and a_{1s} represent sarcomeres a_0 and a_1 at the start of a contraction, and a_{0e} and a_{1e} represent the corresponding sarcomeres after they have reached the equilibrium length (Figure 4.3). During the contraction, sarcomere a_1 lengthens and sarcomere a_0 shortens by the same amount because of the length constraint on the entire fiber. The system would also be stable if the sarcomeres were on separate positively sloped F-L curves with different slopes, for example, the ascending limb and the passive limb of the F-L relation.

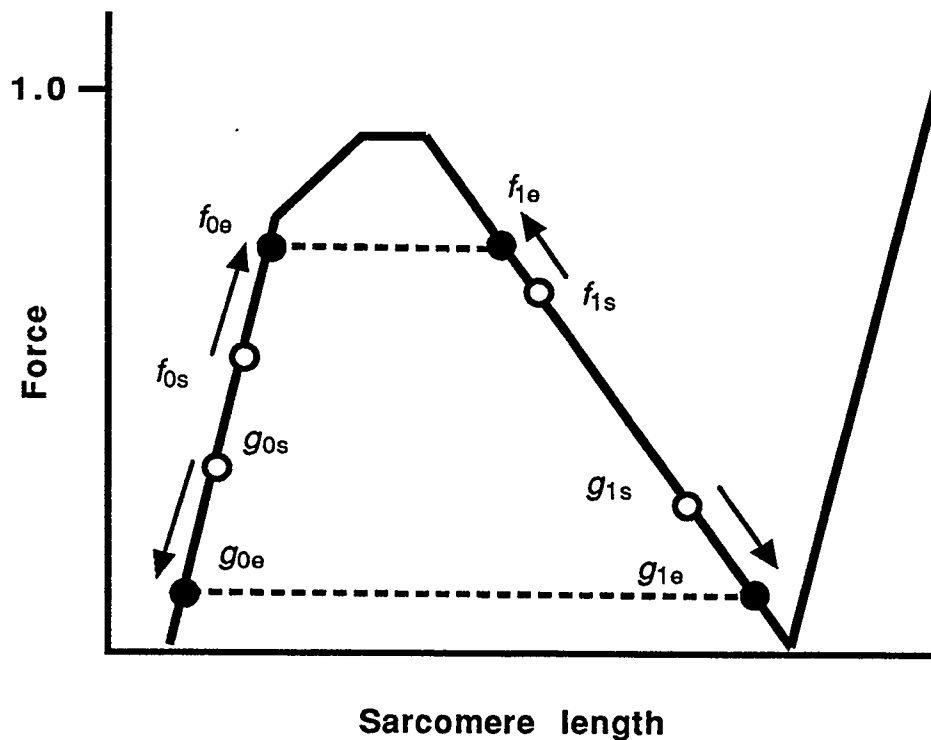


Figure 4.4. Stability -- response of a stable ($k_A > k_D$), two sarcomere model with different initial lengths for case 3. One sarcomere is always on the ascending limb and one sarcomere always on the descending limb. Sarcomeres f_0 and f_1 represent one fiber and sarcomeres g_0 and g_1 represent a different fiber. Initial sarcomere lengths are given by open circles and the stable, steady-state conditions are shown by solid circles.

Case 2: Assume that the fiber consists of two sarcomeres, both located on the descending limb of the F-L relation ($k_0 = k_1 = -k_D$). The stiffness matrix in this case is not positive definite ($|\mathbf{K}| = -2k_D < 0$), and thus, the system is unstable. Sarcomeres d_0 and d_1 , located initially at d_{0s} and d_{1s} (Figure 4.3), are unstable and diverge in length. The sarcomere with the short initial length (d_{0s}) is stronger than the sarcomere with the long initial length (d_{1s}); thus, the short sarcomere will shorten at the expense of the long sarcomere.

Case 3: Assume that the fiber consists of two sarcomeres; one sarcomere located on the ascending, the other on the descending limb of the F-L relation ($k_0 = k_A$ and $k_1 = -k_D$). This case is positive definite and stable if $k_A > k_D$ ($|\mathbf{K}| = k_A - k_D > 0$). The stability of the system is not changed if the negatively sloped curve is at longer or shorter lengths than the positively sloped curve (i.e., if the active or passive ascending limb is considered).

If the sarcomere on the descending limb (f_{1s} , Figure 4.4) is located at a position of higher force than the sarcomere on the ascending limb (f_{0s}), the equilibrium condition (f_{0e} and f_{1e}) will be reached at a force level that is higher than the initial force of each sarcomere. If the sarcomere on the descending limb (g_{1s} , Figure 4.4) is located at a position of lower force than the sarcomere on the ascending limb (g_{0s}), the equilibrium condition (g_{0e} and g_{1e}) will be reached at a force level that is lower than the initial force of each sarcomere.

Stability of an $n + 1$ Sarcomere Fiber

Stability of a fiber containing $n + 1$ sarcomeres can be disproven by determining if the potential energy (PE) of the system is negative for one matrix $[\mathbf{x}]$. For example, choose the $[\mathbf{x}]$ matrix of dimensions $n \times 1$ such that the nodes x_1 and x_n are assigned displacements of zero and the rest of the nodes are

assigned displacements of one,

$$[\mathbf{x}] = \begin{bmatrix} 0 \\ 1 \\ 1 \\ \vdots \\ 1 \\ 0 \end{bmatrix} \quad (3)$$

The potential energy function is, $PE = 1/2 [\mathbf{x}]^T [\mathbf{K}] [\mathbf{x}]$. (4)

Substituting $[\mathbf{K}]$ (eq. 2) and $[\mathbf{x}]$ (eq. 3) into the potential energy function (eq. 4) and performing the multiplication yields,

$$PE = 1/2 (k_1 + k_{n-1}) \quad (5)$$

Therefore, the system is unstable if $k_1 + k_{n-1} < 0$, and this example simplifies to the same result as the fiber containing two sarcomeres.

In general, a fiber is unstable if it contains two or more sarcomeres with a negative stiffness ($-k_D$), because a matrix $[\mathbf{x}]$ can always be chosen such that the sign of the potential energy is negative. The potential energy will be negative when matrix $[\mathbf{x}]$ is chosen such that the two sarcomeres with negative stiffness in the $n + 1$ sarcomere fiber are assigned displacement values of one. Then, the sarcomeres located between these two sarcomeres are assigned a displacement of one and the remaining sarcomeres are assigned a displacement of zero.

For a fiber composed of a large number of sarcomeres in series to be stable, the stiffness properties of all but one sarcomere must be positive in this system, constrained by a constant fiber length. One sarcomere may have a negative stiffness and the system will still be stable provided that the positive stiffness is greater in magnitude than the negative stiffness ($|k_A| > |k_D|$).

Discussion

Conditions of Stability

The mechanical conditions required for a muscle fiber to be stable were determined analytically. From this analysis, it was demonstrated that for stability to occur, at most one sarcomere in a fiber can have a negative stiffness.

Therefore, if we assume that a muscle fiber is inherently stable for any length within the normal range, the sarcomere force-displacement behavior during a fixed-end contraction (a contraction in which the ends of a fiber are fixed while the sarcomeres are allowed to lengthen or shorten) must have a positive slope.

Experimentally, sarcomeres have been shown to have a positive stiffness at sarcomere lengths corresponding to the descending limb of the F-L relation. For example, Ford et al. (1977) found that a small group of sarcomeres subjected to quick releases and stretches corresponded with a sharp decrease and increase in force, respectively. This positive stiffness response to sudden length changes in a group of sarcomeres was associated with cross-bridge mechanics and is commonly referred to as the "cross-bridge stiffness" or the "short-range stiffness."

Cross-bridge stiffness or short-range stiffness is explained with the mechanics of the cross-bridges according to the cross-bridge theory of muscular contraction (Huxley, 1957; Huxley and Simmons, 1971). According to this theory, the cross-bridge consists of a tail portion containing a spring element, and a head portion which attaches to specific sites on the thin myofilament. In an activated fiber many cross-bridges are attached and the spring element is stretched. If the fiber is released or stretched very quickly in this activated state (so quickly that there is no time for the cross-bridges to detach), the spring element of the cross-bridges will shorten or stretch,

respectively, and so give rise to a rapid decrease or increase in force, respectively. The "cross-bridge" stiffness observed for sarcomeres on the descending limb of the F-L relation provides the necessary properties for sarcomere stability on the descending limb of the F-L relation during quick length changes of limited magnitude (i.e., by the changes within the operating range of a cross-bridge; about 6 nm per half sarcomere for shortening (Ford et al., 1977) and 12 nm per half sarcomere for lengthening (Flitney and Hirst, 1978).

Other experimental data also suggest that sarcomeres possess a positive stiffness for length changes larger than a cross-bridge cycle. If a group of sarcomeres is stretched or shortened and then held isometrically, the force produced at the new isometric length does not correspond to the force based on the sarcomere F-L relation. "Effective stiffness" can be defined as the slope of a line connecting the isometric force and length of a sarcomere with no previous length change (F-L relation) and the isometric force and length of a sarcomere after stretching or shortening. Thus, the sign of the effective stiffness property can be used to evaluate whether a sarcomere is stable for larger length changes than a cross-bridge cycle.

Sarcomeres that are stretched and then held at constant length exhibit a positive effective stiffness (Hill, 1977, Figure 2B; Edman et al., 1978, Figure 4B; Edman et al., 1982, Figure 3). On the descending limb of the F-L relation, a sarcomere that is stretched and then held isometric exhibits force levels that are larger than the corresponding isometric force (Hill, 1977; Julian and Morgan, 1979b; Edman et al., 1978; Edman et al., 1982). Thus, sarcomeres that are stretched more than a cross-bridge cycle are stable on the descending limb of the F-L relation because the effective stiffness is positive.

Following shortening on the descending limb of the F-L relation, the isometric force in a small group of sarcomeres has been shown to be lower than the forces obtained isometrically before the shortening (Edman, 1980; Granzier and Pollack, 1989; Sugi and Tsuchiya, 1988), while others have reported an increase in force (Horowitz et al., 1992; Edman et al., 1993). Thus, some studies illustrate a positive effective stiffness and other studies illustrate a negative effective stiffness for sarcomere shortenings greater than a cross-bridge cycle.

The effective stiffness property of sarcomeres after stretches larger than a cross-bridge cycle lend more support for the stability hypothesis. There appears to be contradictory data related to whether sarcomeres that shorten more than a cross-bridge cycle possess an effective stiffness property that supports stability. The area of shortening needs to be investigated further.

It should be noted that the F-L relation (i.e., the total of the active and passive curves in this case) may not possess a negative slope depending on the activation and the passive F-L properties of the muscle. The passive curve for different types of muscles maybe shifted along the length axis of the F-L relation. Some muscles (e.g., frog toe muscle; ter Keurs et al., 1978) have a passive curve that ascends steeply close to optimal length. If such a muscle is only partially activated, the combined effects of the active (at reduced force levels) and passive limbs may produce a total F-L relation with only a positive slope. Thus, the problem of instability may not exist for such a muscle.

Is stability consistent with the descending limb of the F-L relation?

Can a sarcomere exhibit a F-L relation with a negative slope (descending limb) and still be stable? The answer to this question is *yes* and it can be illustrated through a thought experiment.

In this thought experiment the force-length property of a hypothetical sarcomere under isometric conditions is determined. Take two combs and place the bristles end-to-end in a "black box." The black box represents a sarcomere from Z-line to Z-line and the bristles represent the cross-bridges (Figure 4.5A). Assume that the backbone of the comb is rigid and that the bristles are equally

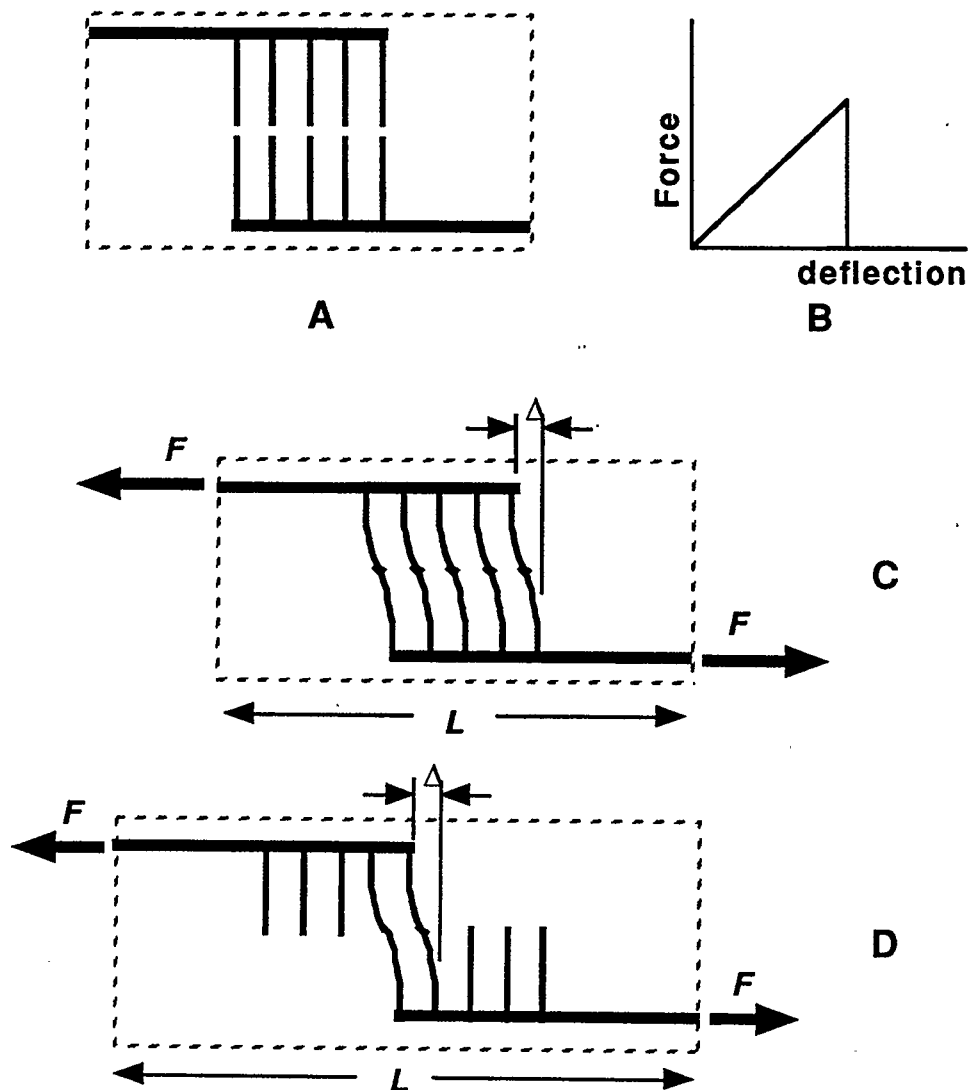


Figure 4.5. Illustration of a comb experiment that demonstrates how a sarcomere can be stable yet possess a F - L relation with a negative slope. A) Combs in resting condition before engaging bristles. B) Force-deflection relation for a single bristle. C) Comb configuration after engaging all bristles and pulling the ends of the comb apart by Δ . D) Comb configuration after engaging two bristles and pulling the ends of the comb apart by Δ .

spaced and have a linear force-deflection relation (positive stiffness, Figure 4.5B).

Begin the experiment with all bristles in contact (representing maximum thin-thick filament overlap in a sarcomere) and pull the combs a given distance (Δ) apart (representing activation of the sarcomere), so that all bristles remain in contact (Figure 4.5C). Record the length of the "sarcomere" (L) and the force level (F) at this isometric condition. Now separate the combs and reengage them so fewer bristles are in contact (representing less thin-thick filament overlap in a sarcomere). Again pull the combs apart by the same amount (Δ) as in the previous trial and record the length of the "sarcomere" and the force (Figure 4.5D). Continue this procedure with a different number of bristles engaged before "activating" the "sarcomere." Now, plot the relation between the "sarcomere" length and the force produced by the "sarcomere".

The resulting F-L curve for this hypothetical sarcomere has a negative slope (Figure 4.6, thick shaded line) similar to the F-L relation found for muscle fibers (Gordon et al., 1966), yet the "sarcomere" is stable, because the force-displacement curve has a positive slope. The solid lines on the F-L plot (Figure 4.6) represent the force-displacement curves for one trial when the number of bristles engaged is fixed. Thus, at full "activation" if the "sarcomere" was shortened, the force would decrease and if the "sarcomere" was stretched, the force would increase (Figure 4.6, line C). The slope of the force-displacement line for a given number of bristle engagements may be represented by the "short-range stiffness" of a sarcomere. Since the slope of the force-displacement curve (short-range stiffness) is related to the number of bristles engaged (thin-thick myofilament overlap), this hypothetical sarcomere also has stiffness properties exhibited by muscle fibers. Short-range stiffness in muscle (as well as in the comb model) is greatest at maximum thin-thick filament

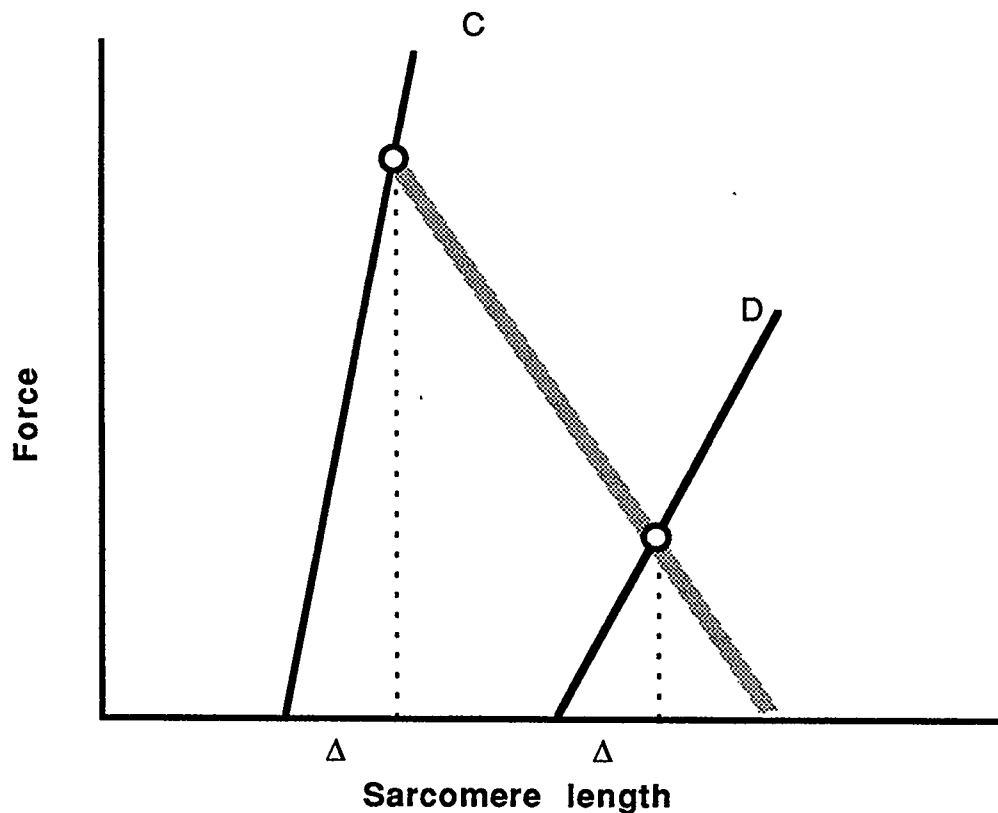


Figure 4.6. F-L plot of the comb experiment. Thick shaded line shows the F-L relation after "activation" when combs are pulled apart a distance Δ . Solid lines represent the force-displacement curves for individual trials with all bristles engaged (C) and with two bristles engaged (D).

overlap and decreases as the amount of thin-thick filament overlap decreases (Huxley and Simmons, 1971).

This thought experiment illustrates how a sarcomere within a muscle fiber can exhibit a negatively sloped F-L relation, yet still remain stable. A microstructure within the sarcomere (e.g., cross-bridge), not accounted for in the usual F-L experiment (Gordon et al., 1966), may have stabilizing properties.

Conclusions

When measuring the F-L properties of a muscle fiber, one observes a decreasing force with increasing sarcomere lengths for the so called "descending limb" of the F-L relation. This behavior, which one might describe as a softening material, has been associated with instability of sarcomere lengths. In this study we have shown that the descending limb of the F-L relation must not necessarily be associated with sarcomere instability. Any positive stiffness behavior on the descending limb will provide stability. Biophysically, it has two candidates for providing a positive stiffness have been identified, the so called "short-range stiffness" (Ford et al., 1977) and the "effective stiffness" (Hill, 1977; Edman et al., 1978). Based on the results of this study it is conceivable that the active force producing process of skeletal muscle provides for stability over the entire range of sarcomeres. Such a hypothesis of stability is very appealing and should be tested in future experiments.

Chapter 5

Force-Length Properties in Stable Skeletal Muscle Fibers -- Theoretical Considerations

Introduction

Skeletal muscle fibers possess a force-length (F-L) or length-tension relation that describes the force-producing potential of a fiber at a given isometric length (ter Keurs et al., 1978; Altringham and Bottinelli, 1985; Martyn and Gordon, 1988; Granzier and Pollack, 1990). Sarcomeres in skeletal muscle fibers also possess an F-L relation (Gordon et al., 1966b; Edman et al., 1987; Bagni et al., 1988; Granzier and Pollack, 1990) that can be described by an ascending limb, a plateau, a descending limb, and a passive limb (Figure 5.1). Because muscle fibers are composed of a large number of sarcomeres in series, the sarcomere F-L relation has frequently been used to represent the F-L relations of fibers or even entire muscles (e.g., Lieber and Boakes, 1988). However, it has been shown convincingly that there is a large difference between the F-L relation of a fiber and the F-L relation of the sarcomeres that make up a fiber, particularly in the region of the descending limb (Figure 5.1; Granzier and Pollack, 1990, their Figure 5; Pollack, 1990, his Figure 2.8).

Differences between the F-L relation of a sarcomere and a fiber have been associated with the methods of length control used experimentally. The F-L relation for a fiber is measured during a fixed-end contraction. In this

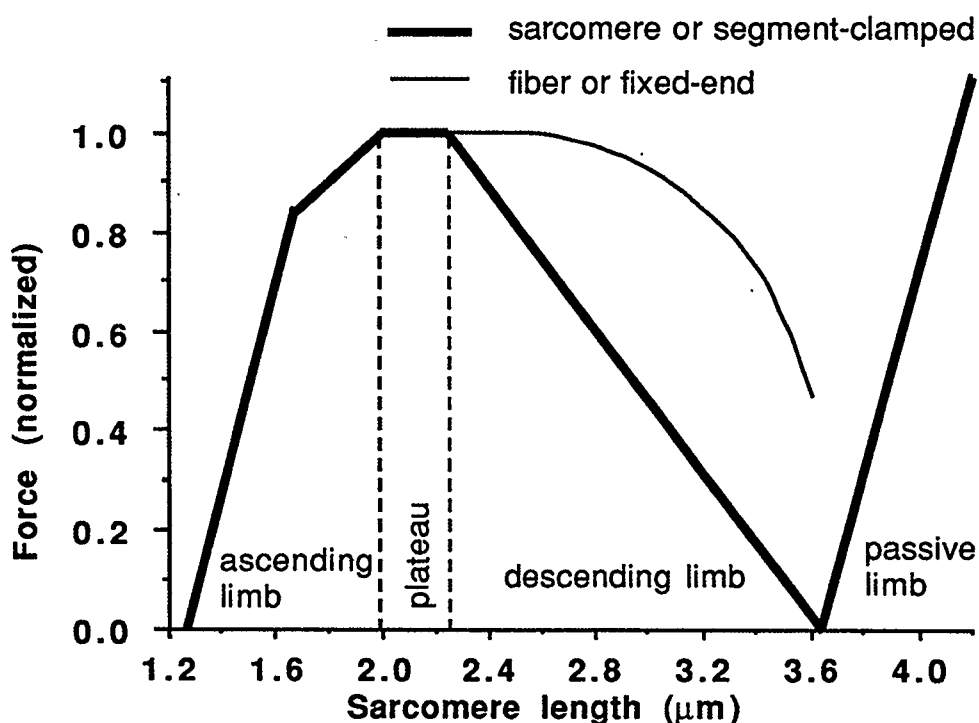


Figure 5.1. Schematic representation of the force-length (F-L) relation for a small group of sarcomeres under isometric contraction conditions using segment-clamping methods (thick line). Also shown is the F-L relation (using average sarcomere length) for a muscle fiber under fixed-end contraction conditions (thin line).

experiment, the fiber as a whole is kept isometric while the sarcomeres within the fiber may change in length. When determining the F-L relation for sarcomeres, a small segment of a muscle fiber (10 mm to 0.07 mm) is held at a constant length throughout the contraction. During this segment-clamped contraction, fiber length may have to be changed actively by the experimenter to keep the segment of interest at a constant length during the contraction (e.g., Gordon et al., 1966a).

A muscle fiber that is tested using the fixed-end method exhibits an extended plateau and larger forces on the descending limb of the F-L relation compared to the same fiber under segment-clamped conditions (Figure 5.1). The force enhancement observed in fixed-end fibers has been associated with

the dynamic changes in sarcomere length during contraction, caused by the inherent instability of sarcomeres on the descending limb of the F-L relation (Hill, 1953; Huxley and Peachey, 1961; Gordon et al., 1966b; Julian et al., 1978; Julian and Morgan, 1979a; Morgan et al., 1982; Lieber and Baskin, 1983; Edman and Reggiani, 1984; Granzier and Pollack, 1990). These studies imply that mechanical properties of the sarcomere (i.e., force-velocity properties) and unstable sarcomere length changes cause the differences between the fiber and sarcomere F-L relations. However, other researchers have stated that sarcomeres should be stable on the descending limb of the F-L relation based on experimental evidence (Délèze, 1961; Hill, 1977; ter Keurs et al., 1978; Pollack, 1990), and can be stable based on theoretical considerations (Pollack, 1983; Chapter 4). If sarcomeres are stable on the descending limb of the F-L relation, instability arguments cannot be used to explain the differences between the fixed-end (fiber) and segment-clamped (sarcomere) F-L relations.

The purpose of this study was to determine the F-L relation of a muscle fiber when sarcomeres were at a stable, steady-state length. Because the fiber F-L relation was determined once the sarcomeres had reached a stable equilibrium position, differences in the F-L relation of fixed-end and segment-clamped preparations were explained based on the mechanical properties of the sarcomeres. Three models of muscle fibers were considered; each model contains sarcomeres that possess properties which have been observed experimentally. The results of this study demonstrate that sarcomeres with F-L properties as measured by Gordon et al. (1966b) cannot predict the F-L relation exhibited by fixed-end fibers. Also, the observation that the F-L relation of fixed-end fibers has an elongated plateau and increased forces compared to the F-L relation of segment-clamped sarcomeres can be predicted using a fiber model of stable sarcomere behavior.

Methods

In order to determine theoretically the F-L properties of a muscle fiber for fixed-end contractions, a fiber was modelled with two sarcomeres in series. The two sarcomeres in a given fiber were assumed to have identical mechanical properties and act independently. The sarcomere lengths at the beginning of each contraction were assumed to differ by 0.1 μm . Because the contractions were started at unequal sarcomere lengths, and therefore unequal sarcomere forces, one sarcomere shortened while the other sarcomere lengthened until a stable equilibrium was achieved. The F-L properties of this fixed-end fiber were calculated by determining the force of the fiber at a number of different fiber lengths. In order to compare the F-L relation of the fiber to that of sarcomeres (Gordon et al., 1966b), the forces were expressed as a function of the mean sarcomere length for the fiber.

Sarcomere properties

Three muscle fiber models were considered, each model possessing sarcomeres with different mechanical properties. The models are referred to as (1) the classic force-length model, (2) the cross-bridge stiffness model, and (3) the effective stiffness model (Figure 5.2).

Model 1: Classic force-length model

In model 1, the mechanical properties of the sarcomeres followed the classic F-L curve found by Gordon et al. (1966b). Force production (F) in a sarcomere was dependent only on the sarcomere length (SL):

$1.27 \mu\text{m} < SL < 1.67 \mu\text{m}$	$F = -2.667 + 2.1 SL$
$1.67 \mu\text{m} < SL < 2.00 \mu\text{m}$	$F = 0.04 + 0.48 SL$
$2.00 \mu\text{m} < SL < 2.25 \mu\text{m}$	$F = 1.00$
$2.25 \mu\text{m} < SL < 3.65 \mu\text{m}$	$F = 2.592 - 0.71 SL$

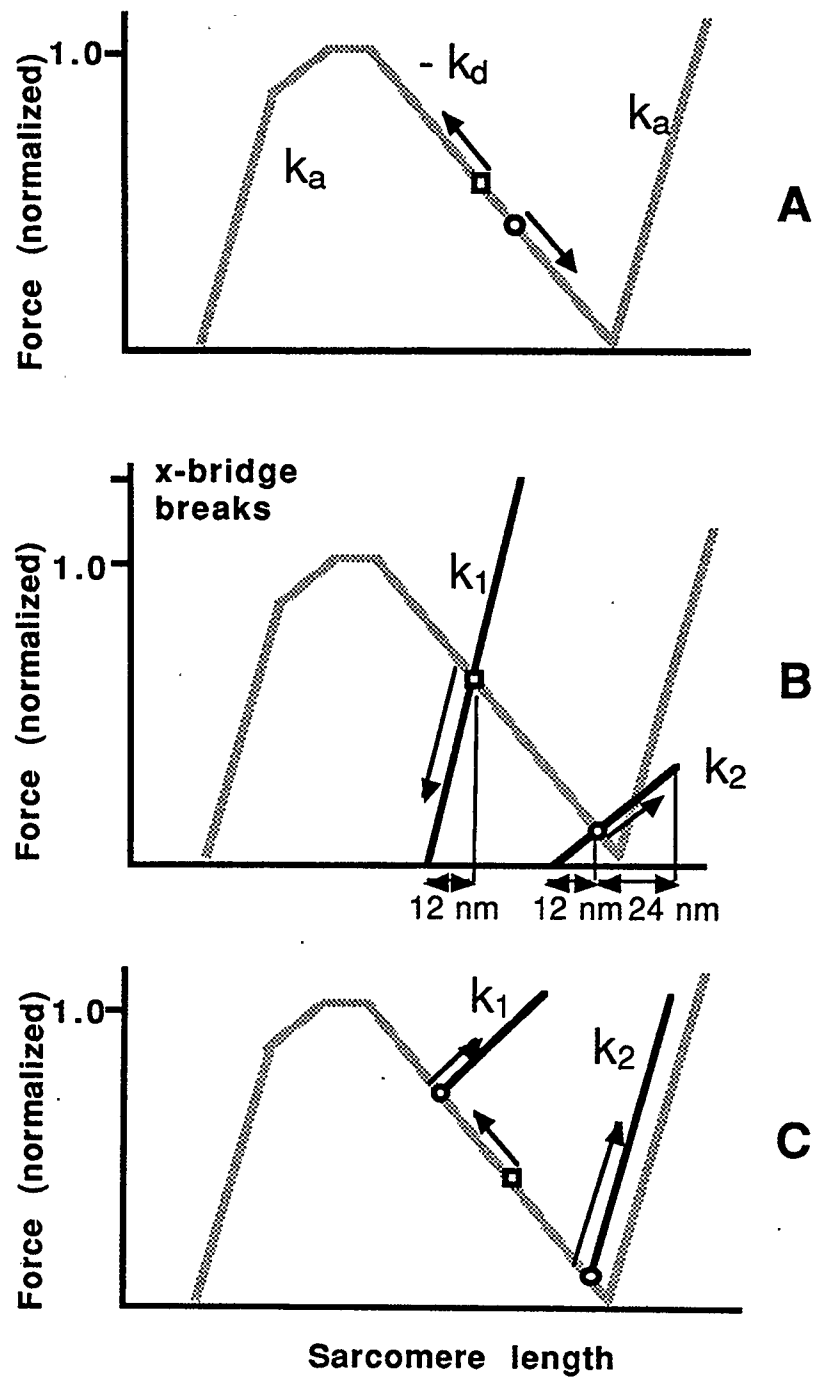


Figure 5.2. F-L properties of individual sarcomeres for model 1 (A), model 2 (B), and model 3 (C). Sarcomeres that shorten are illustrated with squares; sarcomeres that lengthen are illustrated with circles.

The main feature of this model is that the maximal tetanic force of a sarcomere decreases with increasing sarcomere length on the descending limb of the F-L relation (Figure 5.2A, $2.25 \mu\text{m} < SL < 3.65 \mu\text{m}$).

Model 2: Cross-bridge stiffness model

The sarcomeres in model 2 contain cross-bridge stiffness properties superimposed on the classic F-L curve (Figure 5.2B). Cross-bridge stiffness refers to the slope of the force-displacement curve for a sarcomere that is stretched or shortened quickly, resulting in an increase or decrease in force, respectively (Huxley and Simmons, 1971; Ford et al., 1977). Cross-bridge stiffness is typically assumed to originate in an undamped linear spring element in the tail portion (S2 subfragment) of the cross-bridge. Cross-bridge stiffness has a positive slope and is assumed to be proportional to the number of attached cross-bridges, or proportional to the amount of thick-thin myofilament overlap on the descending limb of the F-L relation (Huxley, 1957; Huxley and Simmons, 1971).

Each sarcomere possesses an individual cross-bridge stiffness curve determined by the initial sarcomere length. The cross-bridge stiffness curve is defined as a line intersecting a point on the descending limb of the F-L curve corresponding to the initial sarcomere length, and a point of zero force at a sarcomere length 12 nm / sarcomere shorter than the initial sarcomere length (Ford et al., 1977, their Figure 13). Thus, the cross-bridge stiffness on the descending limb of the F-L relation for frog is defined by $k_i = (2.6 - 0.7 x_i) / 0.012$, where k_i (normalized force / μm / sarcomere) is the slope of the fiber stiffness curve for sarcomere i at the initial length x_i (μm / sarcomere).

Model 3: Effective stiffness model

Model 3 incorporates history-dependent properties of sarcomeres which are stretched or shortened before reaching a stable (isometric) length (Figure 5.2C). After a sarcomere is stretched, during a tetanic contraction and on the descending limb of the F-L relation, its isometric force is larger than the corresponding isometric force without stretch (Hill, 1977; Edman et al., 1978; Julian and Morgan, 1979b; Edman et al., 1982). After a sarcomere is allowed to shorten, during a tetanic contraction, the isometric force is similar to the corresponding isometric force obtained without shortening (Edman et al., 1993). These history-dependent force properties of sarcomeres were modelled using an "effective stiffness" curve.

The effective stiffness curve associated with stretching of the sarcomeres was defined by a straight line connecting a point on the classic F-L relation, determined from the initial sarcomere length, with a point defined by the length and force at an isometric condition following a stretch (Hill, 1977, her Figure 2B). The slope of the effective stiffness curve increased with increasing sarcomere length on the descending limb of the sarcomere F-L relation (Hill, 1977; Edman et al., 1978; Edman et al., 1982). Here, the effective stiffness curve associated with stretch was defined by $k_i = -3.8 + 2.0 x_i$, where k_i (normalized force / μm / sarcomere) is the slope of the curve for sarcomere i at the initial length x_i (μm / sarcomere) (based on data shown by Edman et al., 1978, their Figure 4A). In model 3, sarcomeres that shorten follow the classic F-L curve; sarcomeres that lengthen follow the effective stiffness curve defined above (Figure 5.2C).

Rules of stability

The fixed-end, F-L relation for the three models was determined at stable, steady-state conditions. Stability in this case refers to the condition where any sarcomere perturbed from its equilibrium length will return to its equilibrium length. Stability for a fixed-end fiber composed of a number of independent sarcomeres in series occurs when the stiffness of all the sarcomeres is positive. Stability may also occur when all but one sarcomere have a positive stiffness, provided that the magnitude of the negative stiffness of the one sarcomere (if it occurs) is less than the magnitude of the positive stiffness of the remaining sarcomeres (Chapter 4).

Model 1: Classic force-length model

Instability in model 1 dictates that two sarcomeres cannot be on the descending limb of the sarcomere F-L relation simultaneously. For example, the fiber in model 1 is stable if one sarcomere is on limb A and the second sarcomere is on limb D (sarcomeres ad_1 and ad_2 , Figure 5.3). Similarly, the fiber is stable if one sarcomere is on limb D and the second sarcomere is on limb E (sarcomeres de_1 and de_2 , Figure 5.3). Also, the fiber is stable if both sarcomeres lie on any positively sloped region: A, B, or E (e.g., sarcomeres ae_1 and ae_2 , Figure 5.3). If both sarcomeres are on the plateau, region C, a stable force level is obtained; however, each sarcomere does not have a unique length. Sarcomeres on the plateau region could be considered quasi-stable because they do not alter the fiber F-L relation, but the sarcomeres are not strictly stable based on the stability definition given here.

Model 2: Cross-bridge stiffness model

In the previous model, the fiber is stable on all regions of the F-L relation, except when both sarcomeres lie on the descending limb. In contrast to model

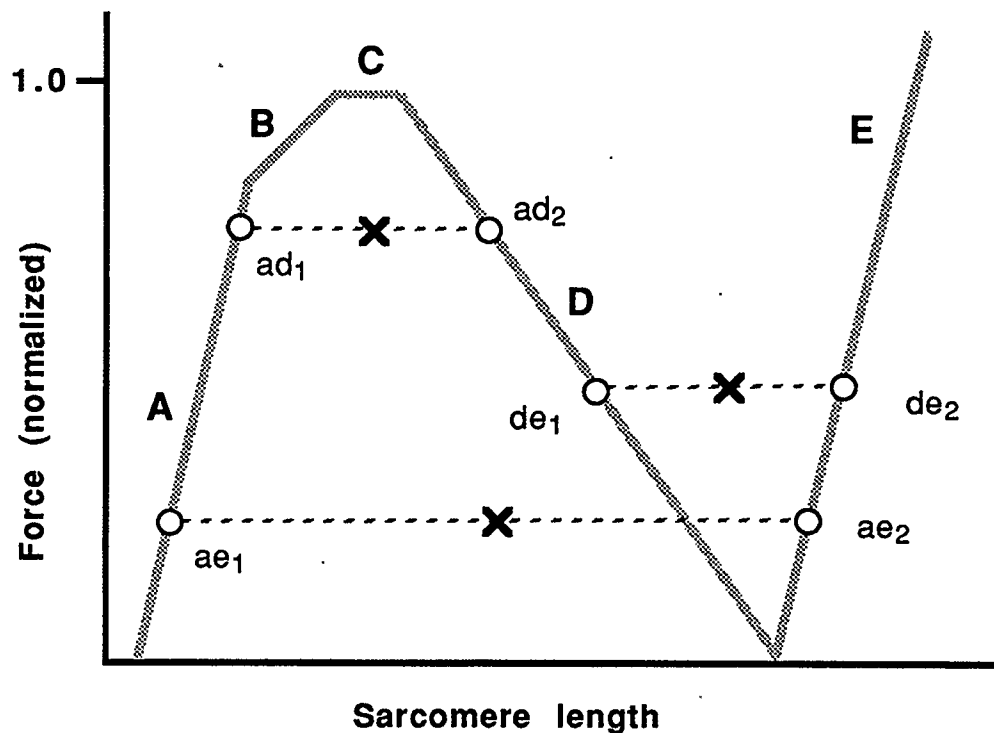


Figure 5.3: Model 1-- stable lengths of sarcomeres (open circles) for average sarcomere lengths of a fiber ("x"). The thick line represents the classic F-L relation for a sarcomere. See text for details.

1, model 2 is stable for sarcomere lengths in all regions of the F-L relation. Specifically, model 2 is stable on the descending limb of the F-L relation because each sarcomere follows a positive stiffness curve (k_1 and k_2 , Figure 5.4). The strong sarcomere will begin on the classic F-L relation (1s) and shorten along its cross-bridge stiffness curve (k_1), while the weak sarcomere will begin on the classic F-L relation (2s) and will be stretched along its cross-bridge stiffness curve (k_2 , Figure 5.4).

Model 3: Effective stiffness model

Like model 2, model 3 is also stable in all regions of the F-L relation except for sarcomere lengths between 2.250 and 2.255 μm . Sarcomeres on the descending limb of the F-L relation are stable (above 2.255 μm) because the magnitude of the effective stiffness for a sarcomere that lengthens is greater

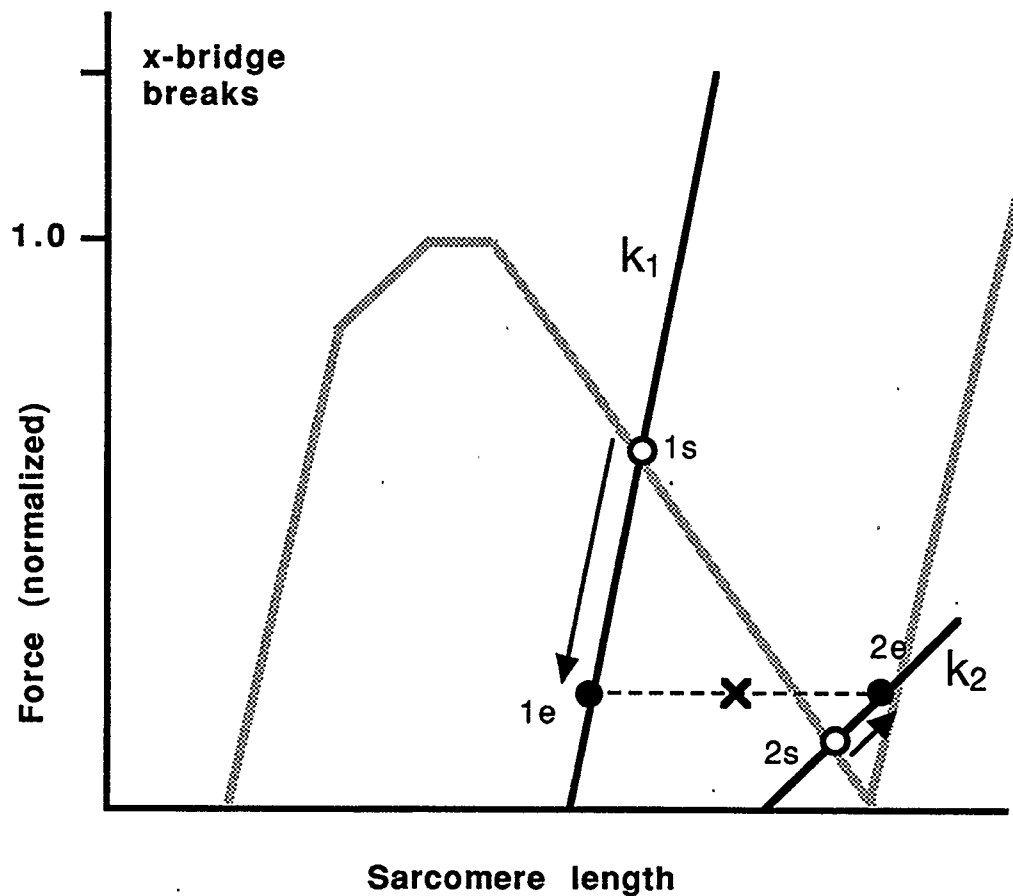


Figure 5.4. Model 2-- behavior of a two-sarcomere model with sarcomeres that follow the cross-bridge stiffness curves (solid lines). "x" indicates the force and average sarcomere length at equilibrium. The classic F-L curve for a sarcomere is represented (shaded line) along with the cross-bridge stiffness curves (solid lines, k_1 and k_2).

than the magnitude of the stiffness for a sarcomere that shortens. For example, for a fiber composed of two sarcomeres labelled 3 and 4, the force initially produced by sarcomere 4 (4s, Figure 5.5) is less than the force initially produced by sarcomere 3 (3s, Figure 5.5) and thus sarcomere 4 lengthens and sarcomere 3 shortens. The force in the sarcomere that is stretched (4) increases more rapidly (along the effective stiffness curve, k_4) than the force of sarcomere 3 that shortens along the classic F-L relation (Figure 5.5). The steady-state lengths of the sarcomeres (3e and 4e) produce a force in the fiber (calculated at

the average sarcomere length) which is higher than the force obtained using the classic F-L relation ("x", Figure 5.5). For sarcomeres near the plateau or with initially unstable mechanical properties, the steady-state may occur with sarcomeres on different regions of the F-L relation. For example, a fiber composed of two sarcomeres (labelled 1 and 2) with initial sarcomeres at lengths $1s$ and $2s$ may reach a steady-state with one sarcomere ($1e$) on the plateau region and the other sarcomere ($2e$) on its effective stiffness curve (k_2 , Figure 5.5).

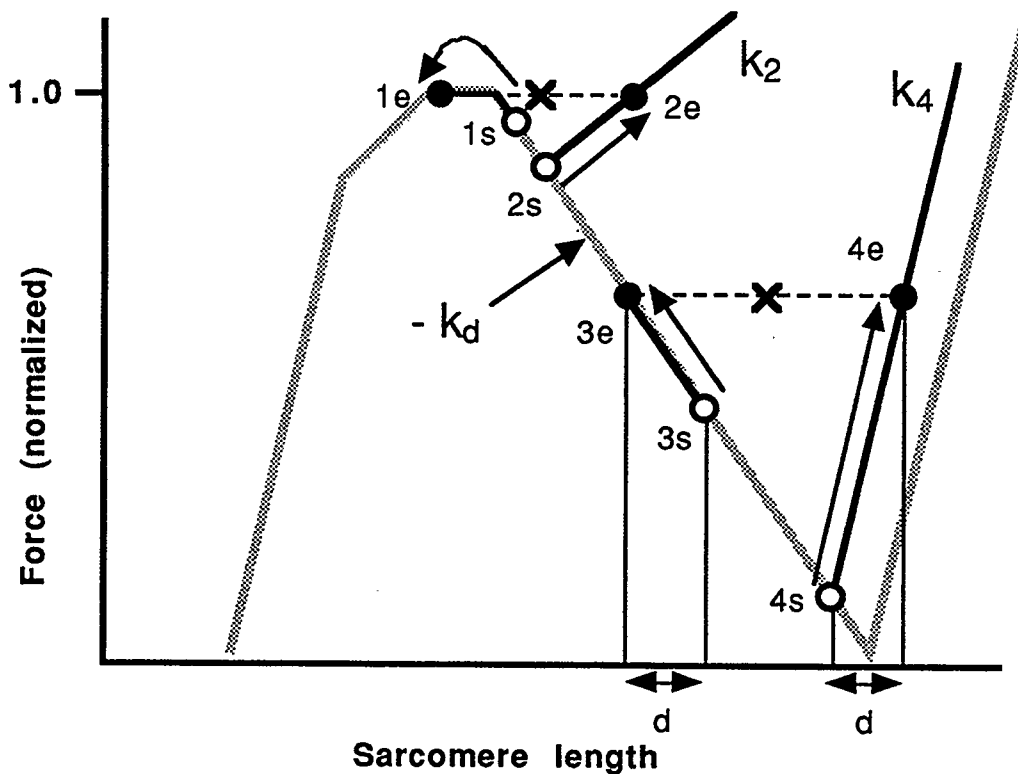


Figure 5.5. Model 3 -- response of a two-sarcomere model with sarcomeres that have individual shortening and stretching behaviors. Shortening sarcomeres follow the segment-clamped F-L curve (shaded line) and stretching sarcomeres follow their effective stiffness curves (k_2 and k_4). Equilibrium (solid circles) is reached at an average sarcomere length and force indicated by "x". Sarcomere behavior for a fiber length near the plateau is illustrated by sarcomeres 1 and 2 with the postscript "s" designating the initial sarcomere length, and "e" the equilibrium sarcomere length. Sarcomere behavior for a fiber at a long length is illustrated by sarcomeres 3 and 4.

Results

Models 1 and 2 did not predict F-L properties of a fixed-end fiber adequately, whereas model 3 did.

Model 1: Classic force-length model

The F-L curve calculated using model 1 consists of three ascending and two descending limbs (thin line, Figure 5.6). If the average sarcomere length of the fiber falls on the active ascending limb (regions A and B) and a portion on the plateau (region C) of the sarcomere F-L curve, the F-L behavior of the sarcomere and the fiber are identical. There is a discontinuity at an average sarcomere length just above 2.20 μm where stability can occur only when one sarcomere is in region A and the other sarcomere is in region D. The first descending limb of the fiber then occurs between 2.20 and 2.46 μm . The fiber has a second ascending limb between 2.46 and 3.075 μm , when one

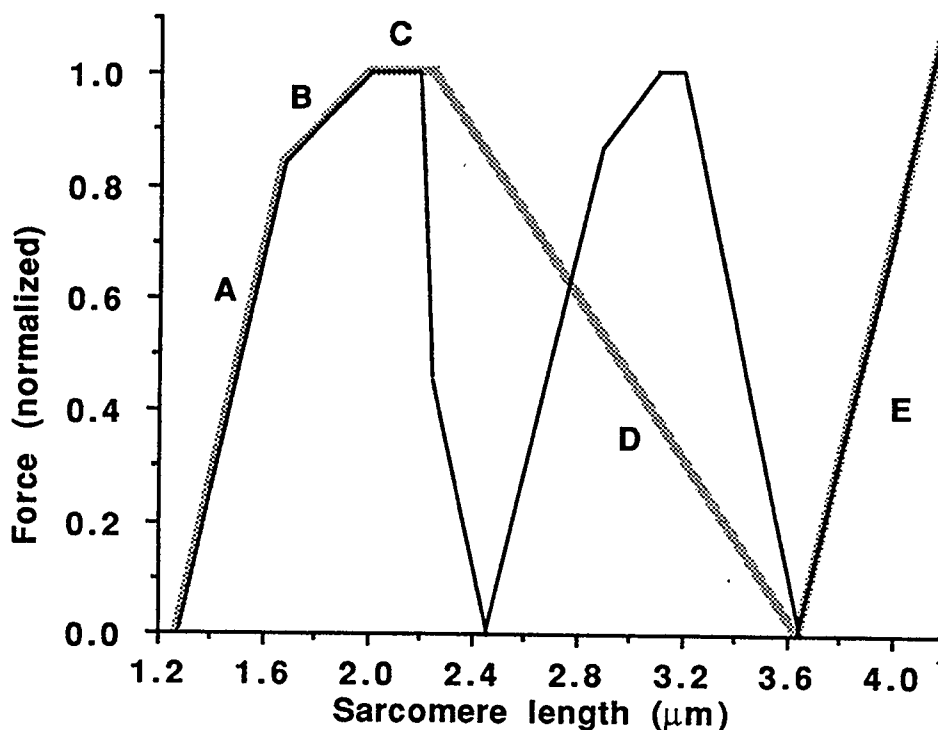


Figure 5.6. Model 1 -- force vs. average sarcomere length for the two-sarcomere model under fixed-end conditions and at stable equilibrium (thin line). The classic F-L curve for a sarcomere is represented by the thick line.

sarcomere is in region A and the other sarcomere is in region E. Between an average sarcomere length of 3.075 and 3.20 μm , a second plateau occurs with one sarcomere in region C and the other in region E. The second descending limb of the fiber occurs when one sarcomere is in region D and the other is in region E (average sarcomere lengths from 3.20 to 3.65 μm). The third ascending limb occurs when both sarcomeres are in region E of the sarcomere F-L curve.

The F-L relation for the fiber in model 1 is radically different than any F-L relation found experimentally. Based on this model, sarcomeres cannot follow the classic F-L relation of single sarcomeres during a fixed-end contraction of a fiber as described by Gordon et al. (1966b).

Model 2: Cross-bridge stiffness model

In model 2, the F-L curve for the two-sarcomere fiber is very close to the F-L properties of the single sarcomere (Figure 5.7). The equilibrium force for the fiber on the descending limb of the F-L curve is slightly lower than the corresponding isometric force of a single sarcomere except near the plateau, because the cross-bridge stiffness curve is greatest at 2.25 μm and decreases towards 3.65 μm (point "x", Figure 5.4). If the local stiffness increased with increasing sarcomere length on the descending limb (e.g., the effective stiffness curve in model 3), the equilibrium force produced by the fiber in model 2 would be higher than the corresponding isometric force of a single sarcomere.

From a practical point of view, the fiber and the sarcomere F-L curves are the same, because the magnitude of the cross-bridge stiffness is very large. Only small changes in sarcomere lengths are required to establish equilibrium for two sarcomeres located on the descending limb of the F-L relation. The close agreement between the F-L curves of the single sarcomere and the fixed-end fiber directly contradicts the corresponding experimental findings (e.g.,

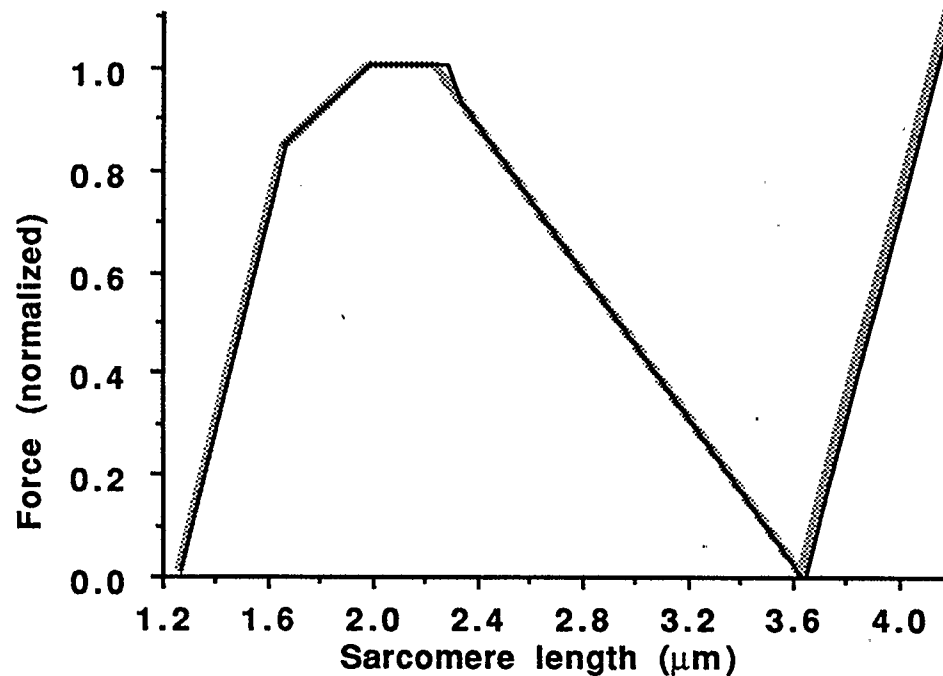


Figure 5.7. Model 2 -- force vs. average sarcomere length for the two-sarcomere model under fixed-end conditions and stable equilibrium (thin line). The classic F-L curve for a sarcomere is represented by the thick line.

Pollack, 1990, his Figure 2.8).

Model 3: Effective stiffness model

The stable F-L relation for the fiber in model 3 is qualitatively similar to what is observed experimentally (Figure 5.8). The fiber exhibits an F-L curve with an extended plateau region when compared to the individual sarcomere F-L curve, and the fiber exhibits force levels consistently higher than those of the individual sarcomere for corresponding lengths on the descending limb. Increasing the initial nonuniformity in sarcomere length shifts the fiber F-L curve to the right (not shown). The sarcomere and fiber F-L relations are identical on the ascending and passive limbs of the F-L relation. The fiber in model 3 qualitatively follows the experimentally observed F-L behavior of a fixed-end fiber (e.g., ter Keurs et al., 1978; Martyn and Gordon, 1988).

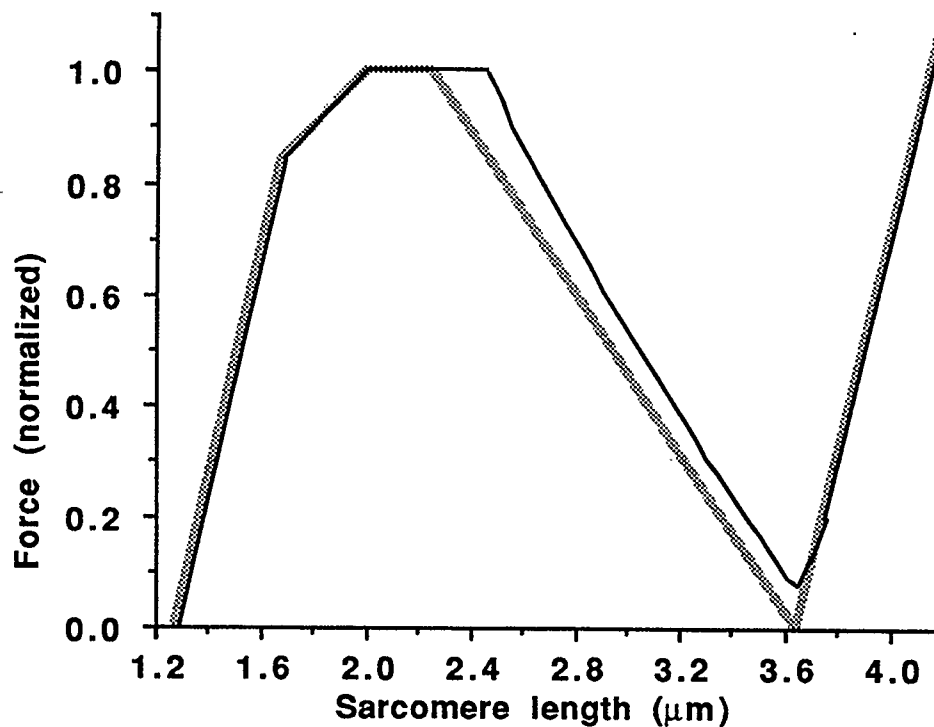


Figure 5.8. Model 3 -- force vs. average sarcomere length for the two-sarcomere model under fixed-end conditions and stable equilibrium (thin line). The classic F-L curve for a sarcomere is represented by the thick line.

Discussion

Evaluation of F-L Properties of the Three Models

Model 1: Classic force-length model

Based on the results of model 1, it appears that individual sarcomeres do not follow the F-L curve during fixed-end contractions as described by Gordon et al. (1966b). If individual sarcomeres or groups of sarcomeres followed the classic F-L curve, the F-L curve for fixed-end contractions would have more than one descending limb (Figure 5.6), which has never been found experimentally for any skeletal muscle preparation.

Large differences in sarcomere length would be expected if sarcomeres in a fiber possessed the F-L properties used in model 1. Based on this finding the difference in the length of two adjacent sarcomeres in the fiber model must

approach 2.40 μm or more (e.g., sarcomeres ae1 and ae2, Figure 5.3). Such large differences in adjacent sarcomere lengths have not been observed experimentally using laser diffraction (Paolini and Roos, 1975; ter Keurs et al., 1978; Tameyasu et al., 1982; Horowitz et al., 1992), light microscopy (Hill, 1977; Edman and Reggiani, 1984), or surface markers (Edman and Reggiani, 1984; Horowitz et al., 1992).

Using sarcomere F-L properties as described by Gordon et al. (1966b), the F-L predictions for a fiber during fixed-end contractions are unrealistic and do not agree with experimental observations. It is safe to conclude that sarcomeres in a fiber during fixed-end contractions will not behave as described by Gordon et al. (1966b).

Model 2: Cross-bridge stiffness model

The fixed-end F-L curve obtained using model 2 was more similar to the F-L relations observed experimentally for fibers during fixed-end contractions than the curves predicted using model 1. However, the fiber F-L relation, when compared to the sarcomere F-L relation, did not exhibit larger forces at corresponding sarcomere lengths on the descending limb of the F-L relation as has been found experimentally (e.g., ter Keurs et al., 1978; Martyn and Gordon, 1988).

The sarcomere properties used in model 2 are those of model 1 with the addition of cross-bridge stiffness on the descending limb of the F-L relation. The cross-bridge stiffness properties are limited in time and distance of relative myofilament movements because cross-bridges are continuously cycling (Huxley, 1957), even if there is no relative myofilament movement. Cross-bridge stiffness also has a limited working range, about 24 nm / sarcomere for stretching and 12 nm / sarcomere for shortening (Flitney and Hirst, 1978 and Ford et al., 1977, respectively). As soon as a cross-bridge detaches, its cross-

bridge stiffness is lost. If a contraction lasts for an extended period of time or involves large length changes, the cross-bridge properties assigned to model 2 would disappear until the cross-bridge reattaches.

If the cross-bridge stiffness properties in model 2 disappeared, the F-L behavior of model 2 would be similar to that predicted for model 1. Once a cross-bridge detaches, it is presumed that the head of the myosin will reattach at the new sarcomere length and produce a force corresponding to the classic F-L curve. For example, if a sarcomere were stretched, its force production would increase along the cross-bridge stiffness curve until cross-bridge detachment occurred. Reattachment of the cross-bridge would occur at a longer sarcomere length and produce a lower force based on this new sarcomere length and the classic F-L relation. This force would be lower than the force level before the detachment and the sarcomere would be stretched until cross-bridge detachment occurred again. Thus, the sarcomere would continue lengthening to a lower force-producing potential while on the descending limb of the classic F-L relation, similar to model 1. The resulting F-L relation for the fiber with cross-bridge detachment would resemble that of model 1. Cross-bridge properties used in model 2 do not illustrate the F-L behavior of a fixed-end fiber, and adding the possibility of cross-bridge detachment did not improve the results.

Model 3: Effective stiffness model

Model 3 exhibits an F-L relation for a fiber during fixed-end contractions that is consistent with the corresponding relations found experimentally (e.g., ter Keurs, 1978; Martyn and Gordon, 1988). The effective stiffness model exhibits an F-L relation for the fiber with an extended plateau region and with forces exceeding the forces of the sarcomere F-L curve at corresponding sarcomere lengths on the descending limb.

Model 3 predicts qualitatively much of the sarcomere and F-L properties observed experimentally in muscles and muscle fibers. These observations are:

- 1) The fixed-end F-L curve has an extended plateau and its forces exceed the corresponding forces of the segment-clamped F-L curve (Pollack, 1990, his Figure 2.8).
- 2) Sarcomere populations diverge slightly in length from their initial lengths until the steady-state is reached -- weaker sarcomeres stretch slightly and stronger sarcomeres shorten slightly (Paolini and Roos, 1975; ter Keurs et al., 1978; Tameyasu et al., 1982; Edman and Reggiani, 1984; Horowitz et al., 1992).
- 3) Length differences between the shortening and lengthening sarcomeres should be small and should not approach $2.4\ \mu\text{m}$ (Paolini and Roos, 1975; Hill, 1977; ter Keurs et al., 1978; Tameyasu et al., 1982; Edman and Reggiani, 1984; Horowitz et al., 1992).
- 4) Sarcomeres approach a constant length at lengths corresponding to the descending limb of the F-L relation (Julian and Morgan, 1979a, Fig. 7; Edman and Reggiani, 1984, Fig. 4; Lieber and Baskin, 1983, Fig. 7; ter Keurs et al., 1978, Figs. 5 and 6).
- 5) Increased nonuniformity in the initial sarcomere lengths results in a more extended plateau and larger forces on the descending limb when comparing the fiber to the sarcomere F-L relation (Edman and Reggiani, 1987; Bagni et al., 1988).

The effective stiffness properties assigned to sarcomeres in model 3 have been observed experimentally, and these properties persist for long periods of time (i.e., seconds, Edman et al., 1982). Also, the predictions of the F-L properties of a fiber during fixed-end contractions using sarcomeres with the effective stiffness properties agree with all the basic observations made

experimentally. However, the effective stiffness properties are associated with a positive slope for sarcomeres that lengthen during the fixed-end fiber contraction, and a negative slope for the corresponding sarcomeres that shorten.

The fiber models considered in this study only contained two sarcomeres; therefore, model 3 could be shown to be stable at virtually all sarcomere lengths. However, a real fiber may contain thousands of sarcomeres. Since the conditions for stability, as defined here, do not allow for more than one sarcomere to have a negative stiffness, no more than one sarcomere is allowed to shorten in model 3. A shortening sarcomere is associated with the classic sarcomere F-L relation (Gordon et al., 1966b) which is negatively sloped on the descending limb. This potential problem with instability may be overcome, at least conceptually, by assuming that the shortening sarcomeres follow a negatively sloped F-L relation, but slight perturbations in sarcomere length would produce a positive stiffness because of the properties of cross-bridges. Further analysis is required to describe the detailed behavior of fibers with a large number of sarcomeres working on a negatively sloped F-L relation.

The force enhancement observed for fixed-end fibers or whole muscles compared to segment-clamped fibers on the descending limb of the F-L relation has been associated with instability of the sarcomeres and nonuniform sarcomere length changes. Based on the present work, we suggest that this force enhancement can be explained, at least in part, by the effective stiffness properties of sarcomeres as observed by Hill (1977), Edman et al. (1978), and Edman et al. (1982). The force enhancement depends on the nonuniformity of the sarcomere length, the effective stiffness properties, and the position of the sarcomeres on the descending limb of the F-L relation. Model 3 can be used to calculate this force enhancement based on these parameters.

Chapter 6

Sarcomere Stability on the Descending Limb of the Force-Length Relation of Mouse Skeletal Muscle

Introduction

The maximal isometric force potential of skeletal muscle, muscle fibers, and small groups of sarcomeres varies as a function of length and is termed the force-length (F-L) relation (Figure 6.1). Because a portion of the F-L relation has a negative slope (descending limb), it has been stated repeatedly that muscle fibers and sarcomeres are unstable when operating at lengths on the descending limb of the F-L relation (Hill, 1953; Huxley and Peachey, 1961; Gordon et al., 1966; Julian et al., 1978; Julian and Morgan, 1979a; Lieber and Baskin, 1983; Edman and Reggiani, 1984).

Stability in a muscle is defined to exist only if the potential energy, which is a function of length, has a minimum. The descending limb of the F-L relation has a negative slope, so the potential energy does not have a minimum over these lengths. Because of this supposed instability, sarcomeres can not reach a steady-state length and remain on the descending limb of the F-L relation.

The instability argument follows this reasoning: muscle fibers are composed of a large number of sarcomeres in series, and an inequality in force

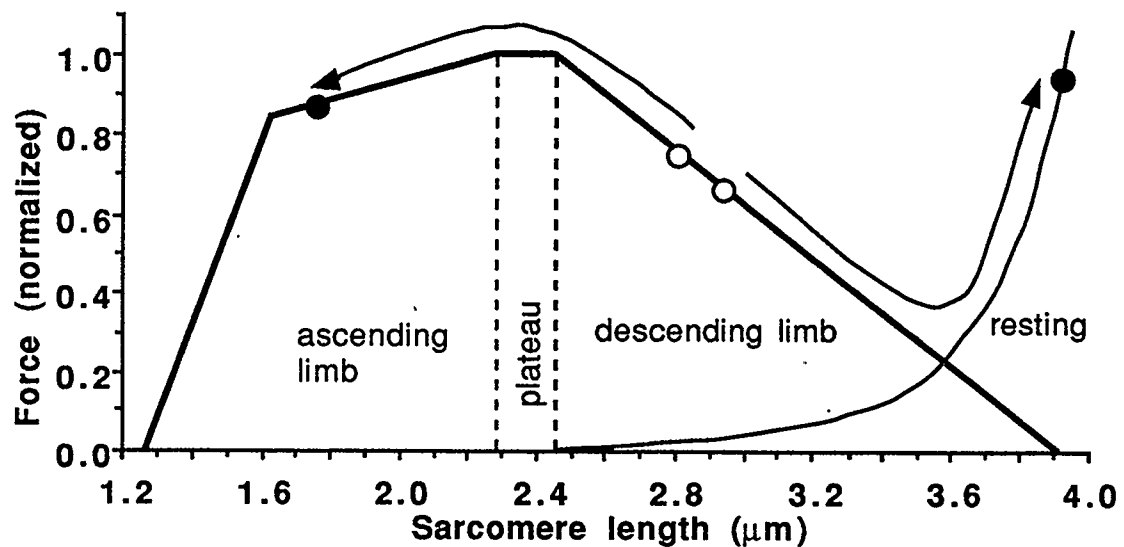


Figure 6.1. Sarcomere force-length relation for mouse skeletal muscle under isometric conditions based on a thin myofilament length of $1.14\ \mu\text{m}$ (Phillips and Woledge, 1992) and a thick myofilament length of $1.63\ \mu\text{m}$ (Sosa et al., 1994). Open circles represent two sarcomeres in the same fiber that begin a contraction at different initial lengths and then become more nonuniform in length during the contraction (an unstable behavior).

production between sarcomeres occurs because of differences in the initial sarcomere length, differences in sarcomere cross-sectional area, or differences in sarcomere activation. Any differences in force production by the sarcomeres would result in some sarcomeres shortening and some sarcomeres lengthening. If the sarcomeres in a fiber follow the F-L relation and are operating at lengths on the descending limb of the F-L relation, unstable behavior will result (Hill, 1953): the weak (long) sarcomeres would be stretched by the strong (short) sarcomeres (open circles, Figure 6.1). Thus, for fibers operating on the descending limb of the F-L relation, some sarcomeres should lengthen onto the resting limb, and some sarcomeres should shorten onto the active, ascending limb of the F-L relation. Differences in sarcomere length of greater than $1.6\ \mu\text{m}$ would occur since no sarcomeres can remain on the descending limb of the F-L relation.

Various techniques have been used to determine that some sarcomeres elongate and some shorten in frog, single fiber preparations during fixed-end contraction (Huxley and Peachey, 1961; Gordon et al., 1966; Julian et al., 1978; Julian and Morgan, 1979a, 1979b; Morgan et al., 1982; Lieber and Baskin, 1983; Edman and Reggiani, 1984; Sugi and Tsuchiya, 1988; Granzier and Pollack, 1990). Many investigators have concluded that the descending limb of the F-L relation is not stable based on these measurements of nonuniform changes in sarcomere length along the length of single fibers (Huxley and Peachey, 1961; Gordon et al., 1966; Julian et al., 1978; Julian and Morgan, 1979a; Lieber and Baskin, 1983; Edman and Reggiani, 1984). They claim sarcomeres will continue shortening or lengthening until a stable condition is reached. Thus, sarcomeres should eventually reach length differences greater than 1.6 μm . Although nonuniformities in sarcomere length may develop during a fixed-end contraction, the sarcomere length-time behavior may exhibit stable behavior.

In spite of the negatively sloped region of the F-L relation and the increase in sarcomere length nonuniformities, some investigators have suggested that sarcomeres in muscle fibers are stable on the descending limb of the F-L relation, but they did not provide rigorous theoretical or experimental evidence for their statements (Délèze, 1961; Hill, 1977; ter Keurs et al., 1978; Pollack, 1983; Pollack, 1990). Recently, it has been demonstrated analytically that a sarcomere with mechanical properties which have been observed experimentally can be stable, yet possess a negatively sloped F-L region (Chapter 4). Two indications of stable sarcomere length behavior have not been investigated: the shape of the sarcomere length-time traces and whether sarcomere length differences become greater than 1.6 μm .

The purpose of this study was to measure the nonuniformities in sarcomere length in mouse skeletal muscle and to determine whether or not sarcomeres exhibit stable length behavior at lengths on the descending limb of the F-L relation during fixed-end contractions. It is demonstrated that the sarcomere length behavior observed in mouse muscle is similar to that of amphibian single fibers. A model is presented that illustrates the expected sarcomere length-time behavior for a stable fiber and an unstable fiber. It is suggested that the sarcomere length-time traces observed here and found in the literature indicate stable rather than unstable sarcomere behavior on the descending limb of the F-L relation.

Although sarcomere length nonuniformities have been measured in many studies using single fiber preparations of frog skeletal muscle, little work is available involving the sarcomere length behavior in whole muscle preparations (amphibian skeletal muscle studies, ter Keurs et al., 1978, and Paolini and Roos, 1975); and in particular, mammalian skeletal muscle. It is not known if the nonuniform sarcomere length behavior observed in single fibers also occurs in muscle preparations. In addition, it is not clear if nonuniform sarcomere length changes necessarily support the instability hypothesis.

Methods

In the first section of the methods, a fiber model is described which demonstrates the expected sarcomere length-time behavior for a stable and an unstable fiber. In the second section of the methods, the experimental approach used to measure the nonuniformities in sarcomere length on the descending limb of the F-L relation in muscle is described.

Stable and unstable fiber models

As defined previously, a stable muscle fiber must possess a minimum in the potential energy function. The potential energy of a fiber is only dependent on the F-L properties of the sarcomeres. Velocity dependent force properties do not affect the potential energy function, so they may be ignored when evaluating the stability of a muscle fiber. A stable fiber may have a transient change in sarcomere length, but the sarcomeres will eventually reach a steady-state length, which can occur on the descending limb of the F-L relation. Sarcomeres in an unstable fiber will never settle to a steady-state length on the descending limb of the F-L relation, but will increase in length, or oscillate with and increasing amplitude in an unbounded manner.

In order to evaluate if the sarcomere length-time traces found experimentally are stable or unstable, models of a stable and an unstable muscle fiber were developed (Appendix). Each fiber was composed of two sarcomeres in series (Figure 6.2A). The force produced by each sarcomere was assumed to be a function of its length (F-L relation, Figure 6.2B) and the speed of contraction (force-velocity relation, Figure 6.2C). The sum of the length and velocity dependent forces was defined as the total force output for each sarcomere. The mechanical properties were based on those of the serratus anterior muscle of the mouse.

Force-velocity properties were included in both fiber models to illustrate that stability is not affected by velocity-dependent properties. Both fiber models had identical force-velocity relations that were assumed to be linear within the range of experimentally observed sarcomere velocities (thick line, Figure 6.2C). Only the period in which the sarcomeres were fully activated was considered. Sarcomeres began the contraction at different initial lengths. The ends of each fiber were fixed to represent a fixed-end contraction.

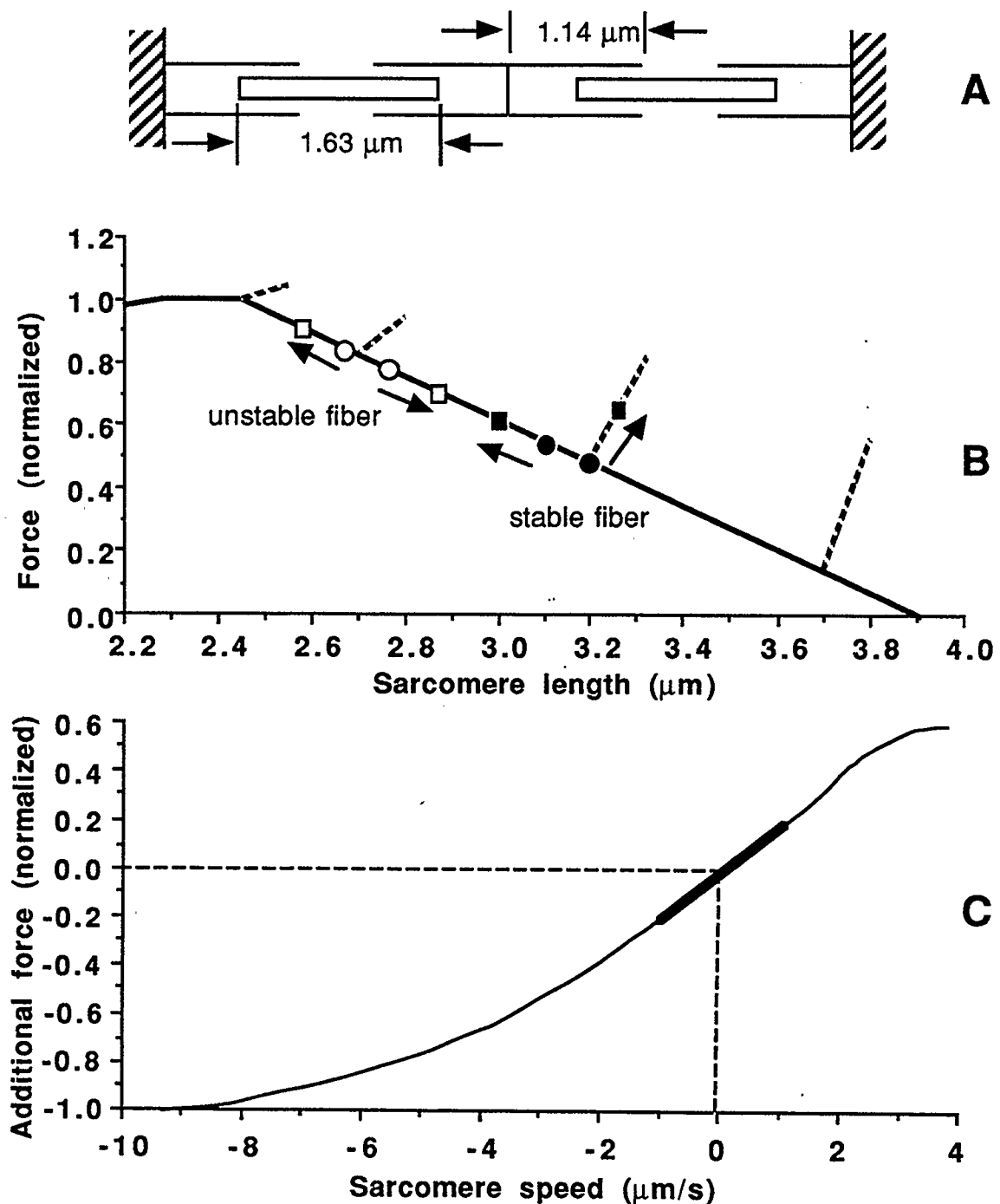


Figure 6.2. (A) Muscle fiber model composed of two sarcomeres. (B) Force-length relation for sarcomeres. The circles represent the initial length of the two sarcomeres and the boxes represent the behavior during contraction. Filled symbols illustrate the behavior of the stable fiber, and the hollow symbols represent the behavior of the unstable fiber. (C) Additional force that depends on the speed of shortening (-) or lengthening (+) and is added to the F-L relation to get the total sarcomere force.

An unstable fiber was developed using the descending limb of the F-L relation from frog single fibers (Gordon et al., 1966b). The force produced by an isometric sarcomere decreased as sarcomere length increased (open symbols, Figure 6.2B). Because of the negative slope of the F-L relation, the potential energy function does not have a minimum and the fiber is unstable.

Sarcomeres in the stable fiber followed different F-L curves depending on whether the sarcomere shortened or lengthened. Shortening sarcomeres followed the descending limb of the F-L relation (Edman et al., 1993), and lengthening sarcomeres followed a F-L curve with a positive slope. The positive slope during lengthening increased with increasing initial sarcomere length, as has been observed experimentally (Abbott and Aubert, 1952; Hill, 1977; Edman et al., 1978; Edman et al., 1982). The slope of the F-L relation for a lengthening sarcomere was greater in magnitude than for a shortening sarcomere. A fiber with these properties has a minimum in the potential energy function and is stable.

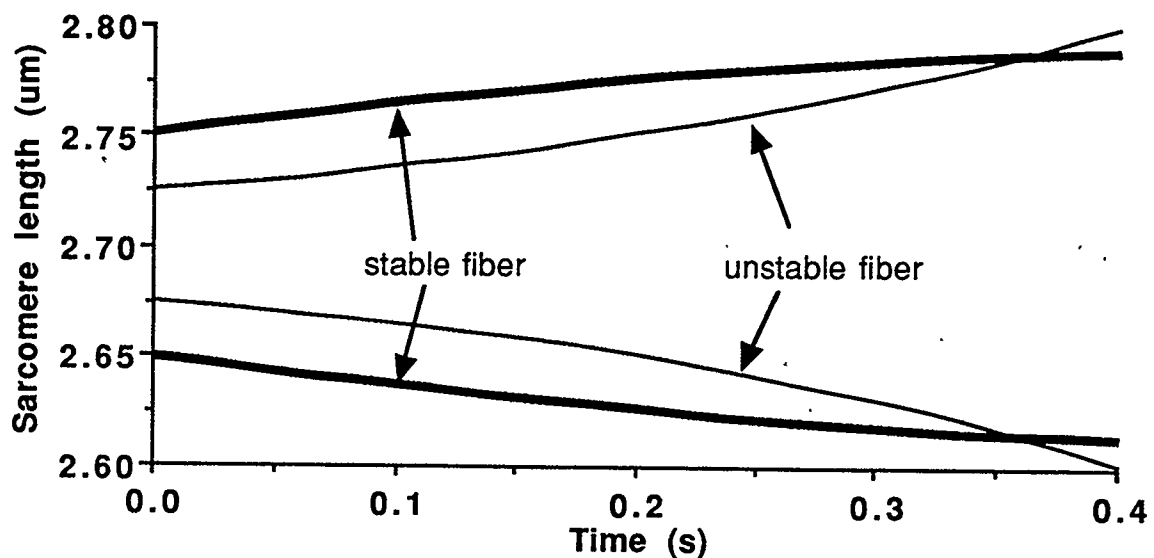


Figure 6.3. Sarcomere length-time behaviors from the unstable (thin line) and the stable (thick line) fiber composed of two sarcomeres. Only the time during contraction is shown.

Results from the model of the stable and unstable fiber illustrate that the sarcomere length for the two sarcomeres diverges in both the stable and unstable fiber models (Figure 6.3). In the stable fiber model, the speed of sarcomere lengthening or shortening decreases asymptotically over time and approaches a steady-state length (zero $\mu\text{m/s}$ change in sarcomere length). In the unstable fiber model, the speed of sarcomere lengthening or shortening increases exponentially in an unbounded manner.

The sarcomere length-time behavior for the stable fiber could be classified as an over damped system. If the sarcomere length changes observed experimentally reversed direction (i.e., shortening to lengthening or lengthening to shortening), this would indicate a stable system that is critically- or under-damped. Thus, another characteristic of stable sarcomere length-time behavior is a reversal in length change

The model of the stable and unstable fiber illustrate that an increase in sarcomere length nonuniformity is not an indication of instability since both the stable and unstable fiber may exhibit such a behavior. Therefore, it is incorrect to conclude that an increase in sarcomere length nonuniformity demonstrates unstable behavior on the descending limb of the F-L relation.

Based on these theoretical considerations, three criteria were identified which could be used to evaluate whether or not the sarcomere length-time traces measured experimentally were stable. Criteria for a stable behavior were: (1) a decreasing rate of sarcomere length change, (2) speed of shortening or lengthening approaching zero (a steady-state length), and (3) a reversal in sarcomere length changes.

Experimental sarcomere length measurements

Preparation

Fifteen muscle preparations were used from the distal head of the mouse serratus anterior (14.9 ± 4.0 g body weight). The distal head of the serratus anterior originates from the vertebral border of the scapula and inserts into rib 7. The fibers in this preparation were fusiform and ran from the scapula to the rib with no visible tendon. Little series elasticity existed in the preparation because of the lack of tendon and the rigid bony attachment sites. The muscle preparation forms a flat band of fibers about 11.1 ± 1.2 mm long (scapula to rib), about 0.7 ± 0.2 mm wide, and about 0.3 ± 0.1 mm thick.

Mice were anaesthetized by interperitoneal injection of sodium pentobarbital ($2 \mu\text{l/g}$ body weight). Muscle tissue was perfused through the left ventricle of the heart with a bathing solution to remove blood from the muscle. The muscle was then dissected from the surrounding tissue under a dissection microscope while submersed in a bathing solution. Fibers in this preparation were disturbed minimally during dissection because the adjacent head of serratus anterior (inserting into rib 6) only attaches to one edge of the distal head (along about half of its length; Figure 6.4A). The scapula was perforated and the rib was cut to fit in the experimental apparatus. The scapula and rib were used as attachment sites to a motor (scapula) and force transducer (rib). Loose connective tissue was removed from the muscle preparation.

Once the dissection was complete, the muscle was placed in the experimental chamber and was allowed to equilibrate. The muscle was exposed to single twitch conditioning contractions (1 Hz) for at least one half hour, followed by several tetanic stimulations before the experimental procedures were started. These contractions were performed at a sarcomere length of about $2.5 \mu\text{m}$.

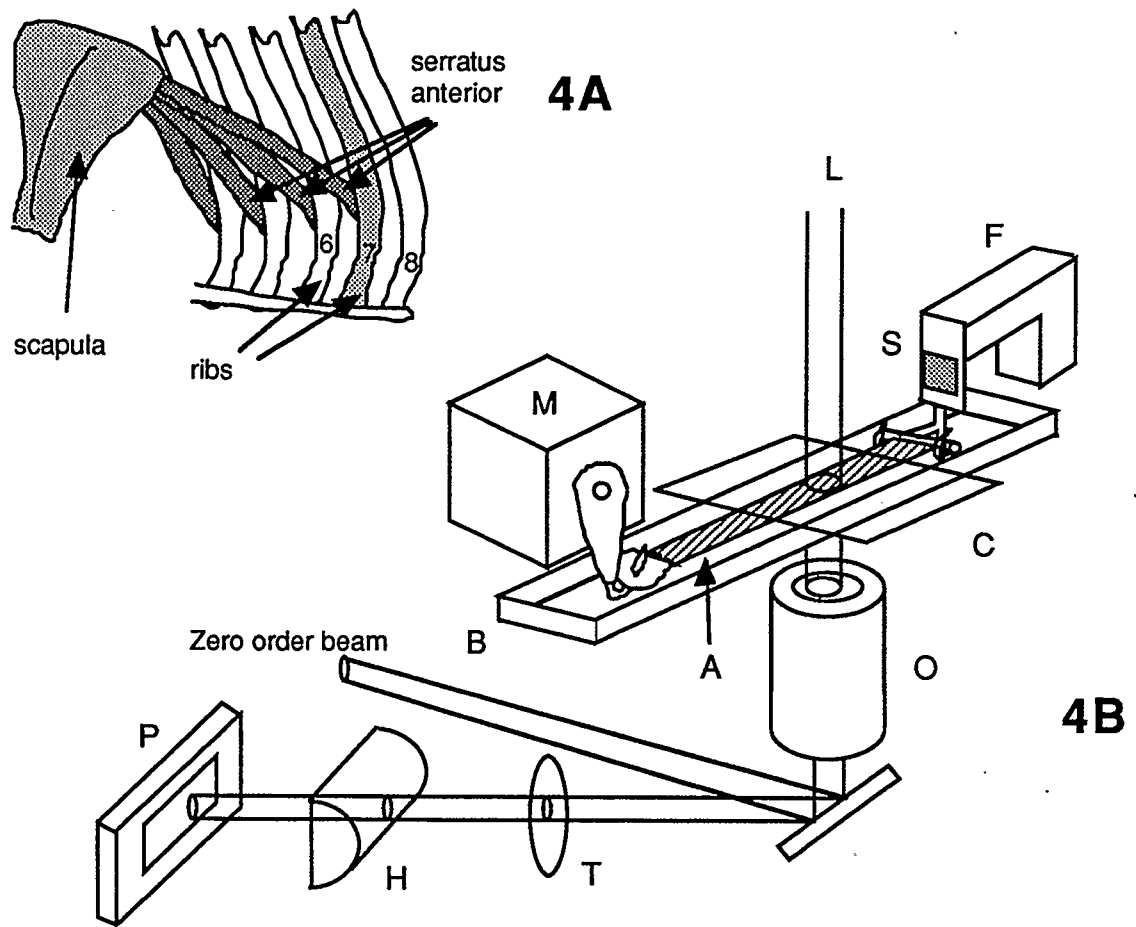


Figure 6.4. Diagram of the serratus anterior muscle as seen from a left lateral view of the mouse (4A). Schematic of the experimental set-up (4B). Bathing solution flowed past the muscle from the force transducer end to the motor end of the bath. A - muscle specimen, B - bath, C - cover slip, F - micro-manipulator, H - half cylindrical lens, L - laser beam, M - motor, O - microscope objective, P - photodiode array, S - strain gauge transducer, T - converging lens.

After the conditioning contractions, the muscle was set at the optimal length ($2.5\ \mu\text{m}$ sarcomere length) and three control contractions were performed. These control contractions were remeasured periodically during testing to determine if muscle force had deteriorated. If the control force decreased by more than 10% from the initial values, the experiment was discontinued.

Bathing solution

The bathing solution used for perfusion, dissection, and during the experiment consisted of 118.1 mM NaCl, 3.4 mM KCl, 0.8 mM MgSO₄, 1.2 mM KH₂PO₄, 1.8 mM CaCl₂, 24 mM NaH₂CO₃, and 10 mM dextrose. The solution was vigorously bubbled with 95% O₂ and 5% CO₂ both during dissection and experimentation (pH 7.5). The bathing solution continuously flowed through both the dissection chamber and the experimental chamber (rate 6 ml/min) at room temperature (20°C).

Experimental apparatus

The experimental apparatus consisted of an experimental chamber, a motor, a force transducer, and a sarcomere length measurement system (Figure 6.4B). The apparatus was mounted on a plate attached to the stage of an inverted microscope.

The experimental chamber was constructed with plexiglass walls and with a glass slide bottom. During the experiment a cover slip was placed over the top of the chamber to remove light aberrations caused by the surface vibrations and meniscus effects of the bathing solution. A motor (Model 6350, Cambridge Technology., Watertown, MA) controlled the length of the muscle at the scapular end.

Muscle force was measured with a semiconductor strain gauge transducer (built in-house) connected to an amplifier (PM1000, CWE Inc., Ardmore, PA) in a half-bridge configuration. The force transducer had a sensitivity of 31 mN/V at an amplifier sensitivity of 10 mV and a resonant frequency of 2300 Hz. The force transducer was attached to a micromanipulator capable of orienting the muscle perpendicular to a laser beam and parallel to the direction of pull of the motor. The force transducer remained in a fixed

position throughout the experiment.

Sarcomere length was measured with a laser diffraction system. When a laser beam is projected through a muscle, the different refractive indices of the A and I bands of the sarcomeres produce a diffraction pattern. Measurement of the deviation of the first-order diffraction peak from the zero-order peak gives a direct measure of sarcomere length. Thus, this system measured the average sarcomere length of the sarcomeres within the region illuminated by the beam (resolution about 5 nm). A 10 mW He-Ne laser (Model 1125, Uniphase, Manteca, CA) with a beam diameter of 0.8 mm was directed through the top of the experimental chamber perpendicular to the long axes of the muscle fibers. The diffracted beam from the muscle was collected in a 10X objective lens (N.A. 0.5, Nikon) and reflected through the access port in the microscope. The diffracted beam was then refracted by a telescopic lens and a cylindrical lens to compress the diffraction pattern onto a photodiode array (RL-128A, Reticon Corp., Sunnyvale, California). An amplifier (ter Keurs et al., 1978) produced an analog signal proportional to sarcomere length based on the median intensity of the first-order diffraction pattern measured by the photodiode array (2000 Hz). The sarcomere length measurement system was calibrated using the 4th, 5th, and 6th order diffraction pattern from a 12.5 μm grating which was placed in the experimental chamber with the bathing solution and the cover slip.

Stimulation

The muscle preparations were stimulated tetanically through two platinum wires running the entire length of the chamber, parallel to the muscle fibers, and attached to the bottom of the test chamber. Tetanic stimulation was achieved using a square wave pulse of 0.5 ms duration at 200 Hz, and a train duration of 250 or 300 ms (Model S88F, Grass Instruments, Quincy, MA). The stimulation voltage was set supramaximally (typically 20-30 V) before the

conditioning twitches, and reset with tetanic contractions before the experimental protocol. A rest period of at least 100 seconds was provided between tetanic stimulations.

Data Collection

Data collection and initiation of the contractions were controlled by a personal computer (IPC 386). The computer digitally recorded muscle length (from motor), sarcomere length (laser diffraction system), and force (force transducer) at a sampling frequency of 1000 Hz and triggered the stimulator. The analog signals from the equipment were collected through an A/D board (DT 2821, Data Translation Inc., Marlborough, MA) and were displayed on the computer monitor. A video camera mounted on a dissecting microscope above the muscle preparation was used to calibrate the muscle length and observe the muscle during testing.

Experimental procedure

Sarcomere length measurements were made at various locations across the width and along the length of the muscle at rest and during contraction. Resting sarcomere length was measured by manually translating the muscle (microscope stage) under the laser beam while the sarcomere length was recorded. Resting sarcomere length across the width of the muscle was performed at two distances from the rib end of one muscle. Sarcomere length along the length of the muscle was measured by translating the muscle under the laser beam along the long axis of the muscle, so the same group of fibers was illuminated by the laser.

Nonuniformities in sarcomere length during contraction were measured across the width and along the length of the muscle under fixed-end conditions (i.e., the ends of the muscle were held stationary). The muscle was stimulated tetanically and sarcomere length was measured at one location on the muscle.

The muscle was then moved using the microscope stage so a different group of sarcomeres was illuminated by the laser beam. Tetanic stimulation and data collection were performed at this new location on the muscle. This procedure was repeated on as many locations as possible on the muscle. The muscle length was then changed and the above procedure was repeated. In order to address any nonuniformities in sarcomere length behavior across the width of the muscle during contraction, sarcomere length was measured at three locations (proximal edge, center, and distal edge near the rib end) perpendicular to the long axis of the muscle. Nonuniformities in sarcomere length during contraction were also measured at different locations along the length of the muscle (parallel to the long axis of the muscle).

Typically, sarcomere length was recorded from three locations on the muscle and at various muscle lengths. However, in some muscle preparations sarcomere length measurements could be made at only one or two locations on the muscle, at different muscle lengths. A total of 143 contractions were collected at 26 locations along the length of 12 muscles.

In order to make sarcomere length measurements from the same group of sarcomeres at different muscle lengths, surface markers (6-0 silk) or natural markers on the muscle (connective tissue) were used to reposition the laser beam. The first contraction at a new muscle length was discarded because the peak force levels were lower than in the successive contractions which were almost identical.

Data analysis

Sarcomere length data were used for analysis only if the intensity of the first-order laser diffraction pattern was clear throughout the contraction. The raw sarcomere length signals were analyzed and are presented here. A moving average filter (± 20 ms) was used to smooth the sarcomere length traces

displayed in the results.

Sarcomere length-time traces exhibited four basic types of behaviors (Figure 6.5). For each sarcomere length-time trace, the mean sarcomere length was determined for three time periods: prior to contraction (resting length, l_r), during early tetanus (25 - 45 ms of contraction, l_e), and during the plateau of the

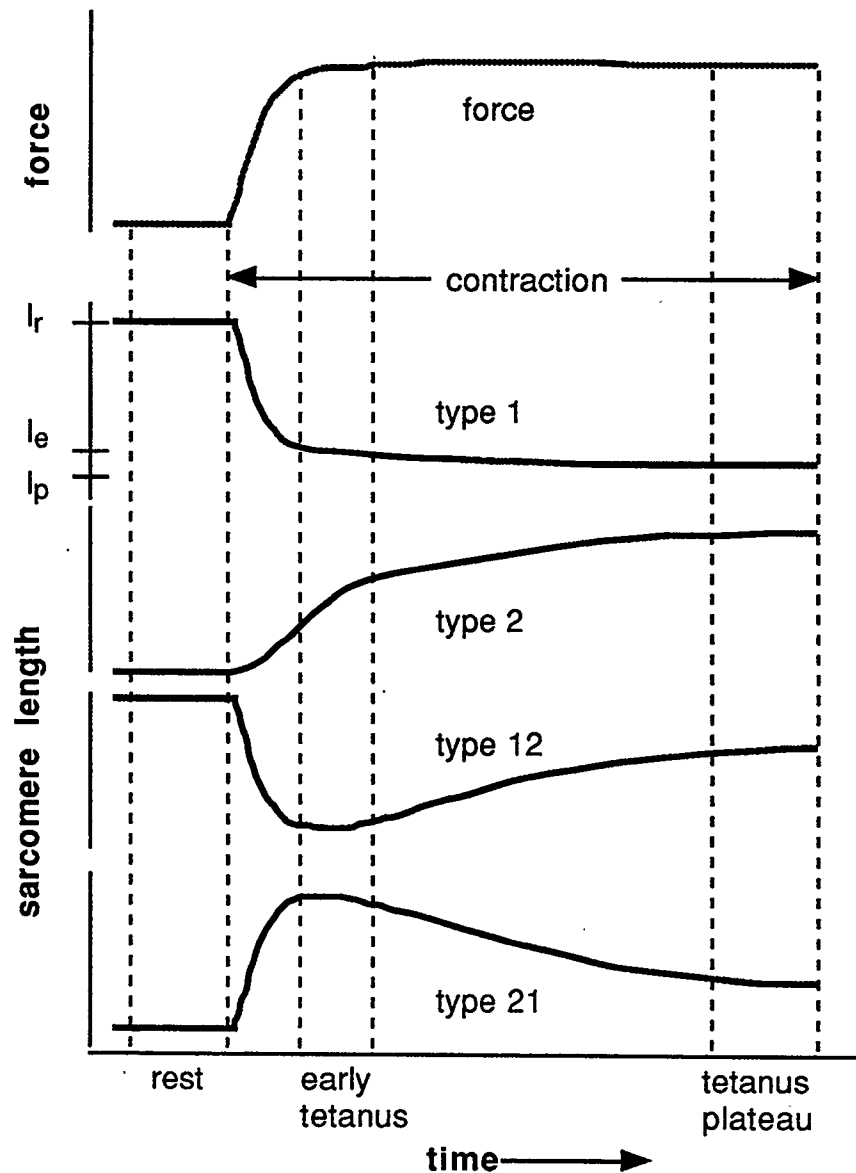


Figure 6.5. Characteristic sarcomere length-time traces which were classified as types 1 (shortening), 2 (lengthening), 12 (shortening-lengthening), and 21 (lengthening-shortening) according to the mean sarcomere length during the time periods shown.

tetanus (last 40 ms of contraction, l_p). Sarcomere length-time traces were classified into four types: type 1 (shortening), if $l_r > l_e > l_p$; type 2 (lengthening), if $l_r < l_e < l_p$; type 12 (shortening-lengthening), if $l_r > l_e$ and $l_e < l_p$; and type 21 (lengthening-shortening), if $l_r < l_e$ and $l_e > l_p$.

The root mean variance (RMV) was a parameter used to evaluate how much the sarcomere length varies for a group of sarcomere length traces (e.g., all type 1 traces) and was calculated as the square root of the mean variance for a specific group of sarcomere length traces. RMV was determined for the four types of traces during the rest period and during the tetanic plateau,

$$RMV = \left(\sum_{i=1}^N \frac{\sigma_i^2}{N} \right)^{0.5} \quad (1)$$

where: σ_i = standard deviation of the mean sarcomere length for the rest period or

the tetanic plateau of sarcomere trace number i .

N = number of sarcomere traces in the group.

Two types of curves were fit to the sarcomere length-time data. A straight line was fit to the data during the tetanic plateau (last 40 ms of contraction) to determine the final sarcomere velocity, v ($\mu\text{m/s}$),

$$SL(t) = u + v t \quad (2)$$

where: SL = sarcomere length (μm)

t = time (s)

u, v = constants

The chi-square merit function was used to explicitly solve for the constants u and v .

An exponential curve was fit to the type 1 and type 2 sarcomere length-time traces over the whole contraction period,

$$SL(t) = a + b e^{-c t} \quad (3)$$

where: a, b, c = constants

e = power of base e

The steady-state sarcomere length was represented by the constant a (μm), and the time constant for the decaying portion of the function was determined as $1/c$ (s). The Levenberg-Marquardt method was used to fit the exponential function to the data. The method was iterative, and it was used with a chi-square merit function to determine the constants a, b , and c . Since the chi-square merit function requires an estimate of the standard deviation, the standard deviation of the data was determined using the previous best fit curve parameters,

$$\sigma_{j+1} = \left(\sum_{i=1}^N \frac{(y_i - SL_j(t_i))^2}{N} \right)^{0.5} \quad (4)$$

where: σ_{j+1} = standard deviation of the data from the fitted curve for iteration $j+1$.

$SL_j(t_i)$ = fitted exponential curve (eq. 3) from iteration j .

t_i = time of data point i .

y_i = sarcomere length of data point i .

N = number of data points.

i = data point identification number

j = iteration number for the fitted curve

Sarcomere length measurement errors

An evaluation of the errors in the sarcomere length measurements during contractions caused by a different group of sarcomeres moving into the test region (under the laser beam) were made. Special care was taken to measure sarcomere length in regions of the muscle that translated less than half the

beam width, so at least half of the sarcomeres that were in the test region before contraction remained in the test region. If sarcomeres in the muscle did translate through the laser beam, the translation (< 0.5 mm) was primarily parallel to the long axis of the muscle.

An evaluation of possible errors caused by the shift of the specimen during contraction was conducted by collecting sarcomere length data in one region of the muscle for three contractions. Following the three contractions, the muscle was translated 0.5 mm along the long axis of the muscle and three repeat contractions were made. The muscle was then translated 0.5 mm to the other side of the initial position, and the sarcomere length measurements were repeated. Results from this test gave a mean (\pm standard deviation) sarcomere length for the rest and the tetanic plateau periods of 2.992 ± 0.021 μm and 2.975 ± 0.014 μm , respectively ($n=9$). The three regions tested all illustrated a type 12 sarcomere length-time behavior. The sarcomere length at rest varied more than during the tetanic plateau. Based on these observations, and the attention paid to this problem during data collection, it was concluded that errors in sarcomere length measurements caused by different sarcomeres moving into the laser beam during the contraction were negligible. Artifacts related to the motion of a group of sarcomeres through the laser beam (< 0.020 μm ; Burton and Huxley, 1995; Altringham et al., 1984) were similar to the magnitude to the precision of the sarcomere length measurements during the plateau of the tetani.

The precision in sarcomere length measurements (RMV) during the rest period and during the tetanic plateau was ± 0.004 μm ($n = 143$) and ± 0.021 μm ($n = 143$), respectively for all muscles combined under tetanic contractions. The decrease in the precision from rest to contraction is probably caused by a decrease in the intensity and an increase in the width of the first-order diffraction

pattern from rest to contraction. However, in some contractions the intensity and width of the first-order diffraction pattern increased from rest to the tetanic plateau. Although the intensity of the first-order diffraction pattern was not quantified, qualitatively our observations agree with the findings of other experiments conducted on amphibian muscle (Paolini and Roos, 1975). The increased width of the diffraction pattern for fiber bundles compared to single fibers is probably related to slight nonuniformities in sarcomere length between individual fibers in the laser beam (Paolini et al., 1976).

Experimental Results

Sarcomere length nonuniformities at rest

A measure of the amount of nonuniformity in sarcomere length for a muscle at rest is the difference between the longest and the shortest group of sarcomeres. Across the width of a muscle at rest, the peak-to-peak variations in

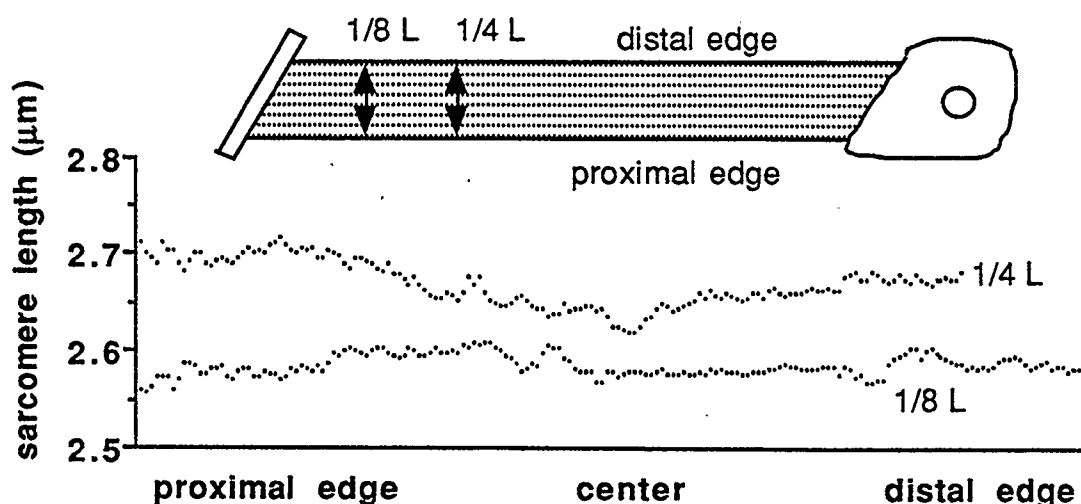


Figure 6.6. Resting sarcomere length measured across the width of a muscle at two distances from the rib end at a constant muscle length. The mean sarcomere lengths of the traces (\pm S.D.) were $2.670 \pm 0.023 \mu\text{m}$ and $2.585 \pm 0.012 \mu\text{m}$ at a distance of $1/8$ [file: f2393.c3] and $1/4$ [file: f2393.c4] of the muscle length from the rib end, respectively. Distances across the muscle width are not to scale.

sarcomere length were $0.099\ \mu\text{m}$ and $0.053\ \mu\text{m}$ at $1/8\ L$ and $1/4\ L$, respectively (Figure 6.6). Peak-to-peak variations in sarcomere length along the length of the muscle were maximally $0.131\ \mu\text{m}$ (C, Figure 6.7) and minimally $0.111\ \mu\text{m}$ (A, Figure 6.7). Sarcomere length varied gradually across the width and along the length of the muscle at rest (Figures 6.6 and 6.7). Because of variations in the speed of muscle translation under the laser beam, the horizontal axis of Figures 6.6 and 6.7 does not correspond directly to the distance across the width or along the length of the muscle.

The muscle at rest had sarcomeres that varied slightly in length, but overall the sarcomeres were very uniform in length. Sarcomere length appears to vary more along the length of the fibers than between sarcomeres of different fibers across the width of the muscle at rest.

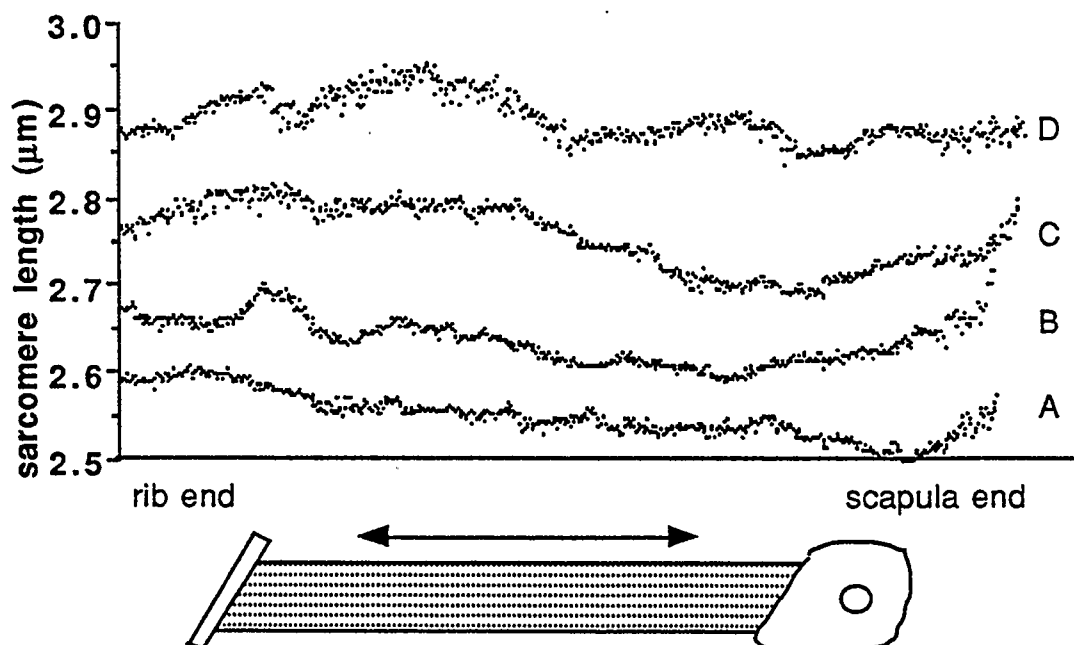


Figure 6.7. Resting sarcomere length along the length of the muscle measured near one edge for four muscle lengths. The mean sarcomere lengths (\pm S.D.) at each muscle length were $2.551 \pm 0.026\ \mu\text{m}$ (A; file: f2493.a7), $2.638 \pm 0.027\ \mu\text{m}$ (B; file: f2493.a9), $2.754 \pm 0.038\ \mu\text{m}$ (C; file: f2493.a13), and $2.890 \pm 0.026\ \mu\text{m}$ (D; file: f2493.a19). Distances along the muscle, parallel to the fiber axes, are not to scale.

Sarcomere length nonuniformities during contraction

During tetanic contraction, muscles held at a constant length exhibited similar sarcomere length behavior across the width of the muscle and dissimilar sarcomere length behavior along the length of the muscle. Sarcomere length-time traces at three locations across the width of one muscle show a similar

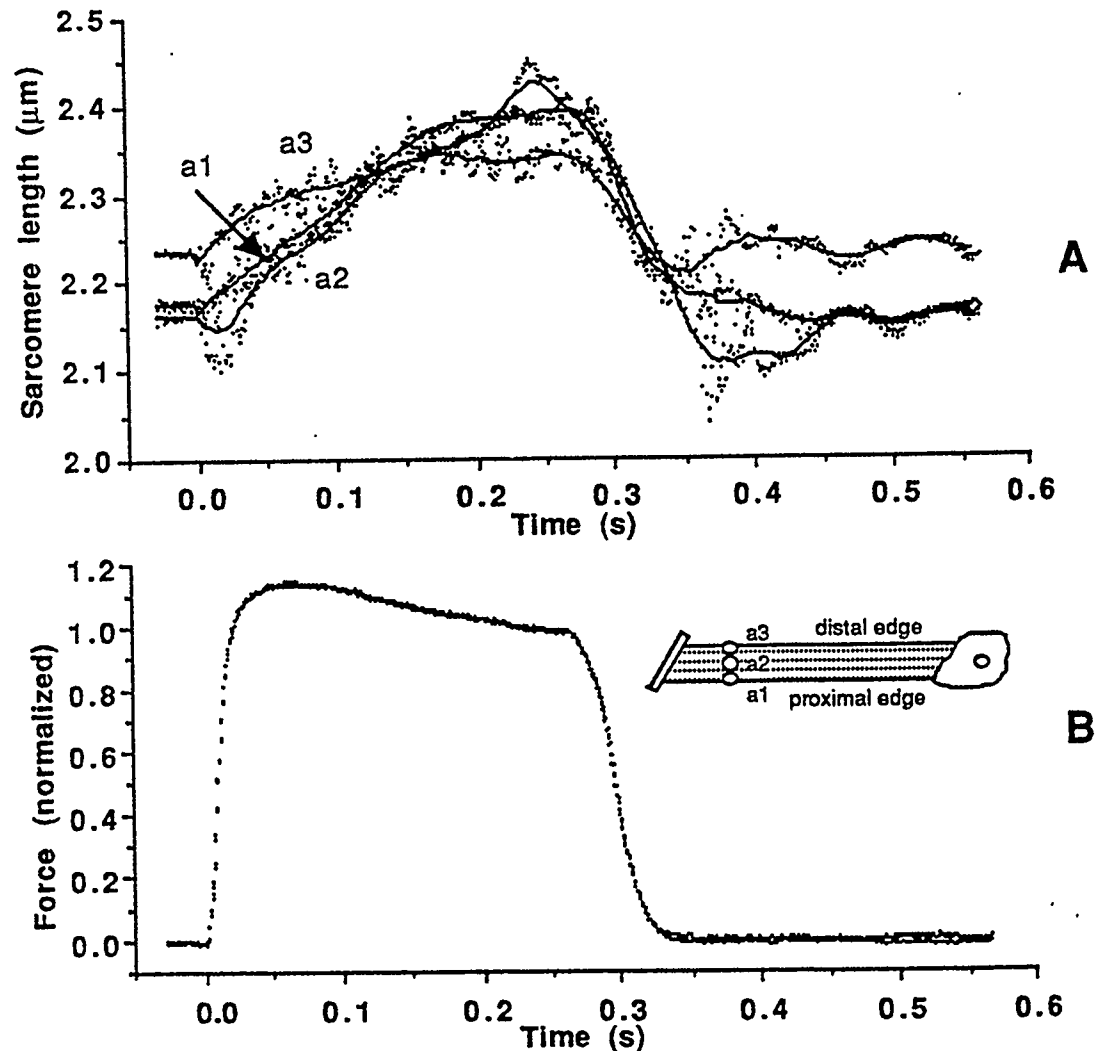


Figure 6.8. (A) Sarcomere length-time traces during a contraction at three positions across the width of a muscle (proximal edge, a1; center, a2; distal edge, a3) near the rib end. Mean and standard deviations of the three traces during rest (0 - 25 ms) and during the tetanic plateau (230 - 270 ms) were $2.19 \pm 0.040 \mu\text{m}$ and $2.380 \pm 0.041 \mu\text{m}$, respectively. (B) Corresponding force-time curves for the above contraction (stimulation 250 ms) [muscle: j293; plateau force 290 mN/mm²; cross sectional area 0.10 mm²].

behavior during contraction (Figure 6.8). The standard deviation of the mean sarcomere length for the three traces was $\pm 0.040 \mu\text{m}$ during the rest period and $\pm 0.041 \mu\text{m}$ during the tetanic plateau. Sarcomeres across the width of this muscle generally displayed uniform length behavior.

Nonuniform sarcomere length behavior was observed along the length of the muscles; some sarcomeres shortened while others lengthened. Typical sarcomere length-time traces at different locations along the length of four of the 12 muscles are shown in Figure 6.9. Force-time traces (normalized to the peak tension during the plateau) corresponding to the sarcomere length-time traces in Figure 6.9 are displayed in Figure 6.10. From rest to the end of the contraction, the differences in sarcomere length grew dramatically for sarcomeres at different locations along the length of the muscle (Figure 6.9). For example, in muscle C the difference in sarcomere length between the two groups of sarcomeres measured increased about 10X from $0.02 \mu\text{m}$ (rest) to $0.2 \mu\text{m}$ (end of contraction). This increase in sarcomere nonuniformity from rest to the tetanic plateau was observed in all muscles where more than one group of sarcomeres was measured along the length of the muscle.

Based on the sarcomere length trace classifications (Figure 6.5), muscles B and C illustrated type 2 [a24; a7] and type 12 [a23; a8] sarcomere length behaviors in the two regions shown. Muscle A had type 1 [a23] and type 12 [a22] curves in the two regions shown, and muscle D contained a type 21 [a20] sarcomere length trace in the region of the muscle illuminated by the laser. A total of 143 measurements in 26 regions of the 12 muscles were made at different muscle lengths along the length of the muscles. Out of the 143 sarcomere length traces collected 31 were of type 1; 60 of type 2; 49 of type 12; and 3 of type 21. These results do not necessarily represent the proportion of sarcomeres that follow these four types of sarcomere length-time behaviors in

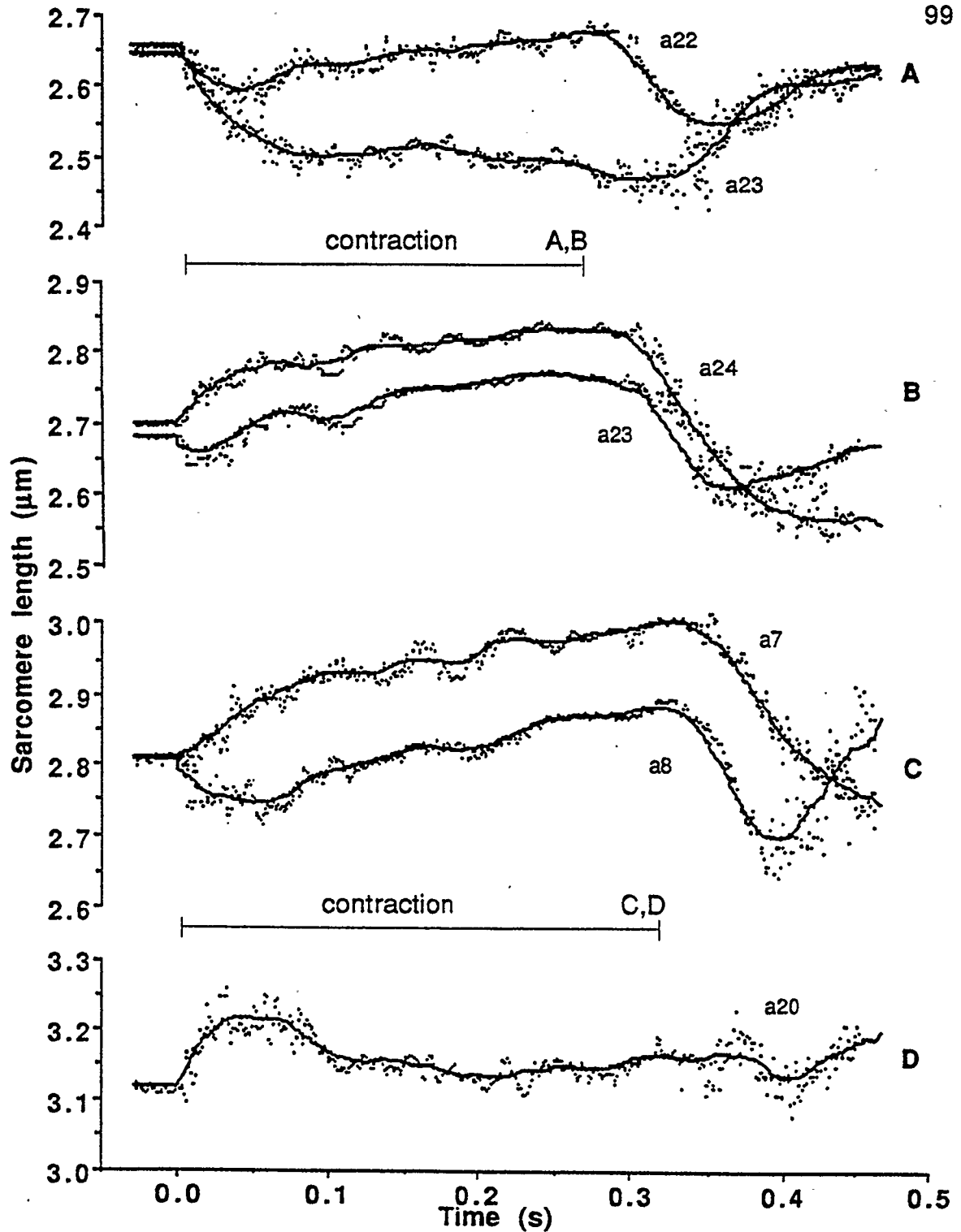


Figure 6.9. Typical sarcomere length-time traces at different locations along the length of four muscles. Traces for a given muscle were at one muscle length. Raw data were represented by dots and the smoothed data by the solid lines. The time of contraction was determined from the force-time traces (Figure 6.10). Stimulation occurred from 0 - 250 ms (A [m994], B [a1994]) and 0 - 300 ms (C [j2293], D [a2894]).

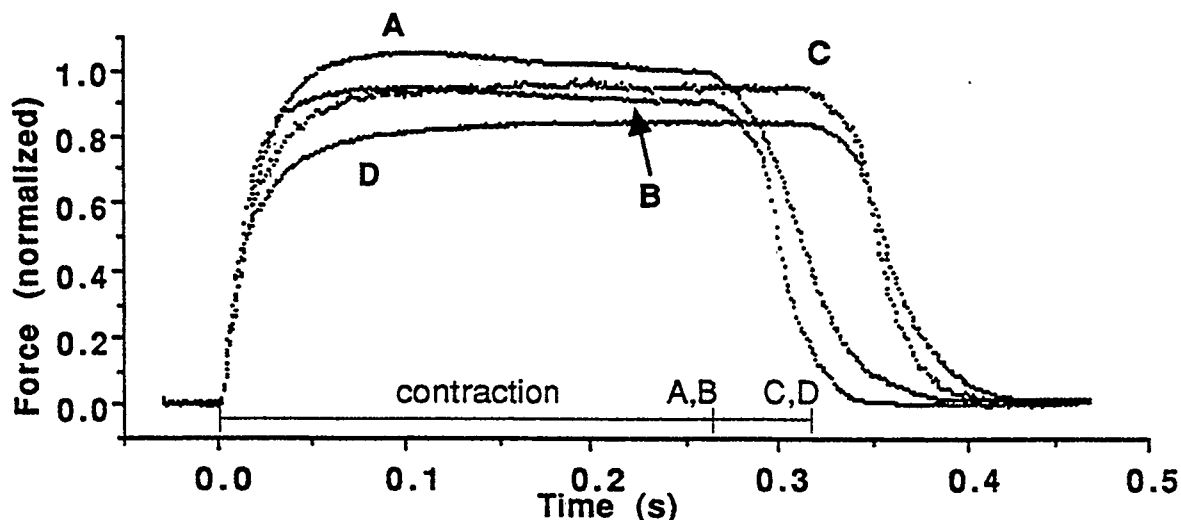


Figure 6.10. Force-time histories for the corresponding traces in Figure 6.9. The forces were normalized to the peak force during the plateau (last 40 ms of contraction). Stimulation occurred from 0 - 250 ms (A, B) and 0 - 300 ms (C, D). Muscles A [m994], B [a1994], C [j2293], and D [a2894] had plateau forces of 86, 75, 490, and 100 mN/mm²; and cross sectional areas of 0.18, 0.08, 0.32, and 0.35 mm², respectively.

the serratus anterior of the mouse, because sarcomere length measurements could be made only from selected regions of the muscle.

Nonuniform sarcomere length behavior was found along the length of the muscle and uniform sarcomere length behavior was found across the width of the muscle. This nonuniform sarcomere length behavior along the long axis of the muscle does not necessarily indicate unstable sarcomere length behavior on the descending limb of the F-L relation, as defined here.

Stability considerations

All of the 143 sarcomere length-time traces collected from the 12 muscles in this study demonstrated stable sarcomere behavior by satisfying at least two of the stability criteria stated in the methods section and 52 sarcomere length-time traces satisfied all three stability criteria.

All of the type 1 and type 2 sarcomere length-time traces exhibited a decrease in the speed of sarcomere shortening or lengthening during the

contraction, respectively (first stability criteria). Upon contraction the sarcomere length changed rapidly during force development and then decreased in speed as the contraction progressed (Figures 6.8 and 6.9). An exponential curve was fit to the type 1 and type 2 sarcomere length traces over the contraction period, $SL(t) = a + b e^{-Ct}$. A typical example of the curve fit is shown in Figure 6.11. The nonlinear curve fitting routine converged successfully for 42 of the 60 type 2 and 15 of the 31 type 1 sarcomere length traces. The root mean variance between the actual data and the fitted curves that converged was $\pm 0.017 \mu\text{m}$ ($n = 42$) and $\pm 0.019 \mu\text{m}$ ($n = 15$) for the type 2 and type 1 groupings, respectively. These root mean variance values are less than those during the tetanic plateau for all contractions combined ($\pm 0.021 \text{ mm}$, $n = 143$). The reason why the exponential curves could not be fitted successfully to all sarcomere length traces was because the change in sarcomere length during the contraction was too small in those cases.

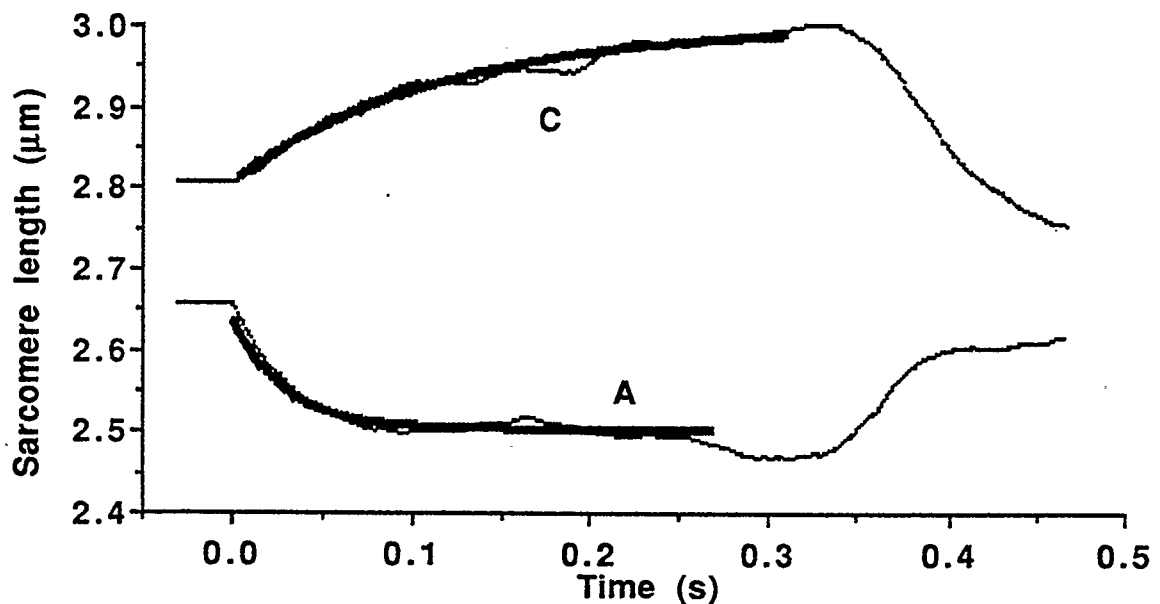


Figure 6.11. Illustration of the exponential ($SL(t) = a + b e^{-Ct}$) approximation during the contraction (thick line) of a type 1 (A; file: m994.a23) and a type 2 (C; file: j2293.a7) sarcomere length-time trace from Figure 6.9.

From the fitted equations for each sarcomere length trace, the time constant ($1/c$) for the logarithmic decrement was calculated. For the type 2 traces, the time constant was 105 ± 8 ms (mean \pm standard error) and for the type 1 traces, the time constant was 55 ± 13 ms (mean \pm standard error). Thus, the shortening regions of the muscle had sarcomeres that approached a steady-state length at a faster rate than the lengthening regions of the muscle.

The sarcomere length behavior for the four types of sarcomere length-time traces approached a steady-state value at the end of the contractions (second stability criteria). The velocity of sarcomere length change at the end of the contraction was determined by fitting a straight line to the last 40 ms of each of the 143 contractions. The mean sarcomere length velocity for the types 1, 2, 12, and all contractions grouped together was $0.132 \mu\text{m/s}$ ($0.055 L_0/\text{s}$) or less (Table 6.1). The type 21 sarcomeres had a larger speed of lengthening during the plateau than the other sarcomere length types, however only three observations of this type of sarcomere length behavior were found. The mean velocity for all types of sarcomere length traces and for all contractions grouped together was not significantly different from zero indicating that a steady-state or nearly steady-state length was achieved by the sarcomeres near the end of the 250 or 300 ms contraction.

Table 6.1. Rate of change in sarcomere length for the last 40 ms of a fixed-end contraction (plateau).

	type of behavior				
	1	2	12	21	all
mean ($\mu\text{m/s}$)	0.080	-0.009	0.132	0.899	0.078
S.E. ($\mu\text{m/s}$)	0.129	0.091	0.090	0.925	0.059
n	31	60	49	3	143
mean (L_0/s)	0.033	-0.004	0.055	0.37	0.032

Note: + lengthening sarcomere, - shortening sarcomere, $L_0 = 2.4 \mu\text{m}$

Stable sarcomere length behavior was indicated by a reversal in sarcomere length changes during the contractions (third stability criteria). Types 12 and 21 of sarcomere length-time traces exhibited reversals in the sarcomere length changes. Also, the sarcomeres classified as types 1 and 2 demonstrated reversals in sarcomere length changes. The type 1 sarcomeres had a mean lengthening velocity ($0.080 \mu\text{m/s}$) while the type 2 sarcomeres had a mean shortening velocity ($-0.009 \mu\text{m/s}$) during the last 40 ms of the contractions. This reversal in sarcomere length changes is characteristic of a stable system with a damped oscillatory motion.

Discussion

Sarcomere length nonuniformity in muscle vs. single fibers

Skeletal muscle exhibits sarcomere length-time behavior similar to that found by other investigators using single fiber preparations and fixed-end contractions. Edman and Reggiani (1984) measured sarcomere length changes in six single fiber preparations of the frog during fixed-end contractions using small segments (0.5 mm long) identified by surface markers. They demonstrated that different segments possess varying amounts of length change and reversals of length change during contractions. Their results (Figures 5 and 6, Edman and Reggiani, 1984) were classified into the four types of sarcomere length behaviors that were used in this study. Comparisons of the results from this study and the study of Edman and Reggiani (1984) show similar findings in the distribution of the four types of sarcomere length behaviors along the length of muscles and fibers (Table 6.2). Their study probably represents the actual distribution of sarcomere length behaviors better than our study since they made measurements along the entire length of the

Table 6.2. Comparison of types of sarcomere length behaviors between muscle (this study) and single fibers (Edman and Reggiani, 1984, Fig. 5 and 6).

type	muscle*		single fiber**	
	number	percent	number	percent
1	31	22 %	47	37 %
2	60	42 %	18	14 %
1 2	49	34 %	62	48 %
2 1	3	2 %	1	1 %
total	143	100 %	128	100 %

* 12 fibers, 26 regions along muscles, various muscle lengths

** 6 fibers, 64 segments along fibers, 2 fiber lengths

fibers. In the present study, measurements could be made only from selected locations along the length of the muscle.

Sarcomere length variations along the length of the muscle were greater than sarcomere length variations across the width of the muscle probably because of the structure of skeletal muscles. Sarcomeres in one fiber may directly exert forces on adjacent fibers through connective tissue (Trotter, 1990; Trotter and Purslow, 1992). Thus, sarcomeres which lie parallel to each other in a muscle would be expected to exhibit a similar length behavior, such as was found in this study. However, large variations in sarcomere length during contraction would be expected along the length of a muscle because consecutive sarcomeres act independently of one another in a single fiber (Huxley, 1957). Slight differences in initial sarcomere length, sarcomere cross-sectional area, and activation for sarcomeres along a fiber could produce the observed variations in sarcomere length (Edman and Reggiani, 1984).

Resting sarcomere length varied gradually along the length of the muscle indicating a shift of the passive force-sarcomere length relation along the length of the muscle. Such a shift in the passive force-sarcomere length relation for

sarcomeres along the length of a muscle could be caused by structures within the sarcomere and/or variations in the amount of connective tissue around different regions of the muscle.

Support for stability

Three characteristics indicating stable sarcomere behavior were found in the sarcomere length-time results of mouse serratus anterior muscle: (1) sarcomere length approached a steady-state length, (2) sarcomere length changes decreased in magnitude with time, and (3) reversals in the sign of sarcomere length changes occurred during contractions.

Decreasing sarcomere length changes with time have also been demonstrated in the literature (Huxley and Peachey, 1961; Julian et al., 1978; ter Keurs et al., 1978; Julian and Morgan, 1979a; Lieber and Baskin, 1983; Edman and Reggiani, 1984; ter Keurs et al., 1984; Sugi and Tsuchiya, 1988; Granzier and Pollack, 1990; Edman et al., 1993). Table 6.3 lists investigations and the number of sarcomere length-time traces shown in these

Table 6.3. List of the number of sarcomere length-time traces demonstrating stable and unstable behavior.

Reference	Figure	stable	unstable	region of muscle	method
Edman and Reggiani, 1984	4	20	0	whole length	segment
	8	8	0	ends	segment
Edman et al., 1993	2b	9	0	whole length	segment
Granzier and Pollack, 1990	2-4, 8, 9	10	0	central	segment & diffraction
Huxley and Peachey, 1961	4	1	0	end	micrographs
Julian et al., 1978	2	2	0	central	segment
Julian and Morgan, 1979a	7, 9	8	0	central	segment
Lieber and Baskin, 1983	2, 5b, 6a, 7	11	0	end and central	diffraction
	4ab, 5a, 6b	0	4	end	diffraction
Sugi and Tsuchiya, 1988	6	10	0	whole length	segment
ter Keurs et al., 1978	5, 6	7	0	central	diffraction
ter Keurs et al., 1984	1	4	0	central	diffraction
	total	90	4		

studies that exhibit a decrease in lengthening or shortening speed during isometric contractions (labelled stable). In the investigations shown in Table 6.3, frog single fibers and different methods of measuring sarcomere length were used. Also, sarcomere behavior was measured at various locations along the length of the fibers. Almost unanimous support for stable sarcomere length behavior was found in these investigations. The four observations listed as unstable (Table 6.3) may in fact be displaying stable behavior, because the contraction time was too short to declare if the sarcomere speed was decreasing or increasing. A reinterpretation of the sarcomere length-time data found in the literature indicates stable sarcomere behavior as defined here on the descending limb of the F-L relation.

Under the premise of unstable sarcomere length behavior, many studies have predicted that long sarcomeres will continue to stretch while short sarcomeres will continue to shorten at lengths on the descending limb of the F-L relation (Huxley and Peachey, 1961; Gordon et al., 1966; Julian et al., 1978; Julian and Morgan, 1979a; Lieber and Baskin, 1983; Edman and Reggiani, 1984). Results from this study demonstrate that the sarcomere velocity near the end of the contractions is zero or very close to zero. The sum of the velocities for all sarcomeres along the length of a fiber should be zero because the fiber remains at a constant length (fixed-end contraction). When the sarcomere length traces were grouped according to type, the mean velocity was also zero or very close to zero towards the end of the contractions. It would be expected that sarcomere length traces that are grouped together because they all shorten, would exhibit a mean shortening velocity throughout the contraction; however, it appears that the sarcomere length in all regions of the muscle approaches a steady-state value (within 300 ms), even at lengths on the descending limb of the F-L relation.

Support for instability

Several arguments have been used to explain sarcomere length behavior under the assumption of instability on the descending limb of the F-L relation -- primarily force-velocity properties of sarcomeres and nonuniform length changes of a few sarcomeres.

It has been argued that the force-velocity properties of sarcomeres provide stability or decrease instability. Force-velocity properties refer to the characteristic of sarcomeres to produce more force during stretch and less force during shortening than the isometric force value at the corresponding sarcomere length. On the descending limb of the F-L relation, the hypothesis of instability predicts that the long sarcomeres are continuously stretched and can produce more force than would be predicted by the F-L relation because of the force-velocity properties. Likewise, the short sarcomeres are shortening, and therefore, produce less force than the isometric value for the same length.

However, force-velocity properties can not produce a stable fiber since they do not influence the existence of a minimum in the potential energy function for sarcomeres on the descending limb of the F-L relation. Force-velocity properties may slow the lengthening of weak sarcomeres and the shortening of strong sarcomeres, but they can not make the system stable. The model of the fiber with sarcomeres possessing unstable F-L properties illustrates this point since the force-velocity properties (Figure 6.8 and Appendix) did not make the sarcomeres stable in the fiber; but, they may have slowed the rate of divergence in sarcomere length.

Nonuniform changes in sarcomere length (i.e., some sarcomeres shorten while others lengthen) have been taken as an indication of sarcomere instability in single fibers (Huxley and Peachey, 1961; Gordon et al., 1966; Julian et al., 1978; Julian and Morgan, 1979a; Lieber and Baskin, 1983; Edman and

Reggiani, 1984). Although nonuniform sarcomere length behavior was found for different groups of sarcomeres along the length of the fibers in these studies and in the muscle of the present study, nonuniformity does not necessarily indicate instability. Nonuniform changes in sarcomere length may occur even in stable fibers (Figure 6.3 and Appendix). However, there exists the possibility that nonuniformities in sarcomere length may develop and remain in the test region which are large enough to demonstrate instability (Morgan, 1990).

If sarcomeres were unstable, large nonuniformities in sarcomere length should develop. However, nonuniformities in the test regions do not increase during tetanic contractions, but reach a steady-state in myofibrils (Fabiato and Fabiato, 1978; Iwazumi, 1987), in frog single fibers (Cleworth and Edman, 1972; Hill, 1977; ter Keurs et al., 1978; Haskell and Carlson, 1981; Tameyasu et al., 1982), and in whole muscle (ter Keurs et al., 1978). Sarcomere length nonuniformities in the test region have been reported to be maximally $0.130\ \mu\text{m}$ (Tameyasu et al., 1982, laser diffraction) in single fibers. In whole muscle, nonuniformities in sarcomere length increase slightly from rest to contraction (2.6% or $0.068\ \mu\text{m}$ at $2.6\ \mu\text{m}$ sarcomere length) but not enough to demonstrate unstable sarcomere behavior (Paolini and Roos, 1975). The uniformities of adjacent sarcomeres in series are probably not a result of an interaction between the sarcomeres, but may be related to stable sarcomere properties (Chapter 4).

Conclusions

Although sarcomeres appear to be inherently unstable on the descending limb of the F-L relation, experimental data support the hypothesis that they are stable. Nonuniform changes in sarcomere length along the length

of a muscle are not necessarily indications of instability. Our interpretation of the sarcomere length-time traces found here for mammalian muscle, and for sarcomere length-time traces found in the literature for frog single fibers, is that sarcomeres are stable at lengths on the descending limb of the F-L relation.

Appendix

An analytical model composed of a fiber that consists of two sarcomeres in series was used to demonstrate the sarcomere length-time behavior for sarcomeres with unstable and stable force-displacement properties. Force-velocity properties were incorporated in this model because they have been suggested to affect stability. The two sarcomeres in each fiber were identical except for the initial sarcomere length. Mass of the sarcomeres relative to its force producing potential was assumed to be negligible, so the force in a sarcomere was related only to the force-length (F_l) and the force-velocity (F_v) properties. Sarcomeres were assumed to produce a force that was linearly related to sarcomere length on the descending limb of the F-L relation,

$$F_{li} = k_i x_i + a_i \quad (a1)$$

where: F_{li} = force at length x of sarcomere i

x_i = length of sarcomere i

k_i, a_i = constants for sarcomere i

Forces were assumed to be linearly related to velocity to provide a force-velocity property to the sarcomeres,

$$F_{vi} = c_i v_i \quad (a2)$$

where: F_{vi} = force for sarcomere i at a given velocity

$v_i = dx_i / dt$ = velocity of sarcomere i

c_i = constant for sarcomere i .

Fixed-end contractions were simulated, so fiber length was kept constant,

$$x_0 + x_1 = L \quad (a3)$$

where: L = fiber length

x_0 = length of sarcomere 0

x_1 = length of sarcomere 1.

The fiber composed of two sarcomeres labelled 0 and 1 must develop the same force,

$$F_{l0} + F_{v0} = F_{l1} + F_{v1} \quad (a4)$$

and substituting equations a1 and a2 into a4,

$$c_0 v_0 + k_0 x_0 + a_0 = c_1 v_1 + k_1 x_1 + a_1 \quad (a5)$$

The sarcomere length behavior over time was found by solving equation a5 for x_0 , subject to the constraint (equation a3),

$$x_0 = (x_0' + D / K) \exp(-K t / C) - D / K \quad (a6)$$

where: x_0' = initial sarcomere length

$$D = a_0 - a_1 - k_1 L$$

$$K = k_0 + k_1$$

$$C = c_0 + c_1$$

$$t = \text{time (s)}$$

For the unstable fiber model, equation a6 was evaluated using the descending limb of the theoretical F-L relation based on the myofilament lengths of the mouse (Figure 6.2B). The thick myofilament length was 1.63 μm (Sosa et al., 1994) and the thin filament length was 1.14 μm (Phillips and Woledge, 1992). Based on these myofilament lengths the values assigned to F-L properties of the unstable model were $k_0 = k_1 = -0.685$ ($F_{\text{normalized}}/\mu\text{m}$) and $a_0 = a_1 = 2.678$ ($F_{\text{normalized}}$).

For the stable fiber model, equation a6 was evaluated assuming that

each sarcomere followed its own F-L curve. A shortening sarcomere (subscripted 0) followed the theoretical F-L relation based on myofilament lengths as in the previous model, $k_0 = -0.685$ (Fnormalized/ μm) and $a_0 = 2.678$ (Fnormalized). This behavior was reported to occur in single fibers of the frog (Edman et al., 1993). A lengthening sarcomere followed its own positively sloped F-L curve. The slope of the F-L curve increased with an increase in initial sarcomere length. These lengthening properties have been shown to exist for quick length changes (Ford et al., 1977), and for slow length changes (Abbot and Aubert, 1952; Hill, 1977; Edman et al., 1978; Edman et al., 1982). This model is stable on the descending limb of the F-L relation, because the slope of the F-L curve for lengthening sarcomeres is greater in magnitude than the slope of the F-L curve for shortening sarcomeres; thus, the potential energy function has a minimum. The slope (k_1) of the force-displacement curve for a sarcomere that lengthens (subscript 1) varied with initial sarcomere length (x_1'), $k_1 = 2 x_1' - 3.8$, so $a_1 = -0.689 x_1' + 2.517 - k_1 x_1'$.

The force-velocity constants were assigned the same values in both the stable and unstable model, $c_0 = c_1 = 0.2$ (Fnormalized/ $\mu\text{m/s}$).

Chapter 7

Reason for the Difference Between the Theoretical and Fixed-end Force-Length Relations in Mouse Skeletal Muscle

Introduction

In order to understand the basic principles of muscle contraction, the force-length (F-L) relation has been studied extensively. The F-L property of muscle describes the relation between active force production and length for isometric tetani. F-L properties of muscle have been studied for sarcomeres, single fibers, fiber bundles, or whole muscles. Generally, the F-L relation consists of three regions of active (stimulation induced) force production: an ascending limb, a plateau, and a descending limb (Figure 7.1). Resting tension results from passive structures in the unstimulated muscle and varies between muscles. The sum of the active and passive tensions is the total force produced during a contraction.

Different methods are used to measure the F-L properties of a muscle preparation. "Fixed-end" methods hold the ends of a fiber, fiber bundle, or muscle fixed (constant length) throughout a tetani (Carlsen et al., 1961; ter Keurs et al., 1978a,b; Altringham and Bottinelli, 1985; Martyn and Gordon, 1988; Granzier and Pollack, 1990). During a fixed-end contraction, sarcomeres within the preparation shorten and lengthen throughout the contraction (Huxley

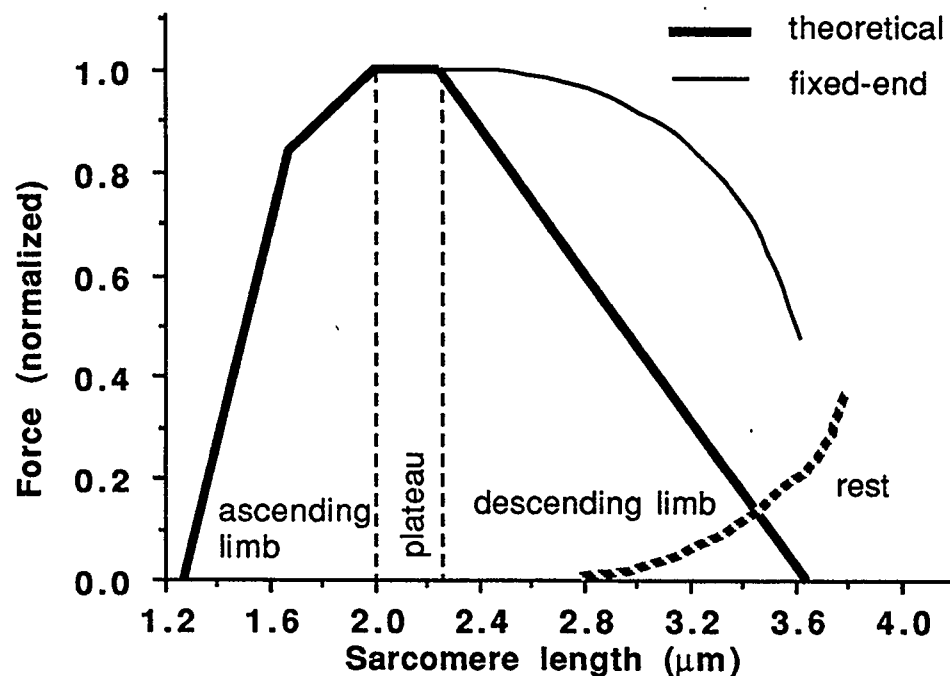


Figure 7.1. Schematic representation of the force-length relations for sarcomeres (thick line) and for fixed-end methods (thin line) from frog single fibers.

and Peachey, 1961; Gordon et al., 1966a; Cleworth and Edman, 1972; Julian et al., 1978; Julian and Morgan, 1979a; Lieber and Baskin, 1983; Edman and Reggiani, 1984), because initial sarcomere length (Edman and Reggiani, 1984), cross-sectional area (Edman and Reggiani, 1984), activation, and maximum velocity of shortening (Edman et al., 1992) vary from sarcomere-to-sarcomere along the length of a fiber. Since individual sarcomeres do not remain constant in the fixed-end experiments, other techniques were developed to measure the “true” isometric force of a sarcomere.

Two major techniques have been used to determine the true isometric force of sarcomeres. The “segment-clamp” technique uses a motor that alters the length of a preparation to keep a small group of sarcomeres (35 - 4000 consecutive sarcomeres) at a constant length throughout a contraction (Gordon et al., 1966a; ter Keurs et al., 1984; Edman and Reggiani, 1987; Bagni et al.,

1988; Granzier and Pollack, 1990). Alternatively, the “extrapolation” technique assumes that the true force of a sarcomere occurs just after full activation and before any slow changes in sarcomere length occur (Gordon et al., 1966b). A straight line is fit through the fast and the slow rise phases of the force-time trace for an isometric contraction. The intersection of these two lines gives the isometric force and the point in time where the length of the sarcomeres is determined. Both the segment-clamp and extrapolation techniques produce a sarcomere F-L relation that corresponds closely to the theoretical F-L relations which have been based on the cross-bridge theory of muscle contraction (Gordon et al., 1966b; Edman and Reggiani, 1987; Bagni et al., 1988; Granzier and Pollack, 1990). According to the cross-bridge theory, the isometric force of a sarcomere is proportional to the number of active cross-bridges which depends on the amount of thick and thin myofilament overlap on the descending limb of the F-L relation (Huxley, 1957).

Differences between the fixed-end and theoretical F-L relations occur on the descending limb. The fixed-end F-L relation has an extended plateau and forces that are larger than the corresponding forces of the theoretical F-L relation (Figure 7.1; Granzier and Pollack, 1990, their Figure 5; Pollack, 1990, his Figure 2.8).

A continuous change in sarcomere length (i.e., some sarcomeres shorten and some lengthen during the contraction) has been thought to cause the differences between the fixed-end and theoretical F-L relations. Sarcomeres generate more force, both actively and passively, while lengthening (force-velocity properties; Hill, 1953; Gordon et al., 1966b; Granzier and Pollack, 1990). Investigations using single fibers have demonstrated that the sarcomeres may lengthen at a velocity that can account for the differences between the sarcomere and fixed-end F-L relation based on force-velocity

properties (Granzier and Pollack, 1990).

Recently, it has been proposed theoretically and demonstrated experimentally that sarcomeres on the descending limb of the F-L relation exhibit stable behavior and achieve a steady-state or near steady-state behavior (i.e., no change in length) during fixed-end contractions (Chapter 4 and 6). If sarcomere lengthening ceases during fixed-end contractions, force-velocity properties cannot be used to explain the difference in the fixed-end and theoretical F-L relations. A model based on stable sarcomere behavior was proposed and used sarcomere properties found experimentally (Chapter 5). In this model, a sarcomere that lengthens follows a positively sloped force curve (positive stiffness), rather than the descending limb of the F-L relation (Abbott and Aubert, 1953; Hill, 1977; Edman et al., 1978; Julian and Morgan 1979b; Edman et al., 1982), and a sarcomere that shortens follows the descending limb of the F-L relation (Edman et al., 1993). The present study was undertaken to determine if the mechanical properties used to explain the differences between the sarcomere and fixed-end F-L relations in the stable sarcomere model (Chapter 5) are found in mammalian skeletal muscle.

The purpose of this study was to determine the theoretical and fixed-end F-L relations in mouse serratus anterior muscle, and to determine the mechanical properties necessary to explain the possible differences between these F-L relations. The results illustrate that the differences between the sarcomere and the fixed-end F-L relations that are typically observed for single fiber preparations also occur in this muscle preparation. The probable cause of the differences between the sarcomere and the fixed-end F-L relations is associated with the changes in the isometric force properties of sarcomeres after stretching or shortening.

In this study the serratus anterior muscle of the mouse was used because little F-L data are available where sarcomere length is measured from mammals or whole muscle preparations that included sarcomere length measurements. Typically, F-L relations have been measured using amphibian skeletal muscle, although some data are available from mammals (extensor digitorum of the rat, ter Keurs et al., 1984). Most F-L studies have used single fiber preparations and little work has been done on whole muscle (frog toe muscle, ter Keurs et al., 1978b; frog sartorius, Paolini and Roos, 1975). Sarcomere behavior may be different in an intact muscle than in a single fiber that has been dissected from its adjacent fibers. The interaction of adjacent fibers may cause different sarcomere behavior in a muscle compared to an isolated fiber.

Methods

Experimental procedure

The experimental setup and preparation have been described in detail previously (Chapter 6). Twelve muscle preparations were carefully dissected from the most distal head of the serratus anterior muscle of the mouse (15.3 ± 4.2 g body weight, mean \pm S.D.). The fibers in this head of the muscle originate from the vertebral border of the scapula and insert into the 7th rib on the lateral thorax of the mouse. Muscle preparations averaged (mean \pm S.D.) 10.9 ± 1.1 mm long (scapula to rib), 0.7 ± 0.2 mm wide, and 0.3 ± 0.1 mm thick at resting length.

This preparation was chosen because it had minimal series elasticity; fibers ran from bone-to-bone with no visible tendon. The bony attachments were easily and rigidly mounted to the experimental apparatus. As a result, fiber length could be held isometrically because of the rigid bony attachments and

low tendon series elasticity. Another advantage of this preparation is that the distal head could be separated with minimal damage from the rest of the serratus anterior muscle. One edge of the muscle was free of attachments, while the other edge was attached through connective tissue along about half of its length to the adjacent muscle head inserting into rib 6 (Figure 7.2A).

The muscle preparation was mounted in the experimental apparatus which consisted of a chamber, a motor, a force transducer, and a sarcomere length measurement system (Figure 7.2) on the stage of an inverted

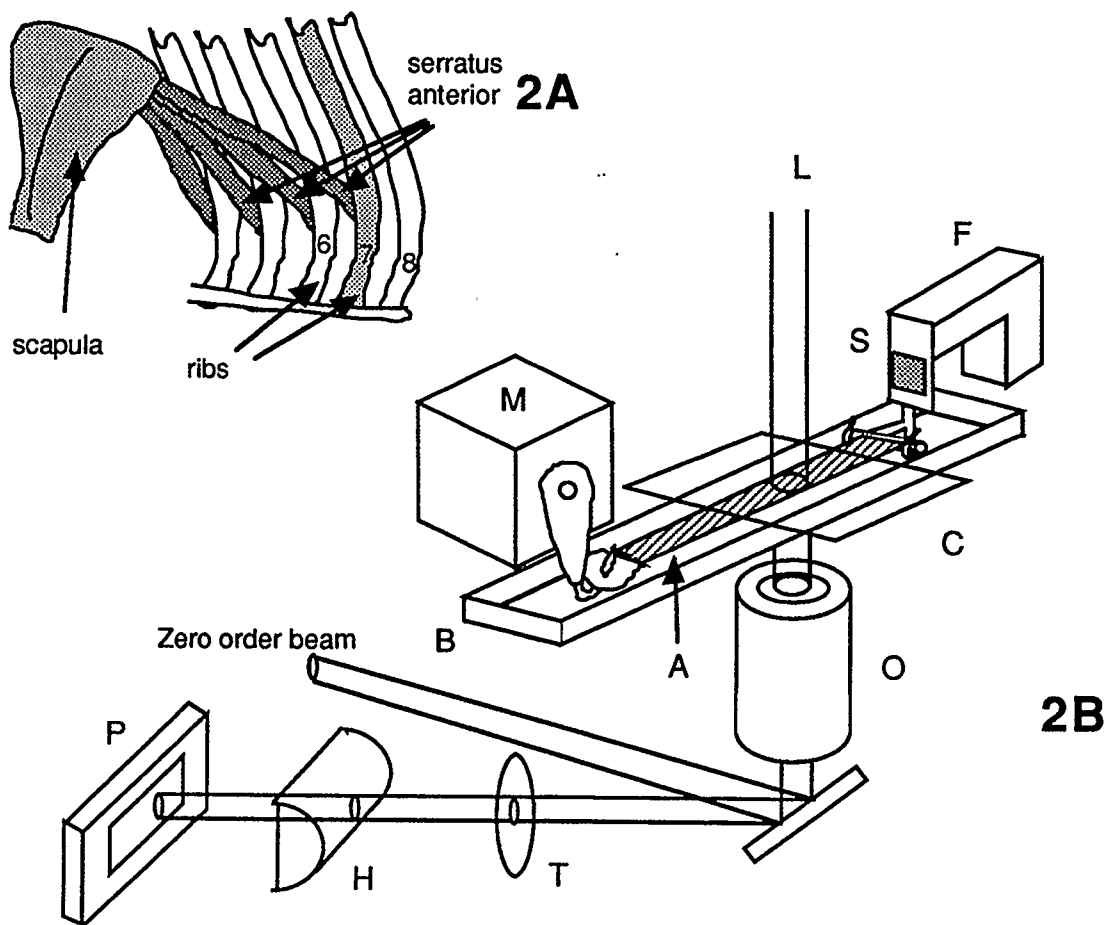


Figure 7.2. Diagram of the mouse serratus anterior muscle during dissection (2A). Schematic drawing of experimental apparatus (2B). Bathing solution flowed past the muscle from the force transducer end to the motor end of the bath. A - muscle specimen, B - bath, C - cover slip, F - micro-manipulator, H - half cylindrical lens, L - laser beam, M - motor, O - microscope objective, P - photodiode array, S - strain gauge transducer, T - converging lens.

microscope. The scapula bone chip was attached to the motor which controlled the muscle length. The rib bone chip was attached to a stationary force transducer (sensitivity 31 mV/mN; resonant frequency of 2300 Hz). Sarcomere length was measured with a laser (He-Ne; 10 mW; beam diameter 0.8 mm) diffraction system that determined the median sarcomere length based on the intensity of the first-order diffraction pattern measured from a photodiode array with a resolution of about 5 nm (ter Keurs et al., 1978). The bathing solution used during the experiment consisted of 118.1 mM NaCl, 3.4 mM KCl, 0.8 mM MgSO₄, 1.2 mM KH₂PO₄, 1.8 mM CaCl₂, 24 mM NaH₂CO₃, and 10 mM dextrose (pH 7.5). The solution was vigorously bubbled with 95% O₂ and 5% CO₂ before flowing through the experimental chamber (rate 6 ml / min, 20°C). Tetanic stimulation was provided by a stimulator through two platinum wires running the entire length of the muscle (square wave pulse, 0.5 ms pulse duration at 200 Hz, train duration 250 or 300 ms, supramaximal voltage, 100 s rest period). Muscle length (from motor), sarcomere length (laser diffraction system), and force (force transducer) data were recorded digitally (1000 Hz) with a personal computer. The computer also triggered the stimulator.

Sarcomere length was measured at different locations along the length of the muscles during fixed-end (constant muscle length) contractions and at various muscle lengths. A region of muscle where the 1st order of the laser diffraction pattern was crisp was positioned under the laser beam and a contraction was performed. Sarcomere length in a different region of the muscle was measured by translating the microscope stage under the laser beam and another contraction was performed. This was continued at a number of locations along the length of the muscle. Then, muscle length was changed and data were collected with the laser beam illuminating the same locations

(sarcomere groups) of the muscle as for the previous length. The first contraction at a new muscle length was discarded, because the force levels were always lower than successive contractions which were almost identical. Typically, sarcomere length could be recorded at a maximum of three locations along the length of the muscle. The laser beam was carefully repositioned over the same group of sarcomeres based on surface markers (6-0 silk) and natural markers on the muscle (connective tissue). Errors associated with measuring the sarcomere length of a different group of sarcomeres that may move into the laser beam during a contraction were negligible (Chapter 6).

Data analysis

The muscle F-L relation was determined from 143 contractions at 26 locations in 12 muscles. Sarcomeres in the muscle demonstrated uniform length behavior across the width of the muscle and nonuniform length behavior along the long axis of the fibers in the muscle (Chapter 6).

Sarcomere length-time traces exhibited four basic types of behaviors (Figure 7.3). For each sarcomere length-time trace, the mean sarcomere length was determined for three time periods: prior to contraction (resting length, l_r), during early tetanus (16 - 36 ms, early tetanic length, l_e), and during the plateau of the tetanus (last 40 ms of contraction, l_p). Sarcomere length-time traces were classified into four types: type 1 (shortening), if $l_r > l_e > l_p$; type 2 (lengthening), if $l_r < l_e < l_p$; type 12 (shortening-lengthening), if $l_r > l_e$ and $l_e < l_p$; and type 21 (lengthening-shortening), if $l_r < l_e$ and $l_e > l_p$. The time interval for the early tetanus was chosen because the average time found from the extrapolation method (explained later) was 26 ms.

An example of the four types of sarcomere length-time traces along with the corresponding force-time curves are shown in Figure 7.3. There were 28 type

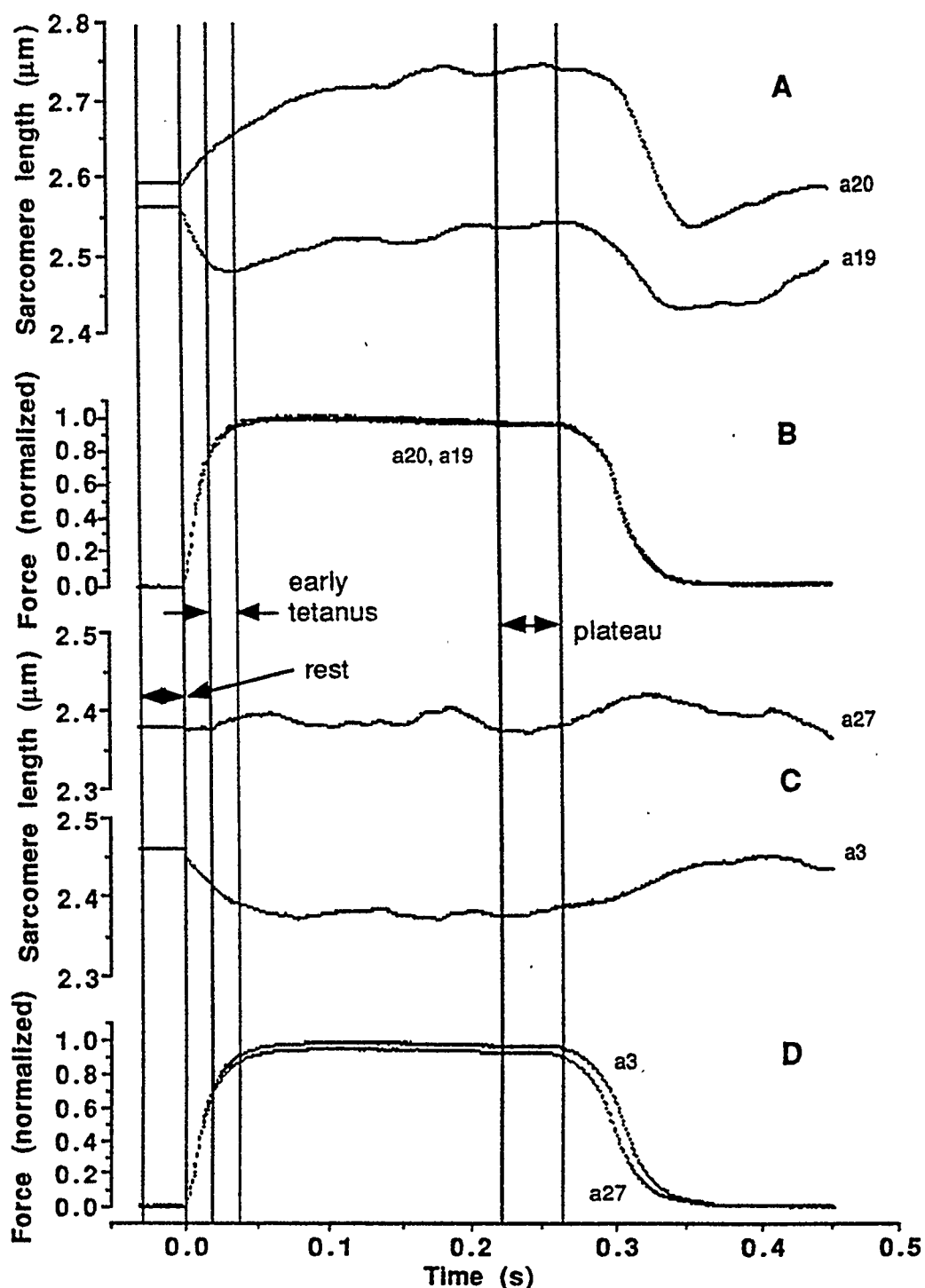


Figure 7.3. Illustration of the four types of sarcomere length-time traces. Two regions in muscle A and C were measured at the same muscle length. Muscle A had type 2 (a20) and type 12 (a19), while muscle C had type 1 (a3) and type 21 (a27) sarcomere length behaviors. Force curves in B and D correspond to the curves in A and C, respectively. Vertical lines indicate time periods where mean sarcomere length was calculated. Stimulation in the two muscles was 250 ms. [A and B from muscle: m994; C and D from muscle: m1894]

1, 55 type 2, 56 type 12, and 4 type 21 sarcomere length-time traces for a total of 143 contractions. All sarcomere length-time traces exhibited a stable behavior and were isometric, or close to isometric, during the tetanic plateau, as described previously (Chapter 6). Sarcomere length traces shown in this paper were smoothed digitally using a moving average filter with a window of ± 20 ms during the contraction and relaxation phases.

The fixed-end F-L relation for the muscle was determined using the mean active force and mean sarcomere length during the tetanic plateau. The active force of the muscle was determined by subtracting the resting force from the total force during the tetanic plateau. Resting force was determined using the sarcomere length during the tetanic plateau and the resting F-L relation.

The sarcomere F-L relation was determined using the so-called extrapolation method (Gordon et al., 1966b). The force-time curve for a fixed-end contraction consisted of a rapid rise in force, followed by a slow rise in force, followed by a plateau. A straight line was fit to the fast rise (first 15 ms of the contraction) and the slow rise portions (55 - 95 ms after the beginning of the contraction) of the force-time curve using a chi-square merit function. The force at the intersection of the fast and slow force rises, and the sarcomere length at this same time, were determined. A plot of the extrapolated force and sarcomere length was used to represent the sarcomere F-L relation. This extrapolation method assumes that the "true" force of a sarcomere occurs at full activation before any slow sarcomere length changes occur, and correlates closely with the theoretical F-L relation for sarcomeres in single fiber preparations (e.g., Gordon et al., 1966b).

The theoretical F-L relation of a sarcomere was based on a thin myofilament length of $1.14 \mu\text{m}$ (end of filament to midpoint of Z-line, from mouse omohyoideus muscle, Phillips and Woledge, 1992); a thick myofilament length

of $1.63\ \mu\text{m}$ (from rabbit psoas muscle, Sosa et al., 1994); and a bare-zone length of $0.17\ \mu\text{m}$ (ter Keurs et al., 1984). The plateau was assumed to occur from $2.28 - 2.45\ \mu\text{m}$, and the descending limb from $2.45 - 3.91\ \mu\text{m}$.

An “effective stiffness” parameter was calculated as the slope of the force-displacement curve for a particular group of sarcomeres. The effective stiffness of the sarcomeres was a measure of how the force producing potential of the sarcomeres changed from one isometric length to a second isometric length after the sarcomeres had shortened or lengthened. The force a sarcomere could produce at the unstimulated sarcomere length (l_r) was determined using the theoretical F-L relation. This point was connected by a straight line to the force and sarcomere length during the tetanic plateau, and the slope of this line was calculated for the type 1 and the type 2 sarcomere length traces. For the type 12 and the type 21 sarcomere length traces, the stiffness was measured in two phases, since these types of traces had a lengthening and a shortening phase, and the transition from shortening to lengthening, or lengthening to shortening, had a sarcomere velocity of $-0.14\ \mu\text{m/s}$ ($-0.06\ L_0/\text{s}$). The first stiffness phase was calculated from the rest stage to the early tetanus, and the second stiffness phase was calculated from the early tetanus to the plateau of the tetanus. Mean forces during the rest stage and the plateau for the type 1 and the type 2 sarcomere length traces were determined over the same time periods used to classify the sarcomere length-time traces. The force during the early tetanus was normalized using the maximum force value during this time interval, not the force at the plateau of the tetanus.

A step-wise linear regression procedure was used to determine the relation between the effective stiffness and the initial sarcomere length. Data points at initial sarcomere lengths of less than $2.28\ \mu\text{m}$ were excluded because

they are located on the ascending limb of the theoretical F-L relation. Because the effective stiffness parameter is numerically sensitive to small changes in sarcomere length, stiffness values were excluded if the change in sarcomere length was less than 30 nm for type 1 and type 2 sarcomeres, and was less than 10 nm for type 12 and type 21 sarcomeres. From the total of 143 contractions, 14 were excluded based on this criteria.

Results

In a given region of the muscle, sarcomere length changes were generally of the same type, independent of the muscle length. Figure 7.4 displays the sarcomere lengths (A) and force-time traces (B) from one region of a muscle at four different muscle lengths. All four contractions exhibit a type 1 sarcomere length trace and reach a near steady-state sarcomere length. Trace a23 demonstrates the sarcomere length for a stimulation of 400 ms (Figure 7.4B).

Different regions along the length of a muscle exhibit different types of sarcomere length behavior. An example of the sarcomere length-time behavior found in three locations along the length of one muscle at two muscle lengths (subscripts 1 and 2) is displayed in Figure 7.5. One region of this muscle (c) had sarcomeres that shortened during the contractions, initially more rapidly than later (Figure 7.5A). The two remaining locations along the same group of fibers (a and b) possessed sarcomeres that shortened and then lengthened during the contraction (Figure 7.5A). Although the three force-time traces at each muscle length were indistinguishable, the sarcomere lengths in the three regions of the muscle were different, and these differences increased from rest to the tetanic plateau. At rest, the differences between the sarcomeres in the

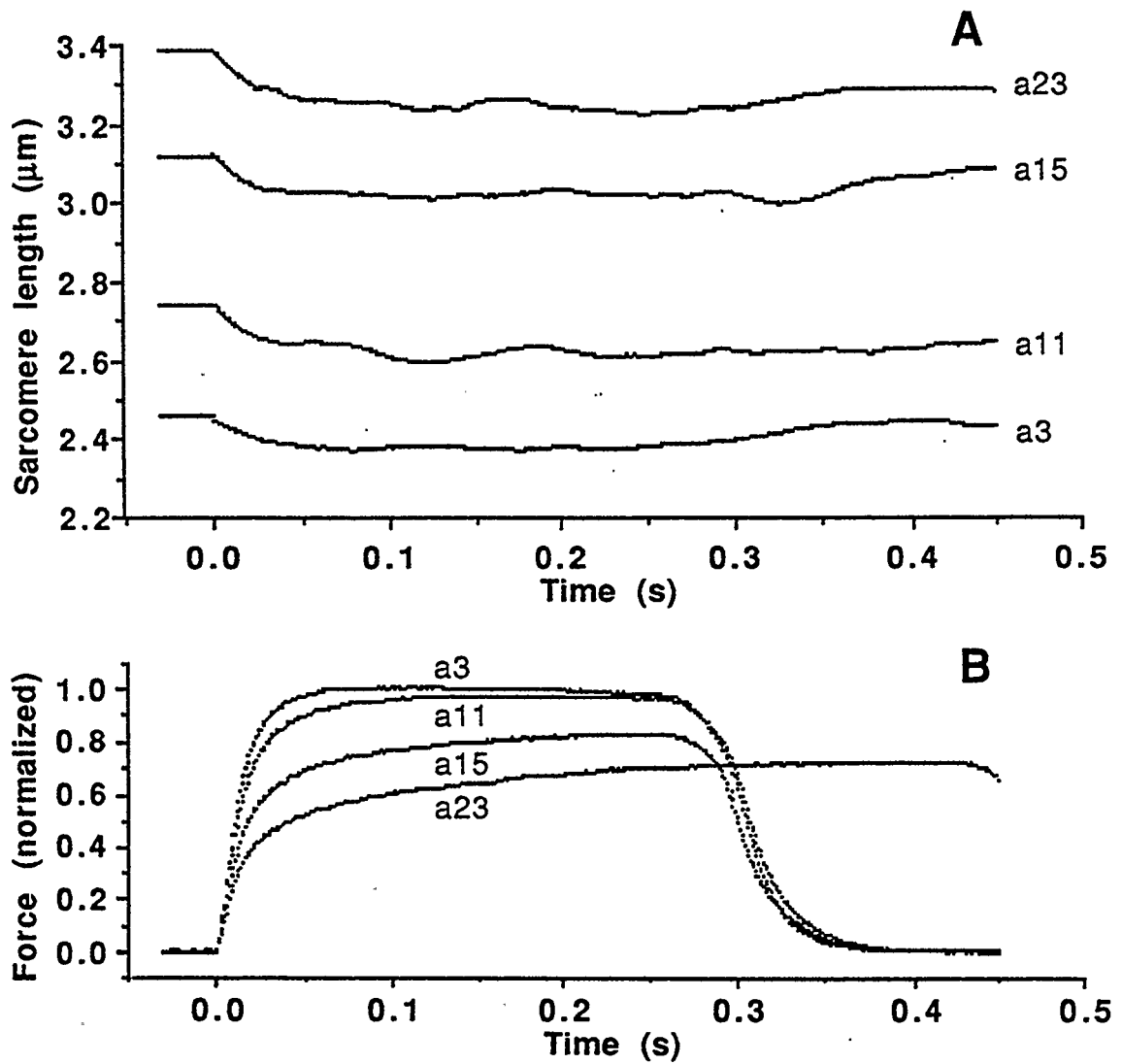


Figure 7.4. Sarcomere length-time (A) and force-time (B) traces at four different muscle lengths. Sarcomere length was measured from the same group of sarcomeres in all four traces. Note, stimulation of a23 was for 400 ms while it was 250 ms for the other three contractions [muscle: m1894].

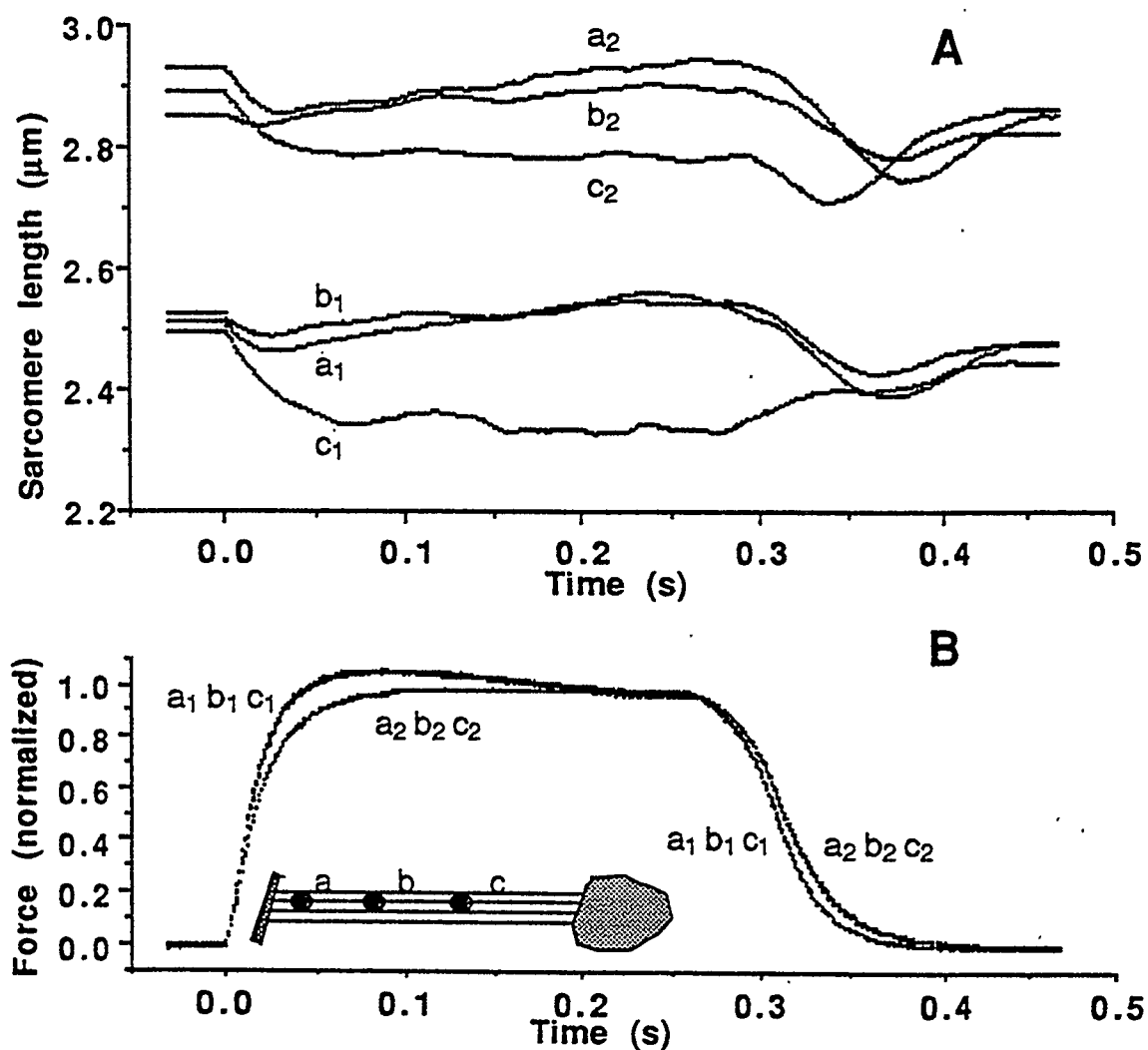


Figure 7.5. Sarcomere length-time (A) and force-time (B) traces for one muscle at two different muscle lengths (subscripts 1 and 2). Sarcomere length was measured at three different location along the length of the muscle (labelled a, b, and c). [muscle: j2293; line-file: a_1 - a_2 , b_1 - a_4 , c_1 - a_5 , a_2 - a_{10} , b_2 - a_{11} , c_2 - a_{12}]

different locations averaged 0.027 and 0.082 μm , and during the plateau the differences increased to 0.223 and 0.139 μm at muscle lengths 1 and 2, respectively (Figure 7.5A).

Figure 7.6 demonstrates how the isometric force changed from rest to the plateau of the tetanus for the muscle shown in Figure 7.4. The points on the theoretical F-L relation were determined using the resting sarcomere length (open squares) and they were connected to the force and length achieved during the tetanic plateau (filled squares). If the sarcomeres in the region measured remained perfectly isometric during the contraction, then the force during the plateau should lie on the theoretical F-L relation; however, the group of sarcomeres shown shortened during all contractions (type 1). At sarcomere lengths greater than 2.6 μm , the forces achieved during the contraction exceeded the predicted isometric forces (theoretical F-L relation) at the corresponding sarcomere lengths (Figure 7.6). At sarcomere lengths less than

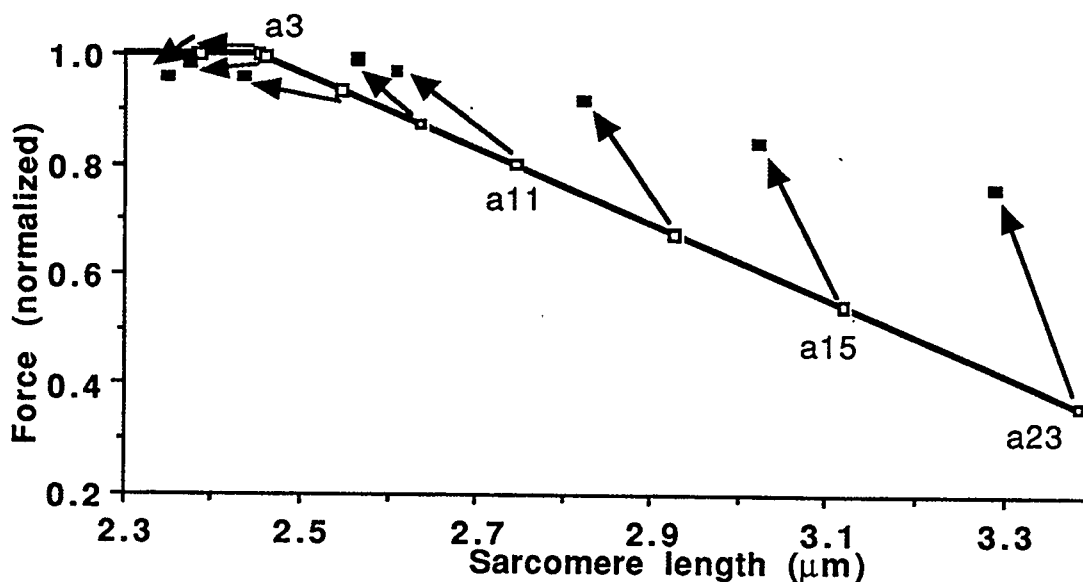


Figure 7.6. Change in force producing potential for one group of sarcomeres at various muscle lengths (same muscle as in Figure 7.4). Arrows connect the theoretical force at the resting sarcomere length (open boxes) with the force and sarcomere length during the plateau of the tetanus (filled boxes).

2.6 μm , the plateau forces were close to the theoretical predictions.

Figure 7.7 displays the forces produced by the muscle shown in Figure 7.5 at the points where sarcomere length had a velocity of zero or close to zero. Three groups of sarcomeres at locations labelled *a*, *b*, and *c* along the length of the muscle were measured for three muscle lengths (identified by triangles, circles, and squares). Sarcomeres in area *c* on this muscle shortened (type 1) during the contraction. As before, a line connects (arrow) the theoretical force at the resting sarcomere length (open symbols) with the force and sarcomere length during the plateau (filled symbols). Sarcomeres in areas *a* and *b* shortened and then lengthened (type 12) during the contraction. A straight line connects the theoretical force at the resting sarcomere length (open symbols) with the force and sarcomere length during the early tetanus phase (diamonds).

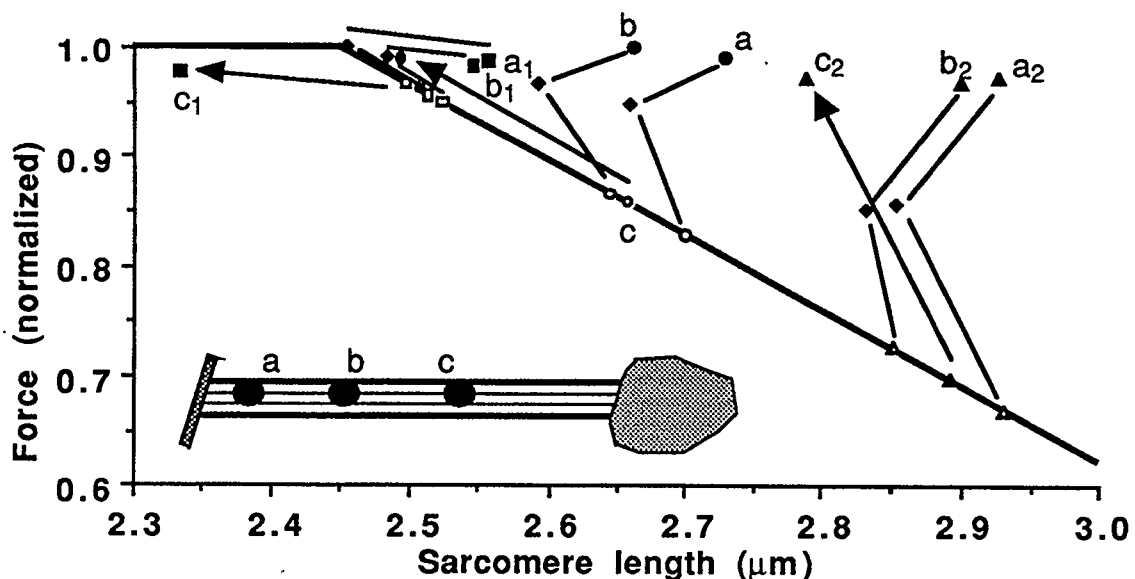


Figure 7.7. Change in force producing potential for three different groups of sarcomeres along the length of the muscle (same muscle as in Figure 7.5). Arrows connect the theoretical force at the resting sarcomere length (open symbols) with the force and sarcomere length during the tetanic plateau (filled symbols) for type 1 sarcomeres. Type 12 sarcomeres have an intermediate point (diamond) after shortening and before lengthening. Letters (*a*, *b*, and *c*) identify the location where sarcomere length was measured. The three muscle lengths are designated by the different symbols (boxes, circles, triangles).

Lines also connect the force and sarcomere length of the early tetanus with the corresponding force and sarcomere length of the plateau (filled symbols).

The straight lines that connect the points in Figures 7.6 and 7.7 establish the change in isometric force with a change in sarcomere length or displacement. The slope of this force-displacement curve is termed the “effective stiffness.” Each group of sarcomeres follows an effective stiffness curve that varies depending on the type of sarcomere length behavior, and depending on the initial sarcomere length.

For sarcomeres that shorten (muscle in Figure 7.6), the effective stiffness was negative for initial sarcomere lengths greater than 2.45 μm and positive for initial sarcomere lengths less than 2.45 μm . For the muscle in Figure 7.7, the effective stiffness was negative for the shortening regions (location *c*) and for the shortening portion of the type 12 sarcomeres (locations *a* and *b*). The lengthening portion of the type 12 sarcomeres exhibited a positive effective stiffness during early tetanus for sarcomere lengths greater than 2.48 μm . Both muscles had an increase in the magnitude of the effective stiffness with an increase in the initial sarcomere length above about 2.45 μm .

Effective stiffness was linearly related to the initial sarcomere length for the shortening sarcomeres (Figure 7.8). Data points of the type 1 sarcomeres (Figure 7.8A) and the shortening phase of the type 12 sarcomeres (Figure 7.8B) are identified by different symbols for each muscle. Since the lines of best fit for the type 1 ($y = 11.6 - 4.73x$, $n = 26$, $r = 0.96$) and type 12 sarcomeres ($y = 11.7 - 5.00x$, $n = 49$, $r = 0.66$) were not significantly different, the data were combined (Figure 7.8C). The effective stiffness was negative and increased in magnitude for sarcomere lengths greater than 2.38 μm ($y = 11.8 - 4.95x$, $n = 75$, $r = 0.71$).

Effective stiffness was also linearly related to the initial sarcomere length for the lengthening sarcomeres (Figure 7.9). Data points of the type 2

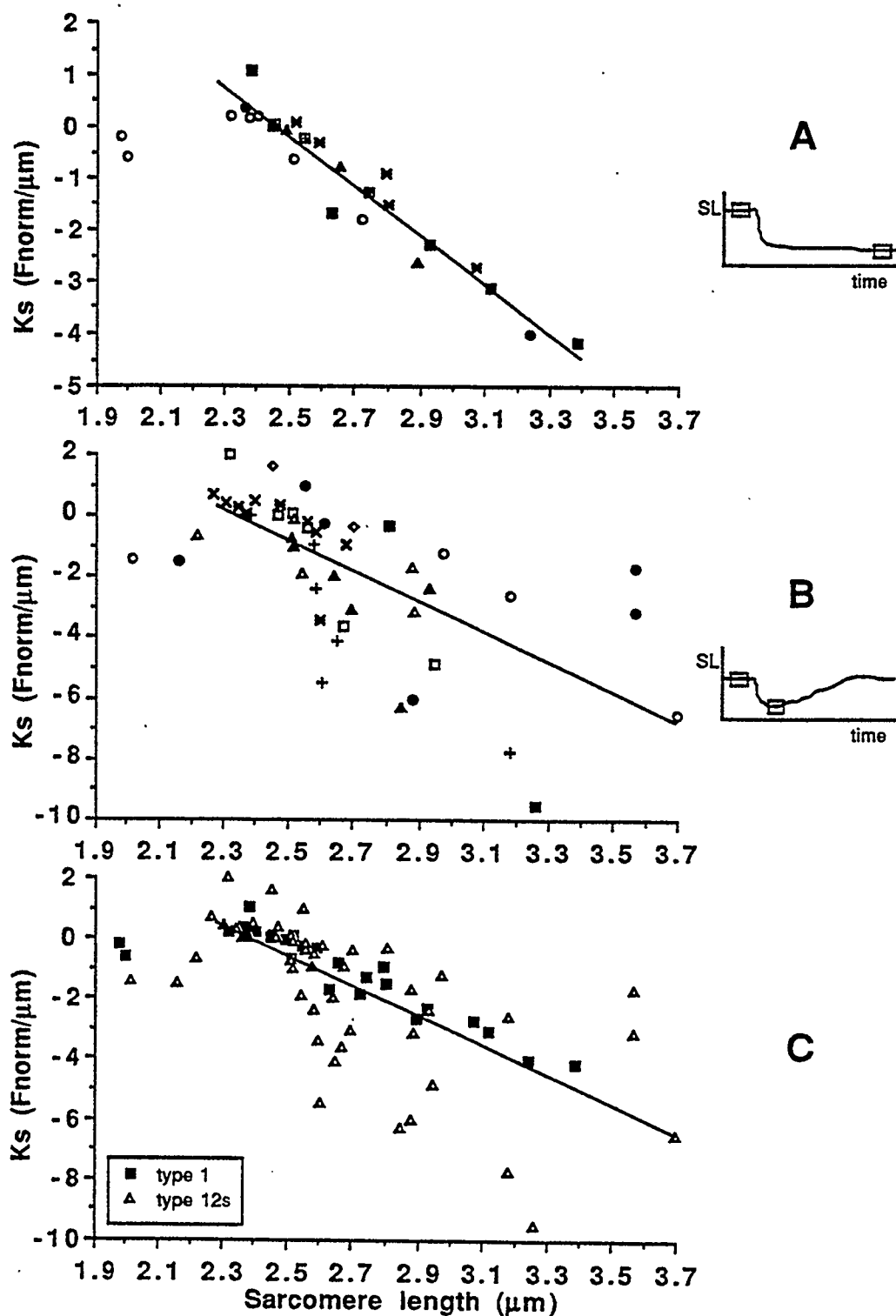


Figure 7.8. Plots of effective stiffness (K_s) for shortening sarcomeres of type 1 (A) and the shortening phase of type 12 (B) sarcomeres. Each symbol represents a different muscle. Combined results of plots A and B are included in C. Insets show the sarcomere length-time trace for each type of behavior between which the effective stiffness was measured.

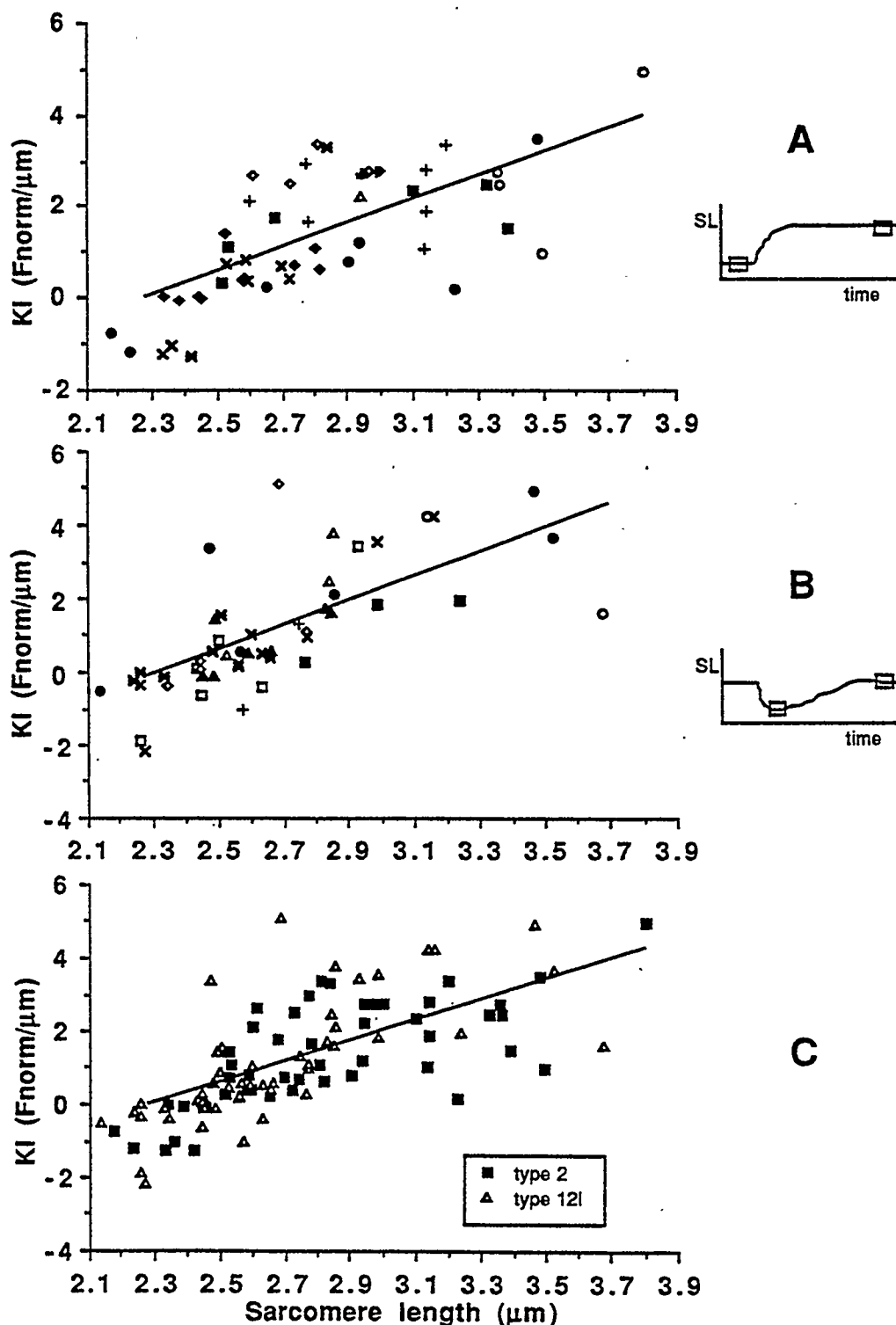


Figure 7.9. Plots of effective stiffness (KI) for lengthening sarcomeres of type 2 (A) and the lengthening phase of type 12 (B) sarcomeres. Each symbol represents a different muscle. Combined results of plots A and B are included in C. Insets show the sarcomere length-time trace for each type of behavior between which the effective stiffness was measured.

sarcomeres (Figure 7.9A) and the lengthening phase of the type 12 sarcomeres (Figure 7.9B) are identified by different symbols for each muscle. The lines of best fit for the type 2 ($y = -6.04 + 2.64x$, $n = 52$, $r = 0.67$) and type 12 sarcomeres ($y = -7.61 + 3.29x$, $n = 49$, $r = 0.66$) were not significantly different, thus the data were combined (Figure 7.9C). The effective stiffness was positive and increased for sarcomere lengths greater than $2.29 \mu\text{m}$ ($y = -6.53 + 2.85x$, $n = 101$, $r = 0.66$).

The fixed-end F-L relation for the serratus anterior muscle had an extended plateau, and forces that were greater than the corresponding theoretical forces on the descending limb of the F-L relation (Figure 7.10). The combined data from the four different types of sarcomere behaviors were fit to a 4th order polynomial ($y = 13.9 - 19.2x + 10.4x^2 - 2.41x^3 + 0.199x^4$, $n = 143$, $r = 0.93$).

The extrapolation method was used to predict the “true” isometric force production of sarcomeres (Figure 7.11). The extrapolated F-L relation obtained

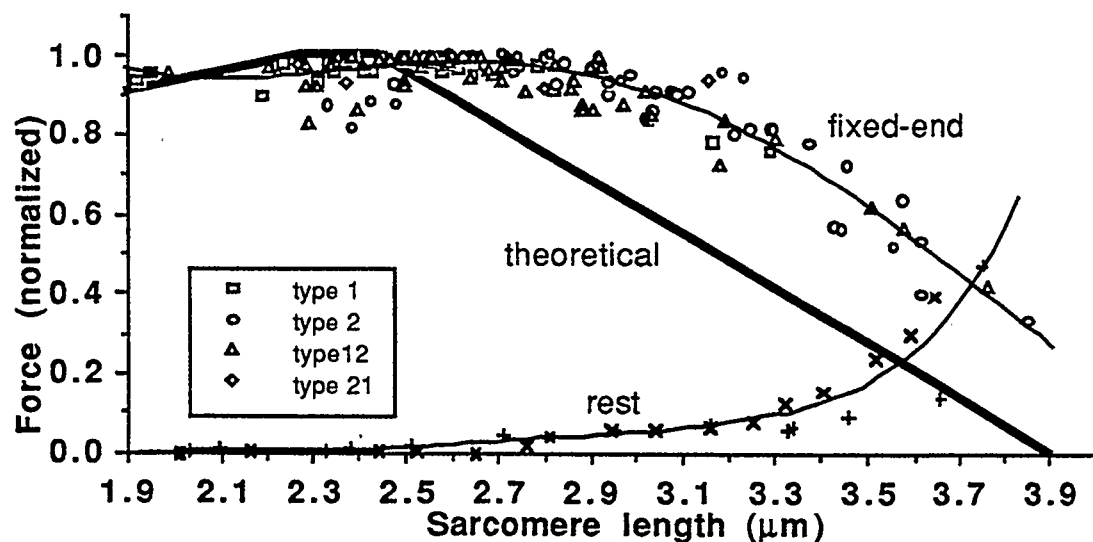


Figure 7.10. Fixed-end F-L relation for all data points ($n = 143$) along with a best fit line (thin line). Also shown are the theoretical F-L relations (thick line) and the resting F-L relation for two muscles (cross and plus symbols [n2492 and a2793.b4]; fit line, $y = -29.2 + 57.7x - 45.2x^2 + 17.5x^3 - 3.37x^4 + 0.257x^5$, $r = 0.93$, $n = 29$).

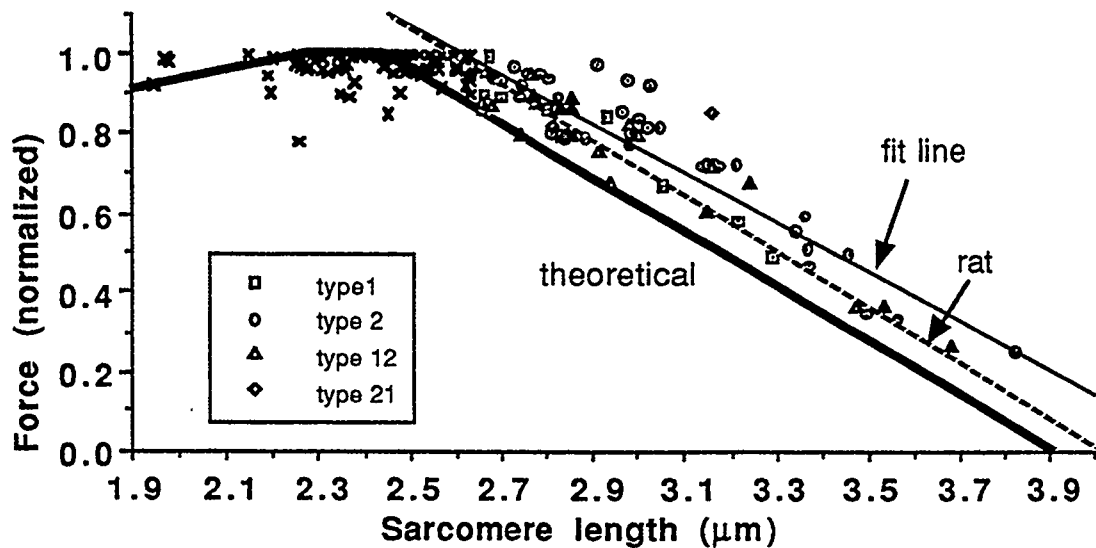


Figure 7.11. Sarcomere F-L relation using the extrapolation method for all data points (12 muscles, $n = 143$) along with a linear fit line for data points above $2.65 \mu\text{m}$ (thin line). Theoretical F-L relations also shown (thick line).

in this study exhibited a linear descending limb that was shifted by about $0.20 \mu\text{m}$ to the right of the theoretical F-L relation at maximum force levels. A straight line was fit using regression ($r = 0.92$) through data at lengths greater than $2.65 \mu\text{m}$. This line had a zero force intercept of $4.23 \mu\text{m}$ and a slope of -0.618 (force-normalized / μm).

As expected, the fixed-end F-L relation had higher forces at corresponding sarcomere lengths on the descending limb when compared to the extrapolated F-L relations (Figure 7.12). Differences between the fixed-end and the extrapolated F-L relations increased from zero at a sarcomere length of $2.65 \mu\text{m}$ to about 20 percent of the maximum force at sarcomere lengths above $3.25 \mu\text{m}$. The difference between these two F-L relations is presumably related to the change in the isometric force produced by a sarcomere after a length change.

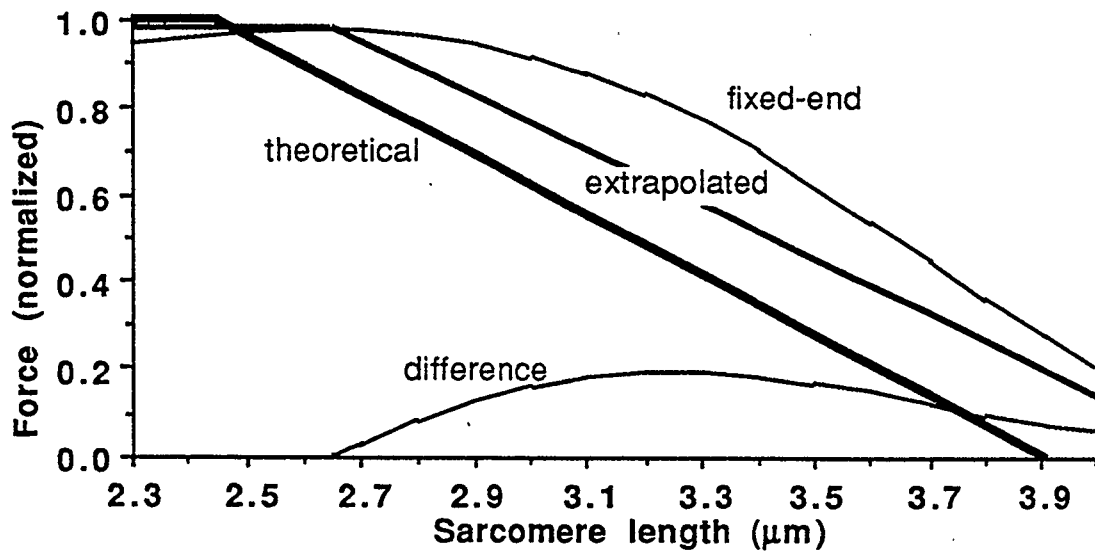


Figure 7.12. F-L relations from lines fit to data of this study. The difference curve computed as the fixed-end minus the extrapolated F-L relations.

Discussion

Comparison with other investigations

The fixed-end F-L relation found here in mouse muscle was qualitatively similar to that of amphibian single fiber and muscle preparations (Carlsen et al., 1961; ter Keurs et al., 1978ab; Altringham and Bottinelli, 1985; Martyn and Gordon, 1988; Granzier and Pollack, 1990). The fixed-end F-L relation had an extended plateau and forces on the descending limb that were greater than those of the theoretical F-L relation.

The F-L relation determined by using the extrapolation technique was expected to produce a curve similar to the theoretical F-L relation based on results from frog single fibers. However, the sarcomere F-L relation found here using the extrapolation technique exhibited higher forces on the descending limb than predicted theoretically. A similar result was found by ter Keurs et al. (1984) using segment-clamping methods for fiber bundles of the rat extensor digitorum longus muscle. They demonstrated a linear descending limb for the

experimentally determined sarcomere F-L relation that was shifted to the right of the theoretical F-L relation at plateau forces, but had a zero force intercept of about 3.90 μm .

The differences between the theoretical and the sarcomere F-L relations found here and by ter Keurs et al. (1984) may be related to the preparation. Fiber bundle or muscle preparations may exhibit a shift in the F-L relation to the right because of slight nonuniformities in the sarcomere length across the width of the muscle.

Another explanation for the differences between the theoretical and the extrapolated F-L relations found here and by ter Keurs et al. (1984) may be that the myofilament lengths are not known accurately. The thin and thick myofilament lengths (1.13 μm and 1.53 μm , respectively) published by ter Keurs et al. (1984) may be corrected for shrinkage assuming that the correct length of the thick myofilament length is 1.63 μm (Sosa et al., 1994). The resulting thin and thick myofilament lengths of 1.20 μm and 1.63 μm , respectively, predict a plateau from 2.40 to 2.58 μm , and a descending limb from 2.58 to 4.03 μm . If these myofilament lengths occur in the mouse serratus anterior muscle, the descending limb of the theoretical F-L relation would not be significantly different from the line of best fit to our data (Figure 7.11).

Stability considerations

Stable sarcomere length behavior, as defined elsewhere (Chapter 6), was found in all 143 sarcomere length-time traces. In order for stability to occur, the force-displacement behavior of the sarcomeres within a fiber must have a positive slope (Chapter 4), i.e., sarcomeres that are stretched must increase in force and sarcomeres that shorten must decrease in force.

The isometric force production of sarcomeres in single fiber preparations does increase after stretch (Abbott and Aubert, 1953; Hill, 1977; Edman et al.,

1978; Julian and Morgan 1979b; Edman et al., 1982). This sarcomere behavior was also observed in the present study. The effective stiffness was positive for sarcomeres that lengthened, if the initial sarcomere length was greater than 2.3 μm . Thus, sarcomeres have an isometric force after stretch that is greater than the isometric force if no stretch had occurred; they do not decrease in force along the theoretical F-L relation as described by Gordon et al. (1966).

It is not clear whether or not the isometric force of sarcomeres decreases following shortening, and thus if sarcomeres possess a positive effective stiffness. Horowitz et al. (1992) demonstrated that after small sarcomere shortenings (0.02 - 0.16 μm / sarcomere) on the descending limb of the F-L relation, the isometric force was greater than the predicted theoretical F-L relation. Edman et al. (1993) found that after sarcomeres had shortened (0.25 and 0.33 μm / sarcomere) onto the plateau of the theoretical F-L relation, the isometric force was maximal. Other researchers have demonstrated a decrease in isometric force below the theoretical F-L relation after sarcomere shortening (Abbott and Aubert, 1952; D  l  ze, 1961; Julian and Morgan, 1979b; Mar  chal and Plaghki, 1979; Edman, 1980; Sugi and Tsuchiya, 1988; Granzier and Pollack, 1989). Results from the present study typically demonstrated an increase in force above the descending limb of the theoretical F-L relation for sarcomeres that shortened during contraction (negative effective stiffness). It appears that there is no conclusive evidence that the force-displacement relation of a sarcomere that shortens has a positive slope, and therefore is known to be stable. More comprehensive research into the force production of sarcomeres after shortening is necessary to fully understand how stability is achieved for these sarcomeres. The cross-bridge stiffness may provide the necessary properties for stability (Chapter 5).

Reason for a shift in the fixed-end F-L relation

Differences between the fixed-end and the theoretical F-L relations can be attributed to the effective stiffness properties of the sarcomeres. Nonuniform changes in sarcomere length (i.e., some sarcomeres shorten while others lengthen) must occur to observe a shift in the F-L relation, otherwise the fixed-end and the theoretical F-L relations should coincide. Also, sarcomeres that change length must produce forces which are different than those of the theoretical F-L relation, as demonstrated here and by others (Hill, 1977; Edman et al., 1978; Julian and Morgan 1979b; Maréchal and Plaghki, 1979; Edman, 1980; Edman et al., 1982; Sugi and Tsuchiya, 1988; Granzier and Pollack, 1989; Horowitz et al., 1992; Edman et al., 1993). In Chapter 5, it was demonstrated theoretically that it is necessary for the effective stiffness to increase with sarcomere length on the descending limb of the F-L relation to get the observed shift of the fixed-end F-L relation relative to the theoretical F-L relation. The results of this study suggest that this change in effective stiffness property exists.

In the past, the shift in the fixed-end F-L relation relative to the theoretical F-L relation was attributed to sarcomeres that are continually changing length (Lieber and Baskin, 1984; Granzier and Pollack, 1990). However, when sarcomeres approach a steady-state length during a contraction (Chapter 6), force-velocity properties of the sarcomeres cannot account for the differences between the two F-L relations because the sarcomeres are no longer changing length. Therefore, the shift in the fixed-end F-L relation may be caused by a change in the isometric force producing characteristics of the sarcomeres caused by the previous sarcomere length changes. These changes in mechanical properties after previous stretching or shortening have been observed here and by other researchers. The precise mechanisms for these

changes in isometric force following length changes in sarcomeres are not known, and cannot be explained using the cross-bridge model of contraction (Huxley, 1957).

Chapter 8

Summary and Conclusions

This dissertation presents theoretical and experimental evidence that sarcomeres are stable at lengths that were previously thought to be unstable (i.e., the descending limb of the F-L relation). Stability was defined to exist if the potential energy function of a fiber had a minimum. Stable sarcomere behavior exhibits a decrease in the speed of sarcomere shortening or lengthening toward a steady-state length, while an unstable sarcomere exhibits an accelerating sarcomere length during contraction (Chapter 6).

Theoretically it was demonstrated that all but one sarcomere must possess a positive effective stiffness (slope of the force-displacement curve) for the fiber to be stable during a fixed-end contraction (Chapter 4). A “comb” model (representing a sarcomere) was used to demonstrate that a stable system can produce an isometric F-L relation with a negative slope (Chapter 4). Previous researchers could have misinterpreted the descending limb of the isometric F-L relation as being unstable, when in fact it is stable.

Sarcomere length-time behavior was found to be stable as measured using the serratus anterior muscle of the mouse (Chapter 6). Sarcomeres within the muscle approached a steady-state length during fixed-end tetani. Nonuniform sarcomere length changes were found along the length of the muscle (i.e., some sarcomeres shortened while others lengthened). Both of

these findings were in agreement with data reported in the literature.

Nonuniform sarcomere length changes have been interpreted by investigators in the past to result from unstable sarcomeres on the descending limb of the F-L relation. However, a fiber model was used to demonstrate that nonuniform sarcomere length changes can be exhibited by a stable or an unstable fiber. The sarcomere length-time traces that were interpreted by others as being unstable, in fact, demonstrate stable behavior (a decreasing speed of lengthening or shortening with time).

The fixed-end F-L relation of the serratus anterior muscle of the mouse exhibited an extended plateau and forces higher than those at corresponding lengths on the descending limb of the theoretical F-L relation (Chapter 7). Differences between the fixed-end and the theoretical F-L relation could not be explained by force-velocity properties, because sarcomeres in the mouse muscle reached a steady-state length (near zero velocity) during fixed-end contractions (Chapter 6). Based on a model of a fiber, sarcomeres must possess an increase in the effective stiffness with an increase in initial sarcomere length to observe the differences typically found between the theoretical and the fixed-end F-L relations (Chapter 5). Effective stiffness properties for sarcomeres which had previously shortened or lengthened were found to increase with increasing initial sarcomere length during fixed-end contractions of mouse serratus anterior muscle (Chapter 7). These effective stiffness properties can be observed from the experimental results of previous investigators and can explain the differences between the theoretical and fixed-end F-L relations.

The serratus anterior muscle from mouse is well suited for in vitro experiments, and has not been previously used. The distal head of the serratus anterior muscle can be isolated with minimal dissection. This preparation has

little series elasticity, since the fibers run from bone to bone with no visible tendon. The bony attachments of the muscle can be rigidly mounted into an experimental apparatus. The preparation is thin enough to measure sarcomere length behavior using laser diffraction in a relatively undisturbed muscle.

Conclusions of this dissertation are that:

- 1) Muscle appears to be stable at sarcomere lengths corresponding the descending limb of the F-L relation.
- 2) Differences between the theoretical and the fixed-end F-L relation can be explained by changes in the force produced in an isometric sarcomere as a result of previous lengthening or shortening (i.e., a history dependent isometric F-L relation).

Chapter 9

References

- Abbott, B.C., and Aubert, X.M. (1952) The force exerted by active striated muscle during and after change of length, *J. Physiol.* **117**, 77-86.
- Altringham, F.D., Bottinelli, R., and Lacktis, J.W. (1984) Is stepwise shortening an artifact? *Nature* **307**, 653-655.
- Altringham, J.D. and Bottinelli, R. (1985) The descending limb of the sarcomere length-force relation in single muscle fibres of the frog. *J. Muscle Res. Cell Motil.* **6**, 585-600.
- Bagni, M.A., Cecchi, G., Colomo, F. and Tesi, C. (1988) Plateau and descending limb of the sarcomere length-tension relation in short length-clamped segments of frog muscle fibres. *J. Physiol.* **401**, 481-595.
- Burton, K. and Huxley, A.F. (1995) Identification of source oscillations in apparent sarcomere length measured by laser diffraction. *Biophys. J.* **168**, 2429-2443.
- Carlsen, F., Knappeis, G.G., and Buchthal, F. (1961) Ultrastructure of the resting and contracted striated muscle fiber at different degrees of stretch. *J. Biophys. and Biochem. Cytol.* **11**, 95-117.
- Cleworth, D.R. and Edman, K.A.P. (1972) Changes in sarcomere length during isometric tension development in frog skeletal muscle. *J. Physiol.* **227**, 1-17.

- Délèze, J.B. (1961) The mechanical properties of the semitendinosus muscle at lengths greater than its length in the body. *J. Physiol.* **158**, 154-164.
- Edman, K.A.P., Elzinga, G. and Noble, M. (1978) Enhancement of mechanical performance by stretch during tetanic contractions of vertebrate skeletal muscle fibers. *J. Physiol.* **281**, 139-155.
- Edman, K.A.P. (1980) Depression of mechanical performance by active shortening during twitch and tetanus of vertebrate muscle fibres. *Acta Physiol. Scand.* **109**, 15-26.
- Edman, K.A.P., Elzinga, G. and Noble, M.I.M. (1982) Residual force enhancement after stretch of contracting frog single muscle fibers. *J. Gen. Physiol.* **80**, 769-784.
- Edman, K.A.P. and Reggiani, C. (1984) Redistribution of sarcomere length during isometric contraction of frog muscle fibres and its relation to tension creep. *J. Physiol.* **351**, 169-198.
- Edman, K.A.P. and Reggiani, C. (1987) The sarcomere length-tension relation determined in short segments of intact muscle fibres of the frog. *J. Physiol.* **385**, 709-732.
- Edman, K.A.P., Caputo, C. and Lou, F. (1993) Depression of tetanic force induced by loaded shortening of frog muscle fibres. *J. Physiol.* **466**, 535-552.
- Fabiato, A. and Fabiato, F. (1978) Myofilament-generated tension oscillations during partial calcium activation and activation dependence of the sarcomere length-tension relation of skinned cardiac cells. *J. Gen. Physiol.* **72**, 667-699.
- Fischer, E. (1926) *Plüg. arch. ges Physiol.* **213**, 352.
- Flitney, F.W. and Hirst, D.G. (1978) Cross-bridge detachment and sarcomere "give" during stretch of active frog's muscle. *J. Physiol.* **276**, 449-465.

- Ford, L.E., Huxley, A.F. and Simmons, R.M. (1977) Tension responses to sudden length change in stimulated frog muscle fibres near slack length. *J. Physiol.* **269**, 441-515.
- Gordon, A.M., Huxley, A.F. and Julian, F.J. (1966a) Tension development in highly stretched vertebrate muscle fibres. *J. Physiol.* **184**, 143-169.
- Gordon, A.M., Huxley, A.F. and Julian, F.J. (1966b) The variation in isometric tension with sarcomere length in vertebrate muscle fibres. *J. Physiol.* **184**, 170-192.
- Granzier, H.L.M. and Pollack, G.H. (1989) Effect of active pre-shortening on isometric and isotonic performance of single frog muscle fibres. *J. Physiol.* **415**, 299-327.
- Granzier, H.L.M. and Pollack, G.H. (1990) The descending limb of the force-sarcomere length relation of the frog revisited. *J. Physiol.* **421**, 595-615.
- Haskell, R.C. and Carlson, F.D. (1981) Quasi-elastic light-scattering studies of single skeletal muscle fibers. *Biophys. J.* **33**, 39-62.
- Hildebrand, F.B. (1965) *Methods of Applied Mathematics*. Prentice-Hall Inc., Englewood Cliffs, N.J. pp. 47-48.
- Hill, A.V. (1938) The heat of shortening and the dynamic constants of muscle. *Proc. Roy. Soc.* **B126**, 136-195.
- Hill, A.V. (1953) The mechanics of active muscle. *Proc. Roy. Soc. Lond.* **B141**, 104-117.
- Hill, L. (1977) A-band length, striation spacing and tension change on stretch of active muscle. *J. Physiol.* **266**, 677-685.
- Horowitz, A., Wussling, H.P.M. and Pollack, G.H. (1992) Effect of small release on force during sarcomere-isometric tetani in frog muscle fibres. *Biophys. J.* **63**, 3-17.

- Huxley, A.F. and Niedergerke, R. (1954) Interference microscopy of living muscle fibres. *Nature* **173**, 971-973.
- Huxley, A.F. (1957) Muscle structure and theories of contraction. *Prog. Biophys. biophys. Chem.* **7**, 255-318.
- Huxley, A.F. and Peachey, L.D. (1961) The maximum length for contraction in vertebrate striated muscle. *J. Physiol.* **165**, 150-165.
- Huxley, A.F. and Simmons, R.M. (1971) Proposed mechanism of force generation in striated muscle. *Nature* **233**, 533-538.
- Huxley, H.E. (1953) Electron microscope studies of the organisation of the filaments in striated muscle. *Biochim. biophys. Acta* **12**, 387-394.
- Huxley, H.E. and Hanson, J. (1954) Change in the cross-striations of muscle during contraction and stretch and their structural interpretation. *Nature, Lond.* **173**, 973-976.
- Iwazumi, T. (1987) Mechanics of the myofibril. In: *Mechanics of the Circulation* (Edited by ter Keurs, H.E.D.J. and Tyberg, J.V.) Martinus Nijhoff Publishers, Dordrecht.
- Julian, F.J., Sollins, M.T. and Moss, R.L. (1978) Sarcomere length non-uniformity in relation to tetanic responses of stretched skeletal muscle fibres. *Proc. Roy. Soc. Lond.* **B200**, 109-116.
- Julian, F.J. and Morgan, D.L. (1979a) Intersarcomere dynamics during fixed-end tetanic contractions of frog muscle fibres. *J. Physiol.* **293**, 365-378.
- Julian, F.J. and Morgan, D.L. (1979b) The effect on tension of non-uniform distribution of length changes applied to frog muscle fibres. *J. Physiol.* **293**, 379-392.
- Kardestuncer, H. (1974) *Elementary Matrix Analysis of Structures*. McGraw-Hill Book Co. pp. 230-231.

- Katz, B. (1939) The relation between force and speed in muscular contraction. *J. Physiol.* **96**, 45-64.
- Lieber, R.L. and Baskin, R.J. (1983) Intersarcomere dynamics of single muscle fibers during fixed-end tetani. *J. Gen. Physiol.* **82**, 347-364.
- Lieber, R.L. and Boakes, J.L. (1988) Sarcomere length and joint kinematics during torque production in frog hindlimb. *Am. J. Physiol.* **254**, C759-C768.
- Maréchal, G. and Plaghki, L. (1979) The deficit of the isometric tetanic tension redeveloped after a release of frog muscle at a constant velocity. *J. Gen. Physiol.* **73**, 453-467.
- Martyn, D.A. and Gordon, A.M. (1988) Length and myofilament-dependent changes in calcium sensitivity of skeletal fibres, effects of pH and ionic strength. *J. Mus. Res. Cell Motil.* **9**, 428-445.
- Morgan, D.L., Mochon, S. and Julian, F.J. (1982) A quantitative model of intersarcomere dynamics during fixed-end contractions of single frog muscle fibers. *Biophys. J.* **39**, 189-196.
- Morgan, D.L. (1990) New insights into the behaviour of muscle during active lengthening. *Biophys. J.* **57**, 209-221.
- Paolini, P.J. and Roos, K.P. (1975) Length-dependent optical diffraction pattern changes in frog sartorius muscle. *Physiol. Chem. & Physics* **7**, 235-254.
- Paolini, P.J., Sabbadini, R., Roos, K.P., and Baskin, R.J. (1976) Sarcomere length dispersion in single skeletal muscle fibers and fiber bundles. *Biophys. J.* **16**, 919-930.
- Peterson, J.N., Hunter, W.C. and Bergman, M.R. (1989) Control of segment length or force in isolated papillary muscle: an adaptive approach. *Am. J. Physiol.* **265(25)**, H1726-H1734.

- Phillips, S.K. and Woledge, R.C. (1992) A comparison of isometric force, maximum power and isometric heat rate as a function of sarcomere length in mouse skeletal muscle. *Pflügers. Arch.* **420**, 578-583.
- Pollack, G.H. (1983) The cross-bridge theory. *Physiol. Rev.* **63**(3), 1049-1113.
- Pollack, G.H. (1990) *Muscles and Molecules*. Ebner and Sons, Seattle. pp. 221-222.
- Smith, J.P. and Barsotti, R.J. (1993) A computer-based servo system for controlling isotonic contractions of muscle. *Am. J. Physiol.* **263**(34), C1424-C1432.
- Sosa, H., Popp, D., Ouyang, G., Huxley, H.E. (1994) Ultrastructure of skeletal muscle fibers studied by a plunge quick freezing method: myofilament lengths. *Biophys. J.* **67**, 283-292.
- Sugi, H. and Tsuchiya, T. (1988) Stiffness changes during enhancement and deficit of isometric force by slow length changes in frog skeletal muscle fibres. *J. Physiol.* **407**, 215-229.
- Tameyasu, T., Ishide, N. and Pollack, G.H. (1982) Discrete sarcomere length distribution in skeletal muscle. *Biophys. J.* **37**, 489-492.
- ter Keurs, H.E.D.J., Iwazumi, T. and Pollack, G.H. (1978a) The length-tension relation in skeletal muscle: revisited. In: *Cross-bridge Mechanism in Muscle Contraction* (Edited by Sugi, H. and Pollack, G.H.), pp. 277-295. University of Tokyo Press, Tokyo.
- ter Keurs, H.E.D.J., Iwazumi, T. and Pollack, G.H. (1978b) The sarcomere length-tension relation in skeletal muscle. *J. Gen. Physiol.* **72**, 565-592.

ter Keurs, H.E.D.J., Luff, A.R., and Luff, S.E. (1984) Force-sarcomere-length relation and filament length in rat extensor digitorum muscle. In: *Contractile Mechanisms in Muscle* (Edited by Pollack, G.H. and Sugi, H.), pp. 511-525. Plenum Press, N.Y.

Trotter, J.A. (1990) Interfiber tension transmission in series-fibered muscles of the cat hindlimb. *J. Morphol.* **206**, 351-361.

Trotter, J.A. and Purslow, P.P. (1992) Functional morphology of the endomysium in series fibered muscles. *J. Morphol.* **212**, 109-122.